

THE INFLUENCE OF TREE TRAITS AND
STORM EVENT CHARACTERISTICS ON STEMFLOW PRODUCTION FROM
ISOLATED DECIDUOUS TREES IN AN URBAN PARK

by

Julie Taylor Schooling

B.Sc., University of Toronto, 1993

B.L.A., University of Toronto, 1993

A THESIS SUBMITTED IN PARTIAL FULFILLMENT OF
THE REQUIREMENTS FOR THE DEGREE OF
MASTER OF SCIENCE IN ENVIRONMENTAL SCIENCES

Thompson Rivers University
Kamloops, British Columbia, Canada

August, 2014

Thesis Examining Committee:

Darryl Carlyle-Moses (PhD), Thesis Supervisor and Associate Professor and Chair,
Department of Geography & Environmental Studies,
Thompson Rivers University

Lauchlan Fraser (PhD), Professor and Canada Research Chair in Community
and Ecosystem Ecology, Department of Natural Resource Science,
Thompson Rivers University

Sharon Brewer (PhD), Associate Professor, Department of Physical Sciences
and Engineering, Thompson Rivers University

Delphis Levia (PhD), External Reader, Professor of Ecohydrology and Director,
Environmental Science and Environmental Studies, Department of Geography,
University of Delaware

© Julie Taylor Schooling, 2014

Thesis Supervisor: Dr. Darryl Carlyle-Moses

ABSTRACT

Urban tree canopy processes affect the volume and biogeochemistry of inputs to the hydrological cycle in cities. We studied stemflow in isolated deciduous trees in a semi-arid climate dominated by small precipitation events. To clarify the effect of canopy traits on stemflow thresholds, rates, yields, percent, and funneling ratios, we analyzed branch angles, bark relief, tree size, cover, leaf size, and branch and leader counts. High branch angles promoted stemflow in all trees, while bark relief influenced stemflow differently for single- and multi-leader trees. The association between stemflow and numerous leaders deserves further study. Among meteorological variables, rain depth was strongly correlated with stemflow yields; intra-storm break duration, rainfall intensity, rainfall inclination, wind speed, and vapour pressure deficit also played roles. Greater stemflow was associated with leafless canopies and with rain or mixed events versus snow. Results can inform climate-sensitive selection and siting of urban trees towards integrated rainwater management.

Keywords: stemflow, canopy water balance, urban hydrology, urban forestry, stormwater management, deciduous trees, branch angles, bark relief

ERRATUM

Throughout this Thesis, American beech (*Fagus grandifolia*) should be replaced with Riversii European beech (*F. sylvatica* 'Riversii').

TABLE OF CONTENTS

ABSTRACT	ii
LIST OF FIGURES	v
LIST OF TABLES	vii
GLOSSARY OF ACRONYMS	ix
ACKNOWLEDGMENTS	xi
CHAPTER 1 INTRODUCTION	1
1.1 URBAN HYDROLOGY CONTEXT.....	1
1.2 TREE CANOPY PROCESSES	1
1.3 STEMFLOW IN CONTEXT.....	2
1.4 FACTORS INFLUENCING STEMFLOW QUANTITY AND QUALITY.....	2
1.4.1 <i>Tree Morphology</i>	2
1.4.2 <i>Storm Meteorology and Seasonal Effects</i>	3
1.4.3 <i>Stemflow Chemistry</i>	3
1.5 OBJECTIVES	4
1.6 REFERENCES	5
CHAPTER 2 THE INFLUENCE OF RAINFALL DEPTH CLASS AND DECIDUOUS TREE TRAITS ON STEMFLOW PRODUCTION IN AN URBAN PARK	7
2.1 INTRODUCTION	7
2.2 METHODS	11
2.2.1 <i>Study Area</i>	11
2.2.2 <i>Precipitation and Stemflow Measurement</i>	12
2.2.3 <i>Tree Selection and Trait Measurement and Derivation</i>	12
2.2.4 <i>Data Analysis</i>	15
2.3 RESULTS	16
2.3.1 <i>Precipitation</i>	16
2.3.2 <i>Study Tree Characteristics</i>	16
2.3.3 <i>Stemflow for Individual Trees as a Percentage of Rainfall</i>	17
2.3.4 <i>Stemflow Funneling Ratios for Individual Trees</i>	25
2.3.5 <i>Stemflow Percent and Funneling Ratios as a Function of Morphological Traits</i>	26
2.4 DISCUSSION	27
2.4.1 <i>Tree Size, Canopy Dimensions, and Branch Metrics</i>	28
2.4.2 <i>Cover Metrics</i>	29
2.4.3 <i>Leader and Branch Characteristics</i>	30
2.4.4 <i>Bark Relief</i>	32
2.4.5 <i>Leaf Size</i>	33
2.4.6 <i>Assessment of Predicted Patterns on an Individual Tree Basis</i>	33
2.5 CONCLUSION.....	35
2.6 REFERENCES	38

CHAPTER 3 TREE TRAITS AND METEOROLOGICAL FACTORS INFLUENCING THE INITIATION AND RATE OF STEMFLOW FROM ISOLATED DECIDUOUS TREES	44
3.1 INTRODUCTION	44
3.2 STUDY AREA AND METHODS	47
3.2.1 <i>Study Area</i>	47
3.2.2 <i>Tree Selection and the Measurement and Derivation of Tree Traits</i>	48
3.2.3 <i>Precipitation and Stemflow Measurement</i>	50
3.2.4 <i>Measurement and Derivation of Meteorological Variables</i>	51
3.2.5 <i>Data Analysis</i>	53
3.3 RESULTS	55
3.3.1 <i>Precipitation Profile</i>	55
3.3.2 <i>Influence of Canopy Characteristics</i>	56
3.3.3 <i>Influence of Meteorological and Seasonal Factors</i>	58
3.4 DISCUSSION	63
3.4.1 <i>Canopy Traits Influencing Stemflow from Rain in Leaf-on Condition</i>	63
3.4.2 <i>Stemflow Initiation Threshold</i>	63
3.4.3 <i>Stemflow Rate</i>	64
3.4.4 <i>Stemflow Percent</i>	68
3.4.5 <i>Funneling Ratios</i>	69
3.4.6 <i>Influence of Leaf Condition on Stemflow from Rain</i>	70
3.4.7 <i>Meteorological Influences on Stemflow from Rain for Various Leaf Conditions</i>	70
3.4.8 <i>Stemflow from Snow and Mixed Events Compared to Rain</i>	73
3.5 CONCLUSION.....	74
3.6 REFERENCES	76
CHAPTER 4 CONCLUSIONS AND RECOMMENDATIONS	82
4.1 SYNTHESIS: TRAIT AND METEOROLOGICAL FACTORS IN STEMFLOW GENERATION	82
4.2 APPLICABILITY OF FINDINGS IN THE CONTEXT OF STORMWATER MANAGEMENT	86
4.3 LESSONS LEARNED	88
4.4 FUTURE RESEARCH	89
APPENDIX A SUPPLEMENTARY TABLES	90
APPENDIX B SUPPLEMENTARY MAPS, PHOTOGRAPHS, AND VIDEOS	99

LIST OF FIGURES

Figure 2.1	Rain depth frequency distribution during the study period compared to Canadian Climate Normals 1981–2010 for station Kamloops A* (Environment Canada, 2014)	17
Figure 2.2a	Boxplots for stemflow % for single-leader (Group A) trees by rain depth class: I (< 2 mm), II (2 to < 5 mm), III (5 to < 10 mm), and IV (\geq 10 mm).....	20
Figure 2.2b	Boxplots for stemflow % for multi-leader (Group B) trees by rain depth class: I (< 2 mm), II (2 to < 5 mm), III (5 to < 10 mm), and IV (\geq 10 mm).....	21
Figure 2.2c	Boxplots for funneling ratio for single-leader (Group A) trees by rain depth class: I (< 2 mm), II (2 to < 5 mm), III (5 to < 10 mm), and IV (\geq 10 mm).....	22
Figure 2.2d	Boxplots for funneling ratio for multi-leader (Group B) trees by rain depth class: I (< 2 mm), II (2 to < 5 mm), III (5 to < 10 mm), and IV (\geq 10 mm).....	23
Figure 3.1	Climograph for the Meteorological Service of Canada’s “Kamloops A*” climate station (50° 42' 08" N, 120° 26' 31" W) (1981–2010 normals; Environment Canada, 2014)	49
Figure 3.2.	Frequency of precipitation events by type and depth class	56
Figure 3.3	Comparison of stemflow volume (L) produced from rain events less than 3 mm by trees in full leaf (\blacktriangle) vs. leafless (\triangle) conditions.....	59
Figure 3.4	Graphs of measured <i>SF</i> generated from rain events (\bullet) and from snow–water equivalent (SWE) depths for snow (\circ) and mixed (\bullet) precipitation events.....	62
Figure 4.1	Range of stemflow colours observed for May 21–23, 2013 rain event (32.7 mm)	87

LIST OF FIGURES (cont'd)

APPENDICES

Figure B.1	Map showing location of study trees, the meteorological station, and manual rain gauges within McArthur Island Park on the north shore of the Thompson River. The inset shows Kamloops in the context of British Columbia and the Pacific Northwest	100
Figure B.2	Aerial view of McArthur Island Park taken from the northwest.....	101
Figure B.3	Meteorological station complete with tipping bucket rain gauge (middle) and separate manual rain gauge (left).....	101
Figure B.4	Stemflow collection system.....	102
Figure B.5	Screen capture of a portion of leafless canopy. Deduction of selected sky pixels from total pixels in Adobe Photoshop® CC yielded canopy cover (%) and wood cover (%).....	102
Figure B.6	Bark with measured bark relief index, <i>BRI</i> , values (from left to right) of 1.00, 1.20, and 1.43	103
Figure B.7	Project sign produced by the City of Kamloops and attached to large maps at key access points around the park	103
Video B.1	Pin oak	103
Video B.2	Silver maple.....	103
Video B.3	American beech	103
Video B.4	American beech (close-up).....	103

LIST OF TABLES

Table 2.1	Single-leader (Group A) and multi-leader (Group B) study trees listed in ascending order of diameter at breast height, <i>DBH</i> , with associated overall height, <i>H</i> , average canopy width, <i>CW</i> , and projected canopy area, <i>PCA</i>	18
Table 2.2	List of selected tree and canopy metrics indicating mean (range) values within Group A ($n = 20$) and Group B ($n = 17$)	19
Table 2.3	Multiple regression equations for stemflow percentages and funneling ratios as functions of tree morphological traits (all coefficients significant at $p \leq 0.05$), generated for single-leader (Group A, $n = 20$) and multi-leader trees (Group B, $n = 17$) in three rain depth classes	27
Table 3.1	Multiple regression equations for stemflow initiation thresholds (P''), flow rates post-initiation (Q_{SF}), and flow rates per unit projected canopy area ($Q_{SF} PCA^{-1}$, $L\ mm^{-1}\ m^{-2}$) as functions of tree morphological traits, generated for single-leader (Group A, $n = 20$) and multi-leader trees (Group B, $n = 17$)	57
Table 3.2	Summary of meteorological variables significantly ($p \leq 0.10$) related to stemflow volume during leaf-on (square), transitional (circle), and leaf-off (triangle) conditions per individual-tree regression equations presented in Tables A.6, A.7, and A.8.....	60
Table 3.3	Summary of means and standard deviations for canopy traits of trees grouped by whether or not each meteorological variable was significant ("occurred", $p \leq 0.10$) in the individual tree's stemflow volume regression equation (between-group differences analyzed via one-way ANOVA, $p \leq 0.10$).....	61

LIST OF TABLES (cont'd)

APPENDICES

Table A.1	Derived values for stemflow initiation threshold, P'' (mm), rate, Q_{SF} ($L\ mm^{-1}$), and rate per unit projected canopy area, $Q_{SF} PCA^{-1}$ ($L\ mm^{-1}\ m^{-2}$), along with measured values for an array of canopy traits for individual single-leader (Group A) study trees (see Glossary for definition of acronyms and units).....	91
Table A.2	Derived values for stemflow initiation threshold, P'' (mm), rate, Q_{SF} ($L\ mm^{-1}$), and rate per unit projected canopy area, $Q_{SF} PCA^{-1}$ ($L\ mm^{-1}\ m^{-2}$), along with measured values for an array of canopy traits for individual multi-leader (Group B) study trees (see Glossary for definition of acronyms and units).....	92
Table A.3	Regression coefficients for stemflow, SF , volume (L) as a function of rainfall depth, P (mm), for study trees in <i>leaf-on</i> condition.....	93
Table A.4	Regression coefficients for stemflow, SF , volume (L) as a function of rainfall depth, P (mm), and actual canopy cover, ACC (%) for study trees in <i>transitional</i> leaf condition	94
Table A.5	Regression coefficients for stemflow, SF , volume (L) as a function of rainfall depth, P (mm), for study trees in <i>leaf-off</i> condition	95
Table A.6	Multiple regression equations for stemflow, SF , volume (L) as a function of meteorological variables, generated for single-leader (Group A, $n = 20$) and multi-leader trees (Group B, $n = 17$) for n rain events during <i>leaf-on</i> condition	96
Table A.7	Multiple regression equations for stemflow, SF , volume (L) as a function of meteorological variables, generated for single-leader (Group A, $n = 20$) and multi-leader trees (Group B, $n = 17$) for rain events during <i>transitional leaf</i> condition.....	97
Table A.8	Multiple regression equations for stemflow, SF , volume (L) as a function of meteorological variables, generated for single-leader (Group A, $n = 20$) and multi-leader trees (Group B, $n = 17$) for rain events during <i>leaf-off</i> condition.....	98

GLOSSARY OF ACRONYMS

<i>AAF</i>	Average branch angle, full canopy average (deg. from horizontal)
<i>AAU</i>	Average branch angle, upper canopy average (deg. from horizontal)
<i>ACC</i>	Actual canopy cover during leaf transition (%)
<i>AIF</i>	Angle of branch intersection, full tree average (deg. from horizontal)
<i>AIU</i>	Angle of branch intersection, upper canopy average (deg. from horizontal)
<i>BA</i>	Basal area (cm ²) of trunk at breast height (1.3 m)
<i>BRI</i>	Bark relief index (dimensionless)
<i>B_n</i>	Branch count
<i>CC</i>	Canopy cover (%)
<i>CH</i>	Canopy height (m)
<i>CW</i>	Canopy width (m)
<i>D_B</i>	Total duration of rain-free within-event breaks of ≥ 30 minutes (h)
<i>DBH</i>	Diameter at breast height (cm), measured at 1.3 m height
<i>D_R</i>	Total duration of rain (not including breaks) (h)
<i>FD</i>	Frequency of discontinuity in branch drainage (dimensionless)
<i>FR</i>	Funneling ratio, the ratio of stemflow volume at the base of a tree to the volume of incident rain that would have accumulated in a gauge with an opening area equal to the tree's basal area (dimensionless)
<i>H</i>	Tree height (m)
<i>HWR</i>	Height-to-width ratio of canopy (dimensionless)
<i>I_c</i>	Canopy interception loss, the proportion of intercepted precipitation that is stored on canopy surfaces and evaporates during or shortly after the event ends
<i>I_{max5}</i>	Five-minute maximum rainfall intensity (mm h ⁻¹)
<i>I_{wt5}</i>	Five-minute weighted average rainfall intensity (mm h ⁻¹)
<i>L_n</i>	Leader count

GLOSSARY OF ACRONYMS (cont'd)

<i>MIP</i>	McArthur Island Park (study site)
<i>MLS</i>	Median leaf size (cm ²)
<i>P</i>	Depth of precipitation (rain or snow-water equivalent) (mm)
<i>P''</i>	Threshold rain depth (mm) required to initiate stemflow
<i>PCA</i>	Projected canopy area (m ²), the area of foliated canopy extending to the dripline and including within-canopy gaps
<i>P_{inc}</i>	Rainfall inclination angle (deg. from vertical)
<i>PWA</i>	Projected wood area (m ²), the product of <i>PCA</i> and percent wood cover
<i>Q_{SF}</i>	Flow rate (L mm ⁻¹) once threshold depth has been satisfied
<i>Q_{SF} PCA⁻¹</i>	Flow rate per m ² of projected canopy area (L mm ⁻¹ m ⁻²)
<i>SF</i>	Stemflow, the proportion of intercepted precipitation channeled through a tree canopy to the base of the trunk
<i>SF%</i>	Stemflow volume as a percentage of the total volume of precipitation incident on a canopy area
<i>TBRG</i>	Tipping bucket rain gauge
<i>TF</i>	Throughfall, the proportion of precipitation that either passes through gaps in a tree's canopy or drips from woody or leafy parts
<i>Vol_C</i>	Canopy volume (m ³)
<i>Vol_W</i>	Wood volume (m ³)
<i>VPD</i>	Vapour pressure deficit (kPa)
<i>WC</i>	Wood cover (%)
<i>W_{wt5}</i>	Five-minute weighted average wind speed (m s ⁻¹)

ACKNOWLEDGEMENTS

For their generous advisory, logistical, and/or financial support, I thank:

- Dr. Darryl Carlyle-Moses, my valued and fully engaged supervisor;
- Advisory Committee members Tony Bradwell (Urban Systems), Dr. Sharon Brewer (TRU), Dr. Lauch Fraser (TRU), and Dr. Valentin Schaefer (University of Victoria);
- TRU faculty Dr. John Church, Dr. Kingsley Donkor, Dr. Nancy Flood, Dr. Tom Dickinson, Dr. Will Garrett-Petts, Dr. John Karakatsoulis, Dr. Walt Klenner, Dr. Shane Rollans, Jacque Sorensen, Dr. Joanne Rosvick, and Peggy-Jo Broad;
- Dr. Del Levia and Dr. David Legates (University of Delaware);
- Our dedicated Research Assistants Kyle Bondarchuk, Scott Borden, Allison James, Stefanie McBride, Megan Osmond-Jones, Will Plommer, Andreas Porman, Jen Powers, and Nikki Willier;
- Volunteers Margaret Graham (for exceptional contribution) as well as Beth and Dennis Andrucson, Shannon Gadsby, Janis Goad, Michelle Gunnlaugson, Alexis Karakatsoulis, Marguerite Machell, Chris McCuaig, Andy Raniseth, and Mandy Schmidt;
- The City of Kamloops' Greg Houghton, a champion throughout, Shawn Cook, Mike de Cicco, Jim Hiebert, Barry Manderson, Garrett Lacey, and Joe Vetere as well as Paul de Zeeuw, Ken Studer, Lisa Hodgkiss, and Joe Luison;
- TRU staff Lincoln Smith and Jerri-Lynne Cameron, Caroline Whitelaw, Johanna Norman, Primo Podorieszach, and Laurel Wale;
- The Kamloops Naturalist Club, especially Jean Crowe, Paul Johansen, and Ken Lipinski, and the Big Little Science Centre's Susan Hammond and Gord Stewart;
- Ray Visser, for mentoring and encouragement;
- The Partnership for Water Sustainability in BC, especially Kim Stephens and Dr. Charles Rowney;
- Environment Canada's Jim Steele (retired);
- Norman and Diana Kopek, hosts of our weather station;
- McArthur Island Lawn Bowling Club for accommodating our equipment; and
- Royal Canadian Mounted Police, Kamloops Detachment, for eyes on the site.

Every dollar received was precious, and allowed us to focus on the project without financial constraint. Thanks to: Golder Associates and the Natural Sciences and Engineering Research Council of Canada (Industrial Post-graduate Scholarship); the Real Estate Foundation of British Columbia; TD Friends of the Environment Foundation; and the Kamloops Foundation.

I thank my many faithful friends—especially Shelley Church, Shannon Gadsby, and Chris McCuaig—and my deeply appreciated family: Roz Isaac, Robyn Brandt, Edward and Janet Taylor, and the resourceful father-son team of Shane and Anthony Schooling.

CHAPTER 1 INTRODUCTION

1.1 URBAN HYDROLOGY CONTEXT

In response to the ecological and socio-economic issues associated with ongoing urbanization, policy makers, resource managers, and urban designers (among others) are exploring ways to preserve, enhance, construct, and maintain “green infrastructure.” For example, urban vegetation can play an important role in rainwater capture and detention as well as filtration of stormwater (Girling and Kellett, 2005). In a study looking at five cities in the United States, McPherson et al. (2005) estimated that the value of benefits per urban tree ranged from \$31 to \$89 USD (net benefit \$1.37 to \$3.09 USD per dollar invested in management annually). This reflected energy savings, atmospheric CO₂ reductions, air-quality benefits, aesthetics and property-value enhancements, and stormwater-runoff reductions. Applied to the City of Kamloops, British Columbia (population ~100,000), which manages over 15,000 trees on public land, this yields an estimated total annual benefit ranging from \$434,000 to \$1.25 million USD. Like many municipalities, the City of Kamloops (2010) has concerns about flooding and erosion; water quality, including quality of stormwater which is not treated prior to entering watercourses; expansion of impervious surfaces; and the cost of new and upgraded stormwater infrastructure. Site- and neighbourhood-level stormwater best management practices are being implemented in new developments. In recognition of increased percentages of impervious surfaces associated with urban and suburban development, stormwater managers have identified source controls as one strategy to minimize water quantity- and quality-related impacts on nearby ecosystems (Xiao et al., 2007).

1.2 TREE CANOPY PROCESSES

Trees are a potential source control (i.e., via canopy interception), but species that effectively funnel rainfall to the base of their trunks as stemflow, *SF*, may contribute

concentrated input to the terrestrial hydrological cycle and soil chemistry (e.g., Levia and Herwitz, 2005). Interception loss, I_c (direct evaporation from canopies) and throughfall, TF (whereby rain falls through gaps in the canopy or drips from leaves and branches), are the other components into which incident rainfall is partitioned (Crockford and Richardson, 2000). Trees can contribute to soil moisture and groundwater recharge (Návar, 2011; Tanaka, 2011), but in areas of soil instability, compaction, or paving, SF can exacerbate the water quality and quantity issues associated with urban or suburban runoff. A better understanding of SF processes in urban environments is needed as the basis of planning, design, and management of urban forests.

1.3 STEMFLOW IN CONTEXT

Globally, SF has been studied far less than TF , likely because percentage-wise it is a relatively small proportion of incident rain (typically 3–10 % vs. 70–80 % for TF in broadleaved deciduous forests). Of the growing number of studies published, most are at the forest-stand scale in rural or agricultural contexts. Over the past decade, a few studies have focused on urban situations (e.g., Xiao and McPherson, 2011; Livesley et al., 2014), single-tree processes (e.g., David et al., 2006; Guevara-Escobar et al., 2007; Levia et al., 2013), meteorological effects (e.g., Van Stan et al., 2014), and seasonal influences (e.g., Levia, 2004; Staelens et al., 2008) on SF . Given the high variability associated with SF yields, more work is needed to discern how urban tree canopy processes differ from those in forests, as they apparently do (Xiao et al., 2000; Asadian and Weiler, 2009).

1.4 FACTORS INFLUENCING STEMFLOW QUANTITY AND QUALITY

1.4.1 Tree Morphology

Stemflow yields, initiation thresholds, and rates are influenced by canopy traits that can differ greatly between species and between age/size classes within a given species. Based on characteristics identified by other researchers as important, this study explored

the effect of size metrics including diameter at breast height, tree height, and canopy width; bark relief; canopy and wood cover fraction; branching angles; and the number of branches and leaders present.

1.4.2 Storm Meteorology and Seasonal Effects

Canopy traits and meteorological variables interact in complex ways to influence *SF* initiation threshold rainfall depth, P'' , flow rates, and volumes. Research shows that rainfall depth and intensity, wind speed and direction, rainfall inclination angle, and vapour pressure deficit can influence *SF* processes (Van Stan et al., 2014). Exposure of an isolated canopy to the elements, whether in an urban or rural situation, changes the dynamics of interacting tree traits and storm meteorology, as does the absence of leaves in the dormant season (Staelens et al., 2008; Van Stan et al., 2014).

1.4.3 Stemflow Chemistry

Many of the trait and meteorological variables listed above play a role in *SF* chemistry, often reflecting residence time in the canopy (Levia and Herwitz, 2002; Staelens et al., 2007; André et al., 2008). In urban areas, airborne pollutants deposited on tree canopies can result in higher concentrations of pollutants as well as the nutrients commonly found in *SF* (Xiao and McPherson, 2011). Detailed examination of *SF* chemistry was beyond the main scope of this study, but results of an exploratory satellite investigation of *SF* chemistry for 12 trees over nine rainfall events may be published at a later date.

1.5 OBJECTIVES

To address gaps and priorities identified in the literature, this research aimed to:

1. analyze the contribution of diverse canopy traits to threshold rainfall depth and post-initiation rate of SF for isolated trees in an urban park in Kamloops, British Columbia, Canada;
2. for this same sample of trees, explore the influence of various storm meteorological characteristics on SF volume, SF as a percent of incident rainfall, and funneling ratios as well as relationships between meteorological and trait variables; and
3. based on synthesized results, provide guidelines to support application of these findings by urban foresters, landscape architects, stormwater managers, and allied professionals.

1.6 REFERENCES

- André, F., Jonard, M., Ponette, Q., 2008. Effects of biological and meteorological factors on stemflow chemistry within a temperate mixed oak-beech stand. *Science of the Total Environment* 393, 72–83.
- Asadian, Y., Weiler, M., 2009. A new approach in measuring rainfall interception by urban trees in coastal British Columbia. *Water Quality Research Journal of Canada* 44, 16–25.
- City of Kamloops, 2010. Sustainable Kamloops Plan: Information Package on Water (Final Version). City of Kamloops.
- Crockford, R.H., Richardson, D.P., 2000. Partitioning of rainfall into throughfall, stemflow and interception: Effect of forest type, ground cover and climate. *Hydrological Processes* 14, 2903–2920.
- David, T.S., Gash, J.H.C., Valente, F., Pereira, J.S., Ferreira, M.I., David, J.S., 2006. Rainfall interception by an isolated evergreen oak tree in a Mediterranean savannah. *Hydrological Processes* 20, 2713–2726.
- Girling, C., Kellett, R., 2005. *Skinny Streets and Green Neighbourhoods*. Island Press, Washington, DC.
- Guevara-Escobar, A., González-Sosa, E., Véliz-Chávez, C., Ventura-Ramos, E., Ramos-Salinas, M., 2007. Rainfall interception and distribution patterns of gross precipitation around an isolated *Ficus benjamina* tree in an urban area. *Journal of Hydrology* 333, 532–541.
- Levia, D.F., 2004. Differential winter stemflow generation under contrasting storm conditions in a southern New England broad-leaved deciduous forest. *Hydrological Processes* 18, 1105–1112.
- Levia, D.F., Herwitz, S.R., 2002. Winter chemical leaching from deciduous tree branches as a function of branch inclination angle in central Massachusetts. *Hydrological Processes* 16, 2867–2879.
- Levia, D.F., Herwitz, S.R., 2005. Interspecific variation of bark water storage capacity of three deciduous tree species in relation to stemflow yield and solute flux to forest soils. *Catena* 64, 117–137.
- Levia, D.F., Michalzik, B., Nätke, K., Bischoff, S., Richter, S., Legates, D.R., 2013. Differential stemflow yield from European beech saplings: The role of individual canopy structure metrics. *Hydrological Processes* 2–9.
- Livesley, S.J., Baudinette, B., Glover, D., 2014. Rainfall interception and stem flow by eucalypt street trees – The impacts of canopy density and bark type. *Urban Forestry & Urban Greening* 13, 192–197.

- McPherson, G., Simpson, J., Peper, P., Maco, S., Xiao, Q., 2005. Municipal forest benefits and costs in five US cities. *Journal of Forestry* 103, 411–416.
- Návar, J., 2011. Stemflow variation in Mexico's northeastern forest communities: Its contribution to soil moisture content and aquifer recharge. *Journal of Hydrology* 408, 35–42.
- Staelens, J., De Schrijver, A., Verheyen, K., 2007. Seasonal variation in throughfall and stemflow chemistry beneath a European beech (*Fagus sylvatica*) tree in relation to canopy phenology. *Canadian Journal of Forest Research* 37, 1359–1372.
- Staelens, J., De Schrijver, A., Verheyen, K., Verhoest, N.E.C., 2008. Rainfall partitioning into throughfall, stemflow, and interception within a single beech (*Fagus sylvatica* L.) canopy: Influence of foliation, rain event characteristics, and meteorology. *Hydrological Processes* 22, 33–45.
- Tanaka, T., 2011. Effects of the canopy hydrologic flux on groundwater, in: Levia, Delphis F., Carlyle-Moses, D., Tanaka, T. (Eds.), *Forest Hydrology and Biochemistry: Synthesis of Past Research and Future Directions*. Springer, Dordrecht, pp. 499–518.
- Van Stan, J.T., Van Stan, J.H., Levia, D.F., 2014. Meteorological influences on stemflow generation across diameter size classes of two morphologically distinct deciduous species. *International Journal of Biometeorology* 1–11.
- Xiao, Q., McPherson, E., 2011. Rainfall interception of three trees in Oakland, California. *Urban Ecosystems* 14, 755–769.
- Xiao, Q., McPherson, E., Simpson, J., Ustin, S., 2007. Hydrologic processes at the urban residential scale. *Hydrological Processes* 21, 2174–2188.
- Xiao, Q., McPherson, E.G., Ustin, S.L., Grismer, M.E., Simpson, J.R., 2000. Winter rainfall interception by two mature open-grown trees in Davis, California. *Hydrological Processes* 14, 763–784.

CHAPTER 2

THE INFLUENCE OF RAINFALL DEPTH CLASS AND DECIDUOUS TREE TRAITS ON STEMFLOW PRODUCTION IN AN URBAN PARK

2.1 INTRODUCTION

Urban trees have been found to be associated with disservices, including maintenance costs, infrastructure damage, health problems (e.g., asthma), and light attenuation (Gorman, 2004; Lohr et al., 2004; Roy et al., 2012). However, trees in urban and suburban environments also provide an array of social, economic, health, and environmental services (Miller, 1997; Tyrväinen et al., 2005; Roy et al., 2012), and these benefits have been found to outweigh associated costs (Peper et al., 2007, 2008; Soares et al., 2011). Specifically, trees in urban areas increase aesthetics and property values (McPherson et al., 1999; Sander et al., 2010), enhance human health (Tzoulas et al., 2007), reduce noise and air pollution (Dwyer et al., 1992; McPherson et al., 1997; Nowak et al., 2006), diminish carbon dioxide concentrations (Liu and Li, 2012; Nowak et al., 2013), lessen energy costs (Akbari et al., 2001; Soares et al., 2011), provide wildlife habitat (Goddard et al., 2010; Stagoll et al., 2012), and decrease stormwater runoff (Sanders, 1986; Soares et al., 2011). The value of stormwater runoff diminution by urban trees and green spaces may not be inconsequential. Soares et al. (2011), for example, found that urban trees in Lisbon, Portugal captured and subsequently evaporated an average of 4.5 m³ of water annually from their crowns and this was equated to a benefit of \$48 USD per tree per year, or \$1.97 million USD annually when all trees in the city are considered. McPherson et al. (2011) suggest that 8 % of the total economic benefit (\$1.33 to \$1.95 billion USD) of the Million Trees Los Angeles initiative—a plan which would see an additional one million trees planted in that city over a 35-year period—would be derived from stormwater runoff reduction.

The decrease in stormwater runoff production by trees in the urban environment has been estimated from the volumetric importance of canopy interception loss (Soares

et al., 2011; Inkiläinen et al., 2013; Pothier and Millward, 2013). Canopy interception loss is the interception, storage, and subsequent evaporation of precipitation by tree crowns and accounts for 10–50 % of annual or season-long rainfall from natural forest systems (Carlyle-Moses and Gash, 2011). Although much less studied within the urban environment, the results available to date suggest that canopy interception loss from city trees is also appreciable and may even be greater than that from natural forests. For example, at the crown scale, Xiao and McPherson (2011) found that canopy interception loss in Oakland, California was 14.3 % of rainfall for an 8.8 m tall sweet gum (*Liquidambar styraciflua* L.) tree, 25.2 % for a 2.9 m tall lemon (*Citrus limon* (L.) Burm. f.) tree, and 27.0 % for a 13.5 m tall ginkgo (*Ginkgo biloba* L.) tree. Guevara-Escobar et al. (2007) concluded that crown-scale canopy interception loss from 19 storms totaling 152 mm was 59.5 % from a single 5.9 m tall weeping fig (*Ficus benjamina* L.) in Queretaro City, Mexico. Asadian and Weiler (2009) derived average interception loss values of 49.1% for three Douglas-fir (*Pseudotsuga menziesii* (Mirb.) Franco) and 60.9% for three western redcedar (*Thuja plicata* Donn ex. D. Don) individuals in North Vancouver, British Columbia for seven selected events. Enhanced canopy interception loss from individual urban trees compared to forested sites may be a consequence of the relatively large structural units (e.g., canopy volume) associated with open-grown canopies (Brooks et al., 2003; Asadian and Weiler, 2009), greater evaporation rates attributable to the urban heat island effect (Asadian and Weiler, 2009), and/or the enhanced influence of wind due to the canopies being isolated from one another rather than being sheltered as in a forest scenario (Xiao et al., 2000b; Asadian and Weiler, 2009; Inkiläinen et al., 2013).

Canopy interception loss is estimated indirectly by taking the difference between precipitation incident upon the canopy and the understory precipitation input to the ground below (Carlyle-Moses and Gash, 2011; Saito et al., 2013; Peng et al., 2014). Understory precipitation takes two forms: throughfall, *TF*, the proportion of precipitation that either passes through gaps in the canopy or drips from foliar and wood components of the canopy; and stemflow, *SF*, the fraction of precipitation that is intercepted by the

tree cover and subsequently flows down the tree bole to the base of the tree (Levia et al., 2011). Interception loss studies conducted within natural forests have often found that *TF* is the dominant volumetric understory rainfall input, with *SF* usually accounting for < 5 % of precipitation at the plot-scale or beyond (Zhongjie et al., 2010; Levia et al., 2011; Carlyle-Moses et al., 2014). However, the proportion of rainfall partitioned into *SF* has been found to greatly exceed 5 % in certain forests. Wei et al. (2005), for example, found that *SF* represented 15.5 % of growing-season rainfall from a Mongolian oak (*Quercus mongolica* Fisch. ex Turcz.) forest in northern China, while Ford and Deans (1978) found that *SF* accounted for 27 % of the 1639 mm annual rainfall input to a 14-year-old Sitka spruce (*Picea sitchensis* (Bong.) Carr.) plantation in southern Scotland. Stemflow studies conducted on individual trees in forest settings have also found relatively high proportions of rain being partitioned into *SF* (e.g., Johnson and Lehmann, 2006; Liang et al., 2009), with some values being as great as 64 % of rainfall on a crown-projection-area basis (Masukata et al., 1990). A review of the interception loss literature suggests that canopy interception loss studies conducted in urban systems typically do not measure *SF* and either consider this input to be negligible (e.g., Asadian and Weiler, 2009) or to be a small and fixed fraction of rainfall based on the results of studies in natural forests (Inkiläinen et al., 2013). However, the aforementioned findings of relatively high *SF* proportions from forests and lone trees in forests, as well as certain studies conducted on isolated trees in urban areas (e.g., Xiao et al., 2000b), suggest that large errors in interception loss estimates may result if *SF* is ignored or assumed to be a small portion of rainfall.

There is growing recognition of the hydrological and biogeochemical importance of *SF* in non-urban forests and plant communities (Levia et al., 2011; Frost and Levia, 2013). Stemflow in these environments has been found to 1) greatly increase soil moisture around and deep beneath the base of the tree or plant, creating a reservoir of water on which the tree or plant can draw in times of need, a phenomenon known as the “nursing effect” (Goodall, 1965; Li et al., 2008); 2) create “fertile islands” where soil nutrients are found in greater concentrations at the tree/plant base than in other areas

(Whitford et al., 1997; Li et al., 2008); 3) be an important point source of groundwater recharge (Tanaka et al., 1996; Taniguchi et al., 1996; Tanaka, 2011); 4) result in localized overland flow (Herwitz, 1986); and 5) even be responsible, at least in part, for the rapid stream response to rainfall inputs under certain conditions (Crabtree and Trudgill, 1985). The potential importance of *SF* in urbanized areas has received little study in either volumetric or biogeochemical terms, despite indications that pollutants concentrate in *SF* (Michopoulos, 2011; Xiao and McPherson, 2011). Given that *SF* is a concentrated point source of water rather than a diffuse source like *TF*, we suggest that *SF* may, in conjunction with canopy interception loss and when infiltration is promoted, serve a role in diverting precipitation from becoming stormwater runoff. Additionally, we suggest that *SF* may also be important from a management perspective because it may lessen tree irrigation water demand. Thus, study is required to determine the quantitative importance of *SF* and to assess the influence rain depth and tree traits have on *SF* production in urban environments so that the role of individual trees in stormwater mitigation in areas of differing rainfall regimes can be more fully understood.

The objective of this study was to determine if *SF* was an important component of the canopy water balance and/or an important point source of water at the base of deciduous trees under full-leaf conditions in an urban park. Specifically, we aimed to:

1. determine the relationship between tree-scale *SF* volume and event-scale rainfall depth;
2. derive the proportion (%) of rain partitioned into *SF* and the *SF* funneling ratios associated with these trees for differing rain depth classes (< 2 mm, 2 to < 5 mm, 5 to < 10 mm, and \geq 10 mm); and
3. define which tree traits influenced the proportion of rain partitioned into *SF* and the magnitudes of *SF* funneling ratios under the differing rain depth classes.

Meeting these objectives will, in part at least, inform stormwater managers and urban foresters of the potential quantitative importance of *SF* when deriving canopy

interception loss estimates and in determining if *SF* serves stormwater management and/or supplemental irrigation roles (Vico et al., 2014). Additionally, meeting the stated objectives will provide information regarding which tree traits and rainfall regimes influence *SF* production in the urban environment.

2.2 METHODS

2.2.1 Study Area

This study was conducted within McArthur Island Park (MIP) in the City of Kamloops, British Columbia, Canada (50° 41' 43" N, 120° 22' 38" W) at an elevation of 344 m a.m.s.l. (Figure B.1). McArthur Island Park is a 51-ha multi-use sport and leisure area bounded to the south by the Thompson River and on other sides by a slough (Figure B.2). Green space at MIP includes several tree stands, including fairly continuous tree and shrub cover in the riparian zone encircling the park. In the more manicured centre of the site, many trees are isolated, meaning that all trees had an unobstructed field of view at least 35° from vertical, centred where the lowest branch met the bole. Although coniferous tree species are present at MIP, including white spruce (*Picea glauca* (Moench.) Voss), most trees are deciduous, including cultivated species of maple (*Acer* spp.), oak (*Quercus* spp.), and ash (*Fraxinus* spp.).

Based on climate normals (1981–2010) for Environment Canada's "Kamloops A*" climate station, situated 4.4 km west-north-west of the study site at an elevation of 345 m a.m.s.l., mean annual temperature for this location is 9.3°C, while mean monthly temperatures range from –2.8°C in January to 21.5°C in July. Mean annual precipitation is 277.6 mm with approximately 224.3 mm (81%) falling as rain and the remainder as snow. Kamloops' mid-latitude, semi-arid steppe climate (BSk Köppen climate type) is modified to a moist, temperate climate (Cwb Köppen climate type) at the study site due to extensive irrigation in the spring and summer months that sustains tournament-standard turf and cultivated, non-native trees.

2.2.2 Precipitation and Stemflow Measurement

Precipitation and *SF* were measured on an event basis from June 12, 2012 to November 3, 2013. Rainfall depth, *P*, was measured using an Onset® tipping-bucket rain gauge (Model # S-RGB-M002) connected to an Onset® Hobo® U-30 USB data logger (Model # U30-NRC) (Figure B.3). The tipping bucket (resolution 0.2 mm tip⁻¹) was situated 1 m off the ground on private property immediately north of MIP.

Accompanying the tipping bucket rain gauge was a manually read polyethylene gauge (diameter 29 cm, depth 36 cm), again positioned at a height of 1 m. The tipping bucket and manually read rain gauge were between 80 and 770 m from the study trees. Eight other manually read gauges were placed within MIP resulting in gauge density of approximately 0.04 km² gauge⁻¹ and a maximum gauge-to-study-tree distance of approximately 215 m.

We collected *SF* using black corrugated polyethylene hose of two diameters: 3.2 cm for 32 trees and 3.8 cm for the five largest trees (Figure B.4). After removal of a lengthwise section of hose, the collar was wrapped twice around the tree at an angle sufficient to ensure flow and one edge was stapled to the trunk. The seam and staples were sealed with 100 % silicone to prevent leaks; collection collars were regularly inspected and repaired throughout the study. The outlet of each open-topped collar was inserted and secured with electrical tape to an intact length of hose which directed *SF* into a 17-L polyethylene pail set within a 114-L lidded polyethylene tote to provide overflow capacity; elastic cord securing PVC plastic over the lid prevented contamination of *SF* by rain, and two 4-L water-filled polyethylene jugs in each tote anchored the reservoir to prevent displacement by high winds.

2.2.3 Tree Selection and Trait Measurement and Derivation

Study trees were: i) deciduous trees in good condition; ii) trees representing a range of canopy characteristics; iii) trees of diverse sizes, but with a minimum diameter-at-breast-height, *DBH*, of 10 cm; and iv) “isolated” trees as defined above.

Basic Tree Size Metrics: Diameter at breast height (cm) was measured using a Lufkin[®] Metric Diameter Tape and tree height, H (m), was measured using a Suunto PM5/SPC clinometer. Dripline radius in eight directions was found using a periscope-style instrument with 5 x 5 dot grid in the viewfinder; the average of these was doubled to calculate average canopy width, CW (m). Areas were calculated using each cardinal-direction dripline radius, and averaged to yield projected canopy area, PCA (m²). Projected wood area, PWA (m²) was the product of PCA and percent wood cover (see below). Side-view leaf-on photographs, also used for side-area calculation (see below), were used to calculate canopy height, scaled in Photoshop[®] CC using an item of known dimension; canopy height-to-width ratio, HWR (dimensionless), was determined using canopy height and CW . To calculate canopy volume, Vol_C (m³), side-view leaf-on area (including gaps; see below) for the view corresponding to the chosen side-view leaf-off tracing was divided by CW to yield average canopy height; this was then multiplied by PCA to give volume. Wood volume, Vol_W (m³), was calculated in the same way.

Side Area Leaf and Side Area Wood: Side-view leaf-on and leaf-off photographs were taken from eight consistent directions at similar heights using a pole-mounted, remotely controlled GoPRO Hero3 camera (7MP resolution, medium field of view). The clearest pair of leaf-on and leaf-off photographs was traced by hand and scanned. Photoshop[®] CC was used to select canopy (leaf-on, including gaps) and wood (leaf-off) areas, and pixels were converted to m² using an item of known dimension in each photo.

Canopy Cover (CC) and Wood Cover (WC): Beneath-canopy skyward photographs of both leaf-on and leaf-off canopies were taken using a Nikon 7100D with lens set to 70 mm focal length mounted on an Optex[®] T25 tripod with level. Six photos were taken at a mount height of 0.3 m along transects extending in each cardinal direction at the following distances relative to the known dripline radius: 0.15 (adjacent to bole), 0.25, 0.5, 0.75, 0.875 (to reflect high variability at this distance), and 1.0 (dripline). Photoshop[®] CC was used to select either cover or open areas within the canopy (Figure B.5), yielding leaf-on CC (%) and leaf-off WC (%) values.

Leader and Branch Characteristics: To sample branch angles, we photographed each “feeder” branch greater than 20 mm diameter that intersected the leader judged to be most central and/or vertical. The number of sizeable secondary leaders was noted (and used to calculate total number of leaders, L_n , at the base of the canopy) and counts (but not angles) of branches intersecting secondary leaders were used to generate a total branch count (B_n) for the tree. Therefore, unless the tree had a single leader, the branch angles calculated are for a subset of feeder branches. Photographs were taken perpendicular to the initial direction of the branch and two angles were determined using ImageJ software: 1) angle of intersection of the branch and leader and 2) average (overall) angle from intersection to furthest extent of the branch (one or both of these could be negative). Canopies were divided into upper, mid-, and lower sections, and average intersection (upper, AIU ; mid, AIM ; and lower, AIL) and overall angles (upper, AAU ; mid, AAM ; and lower, AAL) were found for each section as well as for the full tree (intersection, AIF ; and average, AAF). In addition, the inner, mid, and outer third of each feeder branch was classified as either “continuous” (positive flow towards the bole) or “discontinuous” (flow towards the dripline); if an inner- or mid-canopy segment was discontinuous, so were all further segments of that branch, and if two of three segments drained away from the bole, the branch was given an overall “discontinuous” rating. For each tree, an overall frequency of discontinuous branch segments (FD) was calculated.

Bark Relief Index (BRI): We calculated a quantitative bark relief index using the ratio of the furrowed circumference of the tree to the surface (unfurrowed) circumference at breast height (1.3 m, or slightly higher or lower to avoid branches and deep scars) (Figure B.6). The surface circumference was measured using a flexible measuring tape, while the furrowed circumference was the length of a ribbon pushed into furrows and other surface features around the bole at that same height. This measure is based on the same principles and methods pioneered by Yarranton (1967) and Van Stan et al., (2010) to measure bark microrelief. Overall bark roughness reflects bark relief in conjunction with other characteristics (e.g., bark thickness, texture, and storage capacity; Levia and Herwitz, 2005; Van Stan and Levia, 2010) that were not quantified in this study.

Median Leaf Size (MLS): Samples of between 13 and 49 leaves were taken from each tree (representing a gradient from canopy edge to interior) and were sorted in order of size. The median leaf for each sample was scanned and its area calculated using Photoshop® CC to yield *MLS*.

2.2.4 Data Analysis

Using exploratory cluster analysis (K-means method; IBM® SPSS® Statistics Version 22, hereafter SPSS®) of 34 independent trait variables (not including L_n), the 37 study trees were assigned to clusters that corresponded to two general canopy morphologies: single-leader (main stem with feeder branches intersecting it) and multi-leader (two or more leaders converging at the base of the canopy, each of these intersected by feeder branches). Given observations that *SF* drains to and along the undersides of upright branches (e.g., Herwitz, 1987), it makes intuitive sense that *SF* production processes might differ in trees with single, vertical trunks vs. multiple major leaders. We therefore separated trees into Group A (single leader, $n = 20$) and Group B (multi-leader, $n = 17$) for analysis.

Two measures are commonly used to describe the magnitude and efficiency of *SF* concentration at the base of a tree. Stemflow volume as a percentage of rain incident on the entire *PCA* can be interpreted along with *TF* and interception loss in the context of canopy water balance (Rutter et al., 1975; Guevara-Escobar et al., 2007):

$$SF \% = \frac{SF}{P \cdot CPA}$$

where *SF* is in L, *P* is in mm, and *PCA* is in m². The second measure, *SF* funneling ratio, *FR* (Herwitz, 1986), is the ratio between *SF* volume collected at the base of the tree and the volume that would have accumulated in a gauge the same area as the trunk basal area, *BA* (m²):

$$FR = \frac{SF}{P \cdot BA}$$

Funneling ratio is independent of *PCA*, meaning that broad and narrow trees of similar *DBH* and *SF* with similar *FR* could have very different *SF %* values. For each of these measures of *SF* concentration, data was grouped into four rain-depth classes: I) < 2 mm, II) 2 to < 5 mm, III) 5 to < 10 mm, and IV) ≥ 10 mm. Differences within and between groups were analyzed in SPSS[®] using a one-way ANOVA with Tukey HSD post-hoc (Tukey, 1953; see Zar, 1984). Data was tested for outliers (Grubbs, 1950) as well as normality, and linearity of relationships between dependent and independent variables was assessed. Where justified to improve normality or linearity, one of the following transformations was applied: x^2 , x^3 , $\ln(x)$, x^{-1} , or \sqrt{x} . Stepwise-up multiple regression (Smith's Statistical Package, hereafter SSP) was then used to explore the influence of tree morphological traits for both *SF %* and *FR* for rain depth classes II, III, and IV (given the sparsity of data in class I). Prior to finalizing each regression equation, we confirmed that there was no unacceptable multicollinearity among independent variables (i.e., $r^2 < 0.64$; Hair et al., 1998).

2.3 RESULTS

2.3.1 Precipitation

A total of 327.9 mm of rain fell during 86 events recorded between June 12, 2012 and November 2, 2013, of which over 80 % were < 5 mm, consistent with climate normals for Kamloops (Figure 2.1).

2.3.2 Study Tree Characteristics

The 37 isolated trees selected for this study represented 21 commonly used ornamental species of diverse habits and sizes with *DBH* ranging from 10.2–68.7 cm (Table 2.1). Mean measured or calculated values for the trait variables described above are presented in Table 2.2 along with the range of each value for single- and multi-leader trees. These 37 trees represent almost all isolated deciduous trees in the park; by

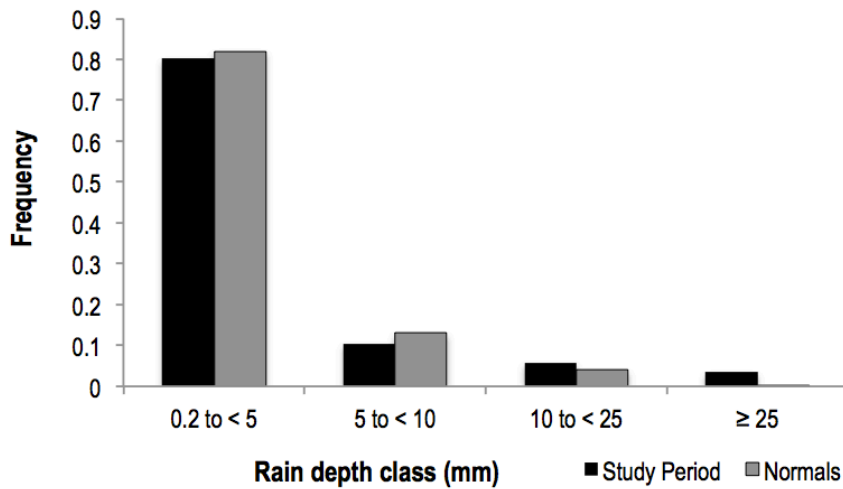


Figure 2.1. Rain depth frequency distribution during the study period compared to Canadian Climate Normals 1981–2010 for station Kamloops A* (Environment Canada, 2014).

calculating rainfall inclination angles and wind directions (section 3.2.4), we verified that rain throughout the research period fell unobstructed on study tree canopies.

2.3.3 Stemflow for Individual Trees as a Percentage of Rainfall

Boxplots of both *SF* % and *FR* data are presented in Figures 2.2a–d. Grubbs’ test was used to verify that none of the mean *SF* % or *FR* values were significant ($p \leq 0.05$) outliers within each tree group for each rain class (Grubbs, 1950).

The percentage of rainfall diverted by the canopies of the 37 study trees into *SF* was largely negligible for events < 2 mm, with 10 of the 20 single-leader and 13 of the 17 multi-leader trees generating no more than < 0.1 % *SF* for any event in this small rain depth class. The smallest rain depth to generate $SF \geq 0.1$ % from single-leader trees was 1.0 mm, which produced 1.5 % *SF* from tree A-1. With the exception of A-1, single-leader trees that produced *SF* did so only during the second largest (1.4 mm) and/or largest (1.6 mm) rain event(s) in the rain depth class. Mean *SF* % for *SF*-producing single-leader trees for these two rainfall events was 0.5 % (SD = 0.4 %) ranging from

Table 2.1. Single-leader (Group A) and multi-leader (Group B) study trees listed in ascending order of diameter at breast height, *DBH*, with associated overall height, *H*, average canopy width, *CW*, and projected canopy area, *PCA*.

ID	Latin name	Common name	<i>DBH</i> (cm)	<i>H</i> (m)	<i>CW</i> (m)	<i>PCA</i> (m ²)
A-1	<i>Cercidiphyllum japonicum</i>	Katsuratree	10.2	5.7	3.7	11.1
A-2	<i>Cercis canadensis</i>	Eastern Redbud	10.5	4.9	4.0	13.5
A-3	<i>Quercus rubra</i>	Red Oak	11.4	6.3	5.1	17.6
A-4	<i>Prunus virginiana</i> 'Shubert'	Shubert Chokecherry	12.7	7.2	4.5	19.5
A-5	<i>Robinia pseudoacacia</i> 'Purple Rain'	Purple Rain Bl. Locust	14.6	7.9	6.9	34.1
A-6	<i>Gleditsia triacanthos</i>	Honeylocust	15.1	9.9	6.4	46.1
A-7	<i>Acer saccharinum</i>	Silver Maple	15.9	9.6	5.1	20.2
A-8	<i>Tilia cordata</i>	Littleleaf Linden	17.2	8.1	4.6	17.5
A-9	<i>Fraxinus pennsylvanica</i>	Green Ash	19.0	10.5	6.0	27.3
A-10	<i>Acer rubrum</i> columnar	Columnar Red Maple	19.0	11.3	5.2	22.4
A-11	<i>Fraxinus pennsylvanica</i>	Green Ash	19.7	10.6	5.6	25.5
A-12	<i>Quercus rubra</i>	Red Oak	20.3	10.1	7.3	44.0
A-13	<i>Quercus macrocarpa</i>	Bur Oak	21.5	9.8	7.5	37.2
A-14	<i>Quercus robur</i> columnar	English Columnar Oak	23.5	14.6	2.8	6.3
A-15	<i>Acer x freemanii</i> 'Armstrong'	Armstrong Freeman Maple	24.1	13.1	3.5	11.1
A-16	<i>Aesculus hippocastanum</i>	Horsechestnut	31.0	10.8	5.8	27.7
A-17	<i>Prunus padus</i> var. <i>commutata</i>	Mayday Cherry	34.3	9.6	8.5	50.3
A-18	<i>Quercus palustris</i>	Pin Oak	43.0	14.1	13.6	149.1
A-19	<i>Quercus palustris</i>	Pin Oak	52.7	13.8	13.7	150.6
A-20	<i>Quercus palustris</i>	Pin Oak	60.7	24.7	14.2	164.8
B-1	<i>Salix babylonica</i>	Weeping Willow	15.2	8.1	5.9	28.9
B-2	<i>Sorbus quercifolia</i>	Oak-leaf Mountain Ash	18.3	6.3	4.4	15.9
B-3	<i>Prunus virginiana</i> 'Shubert'	Shubert Chokecherry	18.8	8.5	6.6	35.2
B-4	<i>Gleditsia triacanthos</i> 'Sunburst'	Sunburst Honeylocust	21.0	8.7	7.8	52.5
B-5	<i>Acer platanoides</i>	Norway Maple	24.6	8.7	8.1	54.2
B-6	<i>Acer platanoides</i> 'Crimson King'	Crimson King Maple	26.0	8.9	5.3	23.4
B-7	<i>Fraxinus pennsylvanica</i>	Green Ash	28.9	12.6	7.5	43.5
B-8	<i>Acer platanoides</i>	Norway Maple	36.9	10.3	10.1	84.7
B-9	<i>Fagus grandifolia</i>	American Beech	38.8	11.0	9.3	65.8
B-10	<i>Aesculus hippocastanum</i>	Horsechestnut	41.3	8.3	7.5	46.5
B-11	<i>Acer platanoides</i> 'Crimson King'	Crimson King Maple	43.0	12.0	10.7	99.7
B-12	<i>Tilia cordata</i>	Littleleaf Linden	46.0	11.2	7.6	43.5
B-13	<i>Fraxinus pennsylvanica</i>	Green Ash	51.8	13.0	14.2	163.8
B-14	<i>Robinia pseudoacacia</i>	Black Locust	54.3	10.5	11.2	103.0
B-15	<i>Catalpa speciosa</i>	Northern Catalpa	58.0	14.2	9.5	79.5
B-16	<i>Eleagnus angustifolia</i>	Russian Olive	66.8	16.8	15.1	206.6
B-17	<i>Acer saccharinum</i>	Silver Maple	68.7	18.6	16.7	214.5

Table 2.2. List of selected tree and canopy metrics indicating mean (range) values within Group A ($n = 20$) and Group B ($n = 17$).

Tree Trait		Group A (single-leader)		Group B (multi-leader)	
		Mean	Range	Mean	Range
Basic Tree	<i>DBH</i> (cm)	23.8	(10.2–60.7)	38.7	(15.2–68.7)
Size Metrics	Tree Height, <i>H</i> (m)	10.6	(4.9–24.7)	11.1	(6.3–18.6)
Canopy Dimension Metrics	Canopy width, <i>CW</i> (m)	6.7	(2.8–14.2)	9.3	(4.4–16.7)
	Canopy height-to-width ratio, <i>HWR</i>	1.49	(0.79–4.13)	1.12	(0.71–1.47)
	Projected canopy area, <i>PCA</i> (m ²)	44.8	(6.3–164.8)	80.1	(15.9–214.5)
	Projected wood area, <i>PWA</i> (m ²)	11.3	(1.4–54.9)	34.1	(2.6–109.4)
	Canopy volume, <i>Vol_C</i> (m ³)	371.2	(28.3–1801.2)	803.6	(56.9–3872.0)
	Wood volume, <i>Vol_W</i> (m ³)	28.4	(1.0–183.5)	120.8	(3.1–551.4)
Cover Metrics	Canopy cover, <i>CC</i> (%)	89.3	(74.9–99.6)	92.4	(80.7–98.8)
	Wood cover, <i>WC</i> (%)	23.1	(10.5–41.0)	37.8	(14.7–68.4)
Branch and Bark Metrics	Branch count, <i>B_n</i> (no. branches)	28.2	(12–52)	59.3	(27–85)
	Leader count, <i>L_n</i> (no. leaders)	1.0	(1–1)	3.6	(2–6)
	Intersection angle, full tree avg, <i>AIF</i> (°)	43.6	(14.3–68.1)	44.8	(25.0–60.2)
	Intersection angle, upper 1/3 avg, <i>AIU</i> (°)	48.0	(20.4–75.1)	46.0	(22.6–58.8)
	Average angle, full tree avg, <i>AAF</i> (°)	43.3	(18.2–77.0)	41.3	(6.5–66.2)
	Average angle, upper 1/3 avg, <i>AAU</i> (°)	49.5	(13.5–83.0)	43.8	(-3.3–66.2)
	Frequency of discontinuity, full tree, <i>FD</i>	0.17	(0.00–0.48)	0.18	(0.00–0.59)
	Bark relief index, <i>BRI</i> (ratio)	1.08	(1.00–1.23)	1.18	(1.00–1.43)
Leaf Size	Median leaf size, <i>MLS</i> (cm ²)	26.8	(1.4–92.2)	23.2	(1.8–71.6)

0.2 % for A-5, A-7, and A-11 to 1.4 % for A-1. The smallest single rain depth to generate $SF > 0.1$ % from multi-leader trees was 0.9 mm, for which SF from trees B-3 and B-9 was 1.0 % and 0.9 %, respectively. The other two multi-leader trees to generate SF in this rain depth class (B-2 and B-5) did so for only the largest rain event (1.6 mm), with both trees partitioning 1.0 % of rain into SF . Stemflow accounted for 2.3 % of this 1.6 mm rain for trees B-3 and B-9.

With the exception of A-14 and A-15, no significant ($p \leq 0.05$) difference in mean SF % was found among single-leader trees across the three rain depth classes greater than

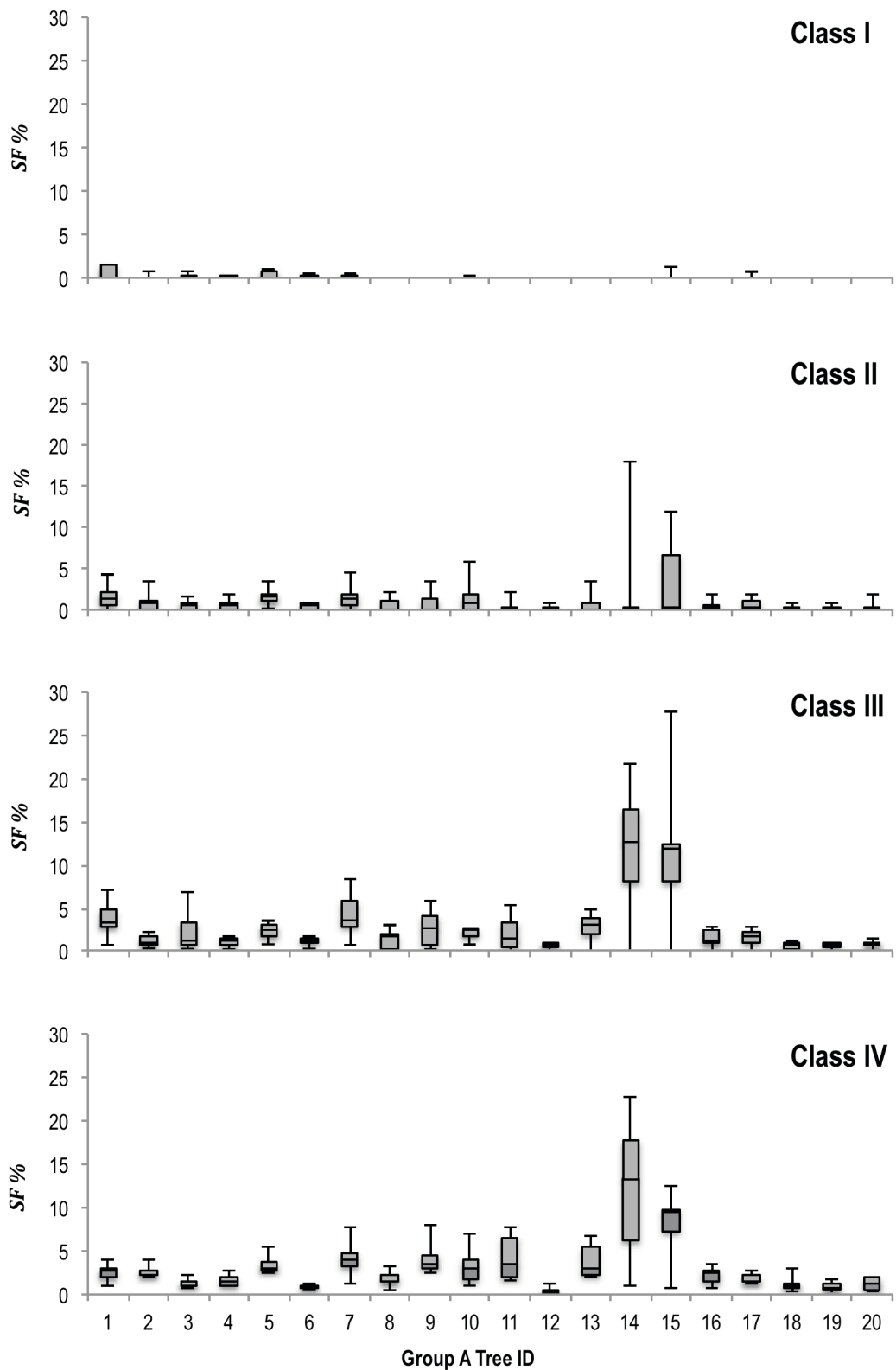


Figure 2.2a. Boxplots for stemflow % for single-leader (Group A) trees by rain depth class: I (< 2 mm), II (2 to < 5 mm), III (5 to < 10 mm), and IV (≥ 10 mm).

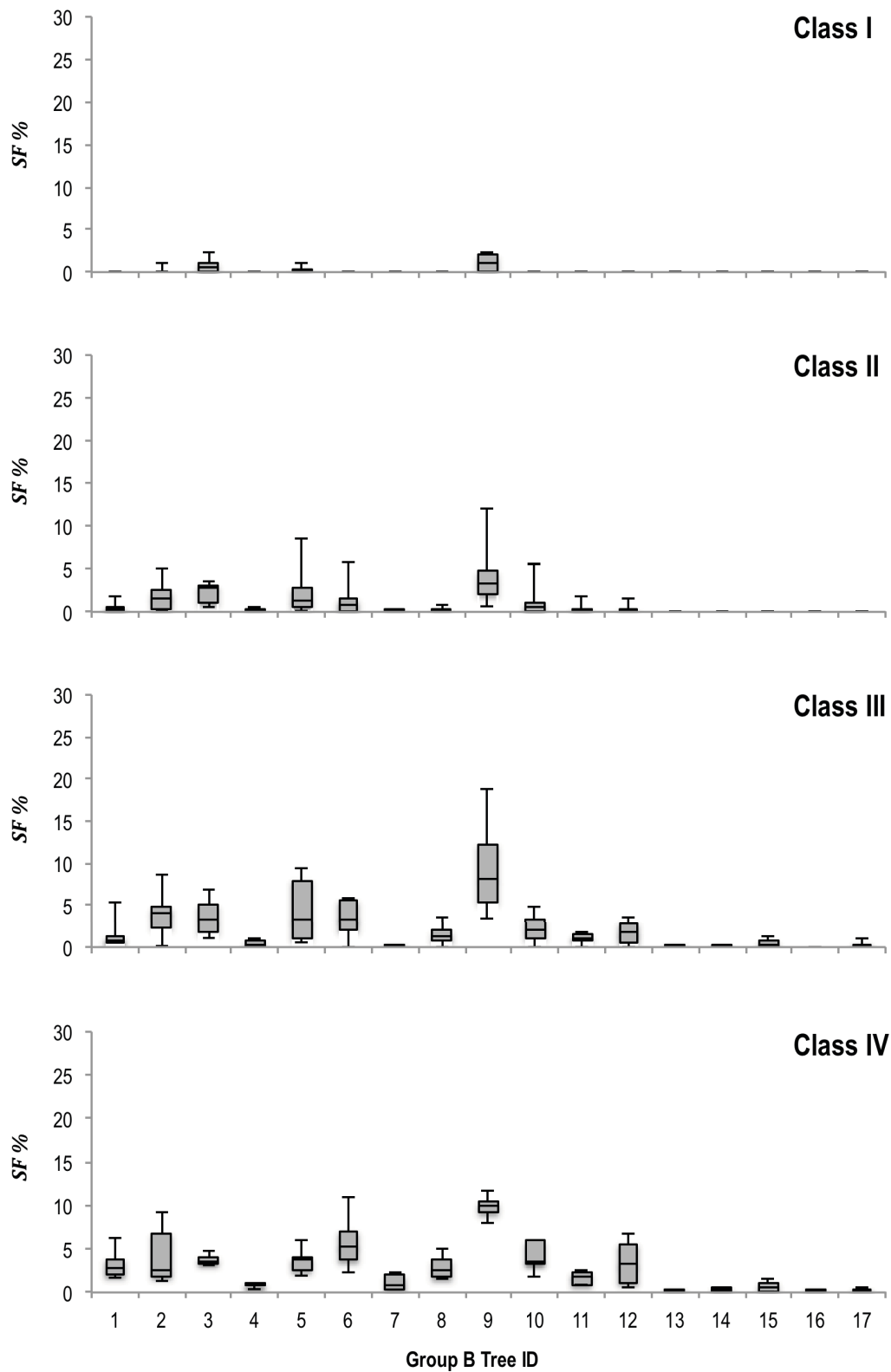


Figure 2.2b. Boxplots for stemflow % for multi-leader (Group B) trees by rain depth class: I (< 2 mm), II (2 to < 5 mm), III (5 to < 10 mm), and IV (\geq 10 mm).

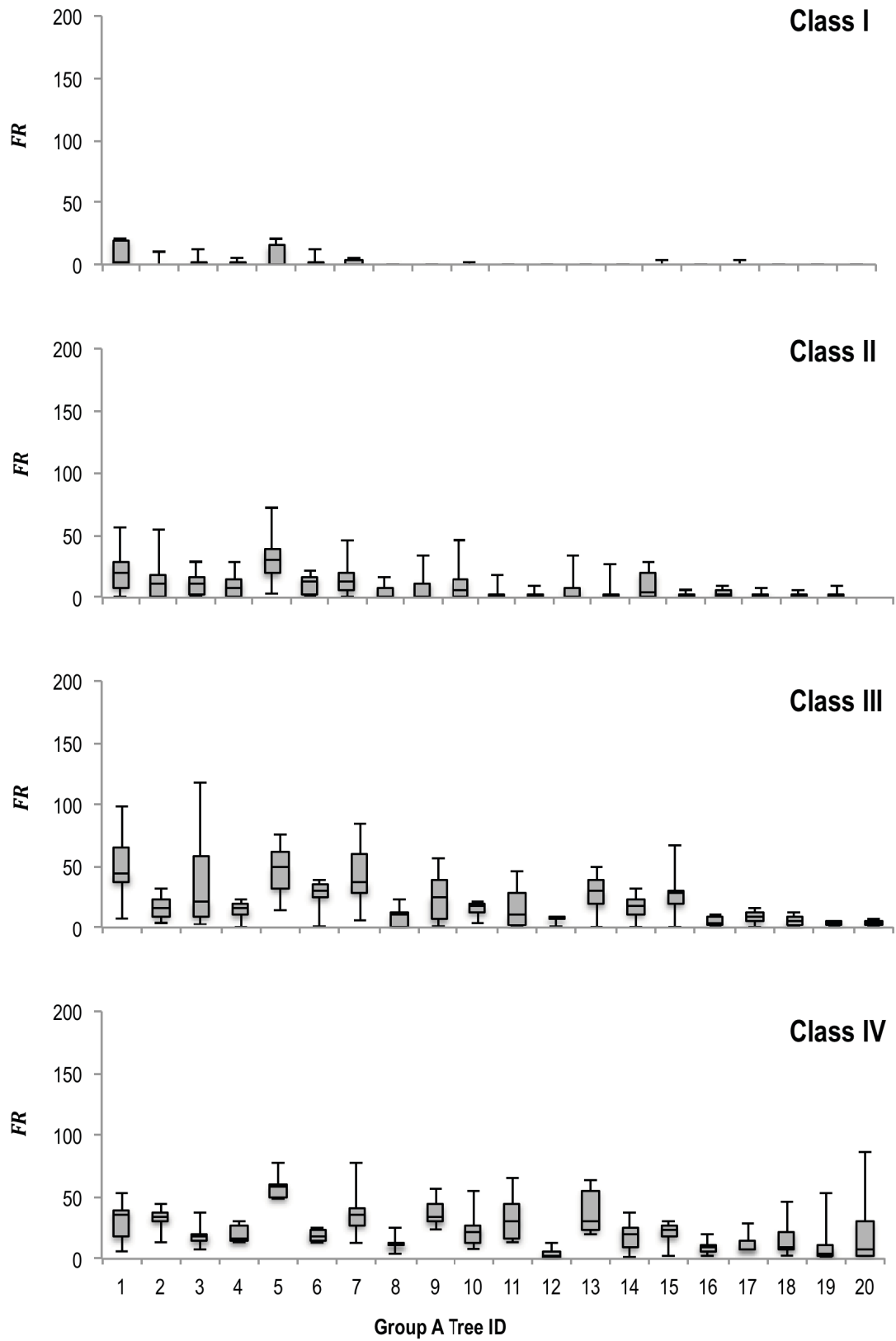


Figure 2.2c. Boxplots for funneling ratio for single-leader (Group A) trees by rain depth class: I (< 2 mm), II (2 to < 5 mm), III (5 to < 10 mm), and IV (≥ 10 mm).

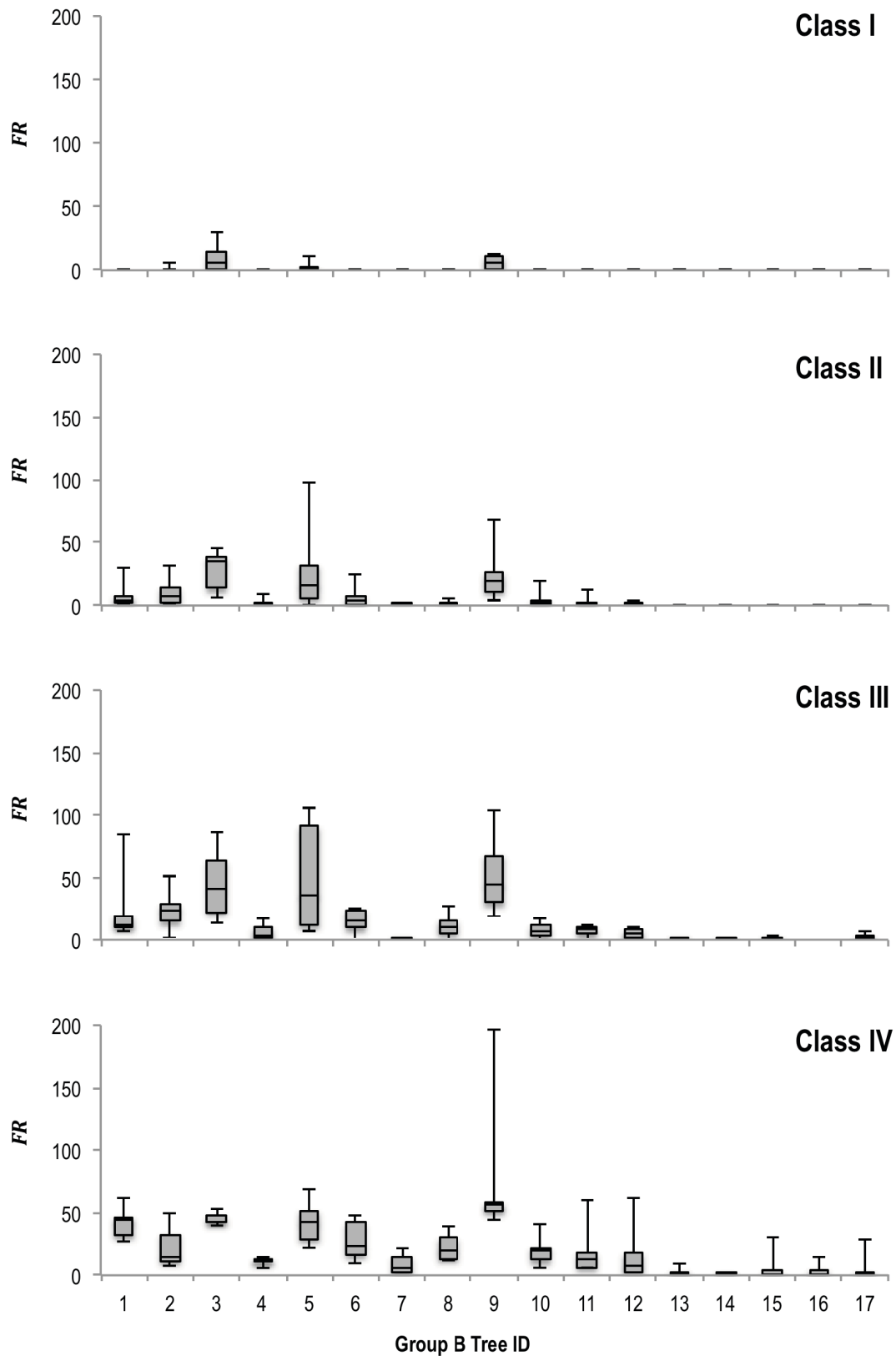


Figure 2.2d. Boxplots for funneling ratio for multi-leader (Group B) trees by rain depth class: I (< 2 mm), II (2 to < 5 mm), III (5 to < 10 mm), and IV (≥ 10 mm).

< 2 mm. Mean average rain depth class *SF* for these 18 trees was $0.7 \pm 0.5 \%$, $1.7 \pm 1.1 \%$, and $2.3 \pm 1.3 \%$ for the 2 to < 5 mm, 5 to < 10 mm, and ≥ 10 mm classes, respectively. Although mean *SF* % for A-14 for the 2 to < 5 mm class ($2.5 \pm 5.9 \%$) was not significantly ($p \leq 0.05$) greater than for other single-leader trees, it was for all but three trees for the 5 to < 10 mm class ($11.8 \pm 9.1 \%$), and for all trees with the exception of A-15 for the ≥ 10 mm class ($12.3 \pm 8.4 \%$). A-15 partitioned a significantly ($p \leq 0.05$) greater percentage of rainfall into *SF* ($3.6 \pm 4.8 \%$) than six other single-leader trees for the 2 to < 5 mm rain depth class, all trees with the exception of A-14 for the 5 to < 10 mm class ($12.0 \pm 10.1 \%$), and 11 of the 19 other single-leader trees for the ≥ 10 mm rain depth class ($8.1 \pm 4.1 \%$). At the individual rain-event scale, *SF* % was found to be quite large for A-14 and A-15 for certain events. For example, A-14 generated 18.0, 21.7, and 22.8 % *SF* for 22.4, 8.8, and 25.6 mm rainfall events, respectively, while A-15 generated 12.3, 12.5, and 27.9 % *SF* for 7.8, 32.7, and 5.2 mm events, respectively. Stemflow % was also found to be highly variable for A-14 and A-15, even for rainfalls of similar depths. A-14, for example, although producing 13.1 % *SF* for a 4.6 mm rain event, did not partition any rainfall to *SF* for a 5.6 mm event, while A-15 partitioned 11.1 % of a 2.9 mm rain event into *SF*, but none of a 3.1 or 3.2 mm rainfall.

Under the 2 to < 5 mm rain depth class, multi-leader trees B-3 ($2.3 \pm 1.2 \%$), B-5 ($2.2 \pm 2.5 \%$), and B-9 ($4.3 \pm 3.6 \%$) had significantly ($p \leq 0.05$) greater mean *SF* % than 4, 10, and 14 other multi-leader trees, respectively. Excluding B-3, B-5, and B-9, average mean *SF* % for the 2 to < 5 mm rain depth class was $0.4 \pm 0.5 \%$, ranging from $< 0.1 \pm < 0.1 \%$ for the five largest *DBH* trees in this tree group (B-13–B-17) to $1.4 \pm 1.9 \%$ for B-6. For the 5 to < 10 mm rain depth class, *SF* % ($9.6 \pm 6.7 \%$) for B-9 was significantly ($p \leq 0.05$) greater than for 13 other multi-leader trees whose average mean *SF* % was $1.1 \pm 1.1 \%$. Mean *SF* % values for trees B-2 ($4.0 \pm 3.2 \%$), B-3 ($3.6 \pm 2.6 \%$), and B-5 ($4.4 \pm 4.0 \%$) were not significantly ($p \leq 0.05$) greater than these 13 trees, nor were they significantly smaller than B-9 *SF* %. In the largest rain depth class, ≥ 10 mm, B-9 *SF* % was significantly ($p \leq 0.05$) larger than all other multi-leader trees ($9.9 \pm 1.4 \%$), while B-6 partitioned a greater percentage ($p \leq 0.05$) of rainfall into

SF (5.9 ± 3.4 %) than eight other trees in this group, including B-4 (0.7 ± 0.2 %), B-7 (1.2 ± 0.7 %), B-11 (1.7 ± 0.8 %), and the four largest *DBH* trees in this group (B-14–B-17) whose *SF* % values ranged from 0.1 ± 0.1 % for B-16 to 0.7 ± 0.6 % for B-15. In addition to the aforementioned statistically differing *SF* % values for this largest rain depth class, B-13 *SF* % (0.2 ± 0.1 %) was also found to be significantly ($p \leq 0.05$) lower than that of B-2 (4.3 ± 3.5 %), B-3 (3.8 ± 0.6 %), and B-10 (4.1 ± 1.9 %), while B-16 and B-17 (0.2 ± 0.2 %) *SF* % values were found to be significantly ($p \leq 0.05$) lower than that of B-2, and *SF* % for B-17 was significantly ($p \leq 0.05$) lower than B-10. At the individual rain-event scale, some notably large *SF* % values from multi-leader trees included 12.1 and 18.7 % from B-9 associated with 4.6 and 8.8 mm rain events, respectively, as well as 11.0 % *SF* from B-6 during a 32.7 mm event and 9.4 % *SF* from B-5 from a 9.7 mm event.

2.3.4 *Stemflow Funneling Ratios for Individual Trees*

Event-scale *FR* values from single-leader trees in the < 2 mm rain depth class ranged from zero for the 10 trees that did not produce *SF* in the class to 21.5 from A-5 during a 1.4 mm rain event. The 1.0 mm rain event that produced *SF* from A-1 had an associated *FR* value of 20.6. Mean *FR* values for the two largest rain events in this class (1.4 and 1.6 mm) from the 10 *SF*-producing single-leader trees in this rain depth class were 4.8 ± 8.6 and 9.4 ± 6.4 , respectively. For the multi-leader trees that produced *SF* for events < 2 mm, B-3 and B-9 had *FR* values of 12.5 and 5.6, respectively, during a 0.9 mm rainfall, while for the 1.6 mm event, B-3 and B-9 had *FR* values of 30.8 and 13.5, respectively, and B-2 and B-5 had values of 6.4 and 11.1.

For the 2 to < 5 mm rain depth class, the mean *FR* value of A-1 was found to be 20.8 ± 14.5 and was significantly ($p \leq 0.05$) greater than that of A-11 (2.4 ± 5.7), A-12 (1.4 ± 3.0), and the five largest-*DBH* single-leader trees, whose mean *FR* values ranged from 0.7 ± 1.6 for A-19 to 3.4 ± 3.9 for A-17. The mean *FR* value associated with A-5 (31.5 ± 20.9) for the 2 to < 5 mm rain depth class was significantly ($p \leq 0.01$) larger than all single-leader trees with the exception of A-1 and A-2. Funneling ratios for the multi-

leader trees in this rain depth class averaged 6.4 and ranged from $< 0.1 \pm < 0.1$ for trees B-14 and B-16, to 28.6 ± 15.0 for B-3. At the individual event scale for rain depths 5 to < 10 mm, *FR* values were found to be as high as 56.4 from single-leader trees (A-1, 4.6 mm event) and 96.8 from multi-leader trees (B-5, 4.6 mm event). Although the range in mean *FR* values for single-leader and multi-leader trees was large for the 5 to < 10 mm rain depth class (3.2 ± 2.4 for A-19 to 50.7 ± 33.6 for A-1; $< 0.1 \pm < 0.1$ for B-16 to 53.4 ± 37.1 for B-9), the small number of events ($n = 6$) combined with the large variability of *FR* in this rain depth class (mean coefficient of variation = 78.0 % for single leader trees, 106 % for multi-leader trees) meant that no significant ($p \leq 0.05$) differences in *FR* were found among the single-leader or multi-leader trees. For rain events > 10 mm, A-5 had a mean *FR* value (58.6 ± 12.0) that was significantly greater than 12 of the 19 other single leader trees, while A-12 had a significantly ($p \leq 0.05$) greater mean *FR* value (38.4 ± 18.6) than did A-13 (4.8 ± 5.5). For multi-leader trees, with the exception of B-1 (49.4 ± 22.7), B-3 (45.1 ± 5.2), and B-5 (42.9 ± 18.6), B-9 (81.3 ± 64.9) had a mean *FR* that was significantly ($p \leq 0.05$) greater than the other 13 multi-leader trees, which averaged 13.4 and ranged from 1.1 ± 1.3 (B-14) to 28.1 ± 16.6 (B-6). Notable *FR* values for individual events ≥ 10 mm include 117.8 by A-3 during a 9.7 mm event and 196.9 for B-9 during a 25.6 mm event.

2.3.5 *Stemflow Percent and Funneling Ratios as a Function of Morphological Traits*

As noted above, we observed high variability in event-scale *SF %* and *FR* within and between tree Groups A (single-leader) and B (multi-leader) as well as for individuals and groups between rain depth classes. Results of multiple regressions (Table 2.3) indicate that different tree traits were associated with *SF %* vs. *FR* and with smaller vs. larger rain depth classes, both within and between groups.

Table 2.3. Multiple regression equations for stemflow percentages and funneling ratios as functions of tree morphological traits (all coefficients significant at $p \leq 0.05$), generated for single-leader (Group A, $n = 20$) and multi-leader trees (Group B, $n = 17$) in three rain depth classes.

Group A – Single leader	Group B – Multi-leader
<i>SF</i> %, 2 to < 5 mm	
$e^{(0.05 AIF - 0.28 \ln Vol_C - 1.23)}$ $SEE = 0.330, r^2 = 0.901$	$e^{(-0.14 DBH + 5.15 HWR + 1.71 L_n - 8.84)}$ $SEE = 1.229, r^2 = 0.882$
<i>SF</i> %, 5 to < 10 mm	
$e^{(0.44 AIF + 0.02 WC + 0.02 AAU - 2.58)}$ $SEE = 0.357, r^2 = 0.873$	$(7.39 \left(\frac{1}{BRI}\right) + 0.03 CC + 0.06 AIU - 0.03 AIF - 9.19)^2$ $SEE = 0.333, r^2 = 0.881$
<i>SF</i> %, ≥ 10 mm	
$e^{(0.05 AIF + 0.03 CC + 3.20 BRI - 6.95)}$ $SEE = 0.296, r^2 = 0.890$	$(-0.18 CW + 0.0002 WC^3 - 2.55 BRI + 0.41 L_n^3 + 4.31)^2$ $SEE = 0.263, r^2 = 0.921$
<i>FR</i> , 2 to < 5 mm	
$e^{(-1.17 \ln DBH - 0.37 HWR + 0.03 AIU - 0.02 B_n + 4.74)}$ $SEE = 0.402, r^2 = 0.886$	$74.87 \left(\frac{1}{BRI}\right) - 57.65$ $SEE = 7.542, r^2 = 0.438$
<i>FR</i> , 5 to < 10 mm	
$-14.56 \ln DBH - 0.68 CC + 0.58 AIU + 97.86$ $SEE = 8.498, r^2 = 0.729$	$-990.10 \left(\frac{1}{AIU}\right) + 151.11 \left(\frac{1}{BRI}\right) - 91.20$ $SEE = 12.906, r^2 = 0.573$
<i>FR</i> , ≥ 10 mm	
$646.86 B_n - 10.45 \ln DBH + 118.25 BRI - 97.83$ $SEE = 7.902, r^2 = 0.676$	$(-12.99 BRI + 0.16 AIU + 125.95 \left(\frac{1}{AIF}\right) + 9.18)^2$ $SEE = 1.066, r^2 = 0.792$

2.4 DISCUSSION

It is well established that complex meteorological as well as tree morphological factors contribute to observed variation in stemflow, *SF* (Levia and Frost, 2003; Van Stan et al., 2011; Pypker et al., 2011). Chapter 3 will explore the role of both canopy traits and storm meteorology on stemflow initiation thresholds, P'' , and flow rates, Q_{SF} , as well as seasonal aspects of this 37-tree study. This chapter analyzes the influence of canopy traits on variation in *SF* % and *FR*.

2.4.1 Tree Size, Canopy Dimensions, and Branch Metrics

Numerous studies have found that diameter at breast height, *DBH*, positively predicts *SF* volume. For example, Germer et al. (2010) found that *SF* yields in two tropical tree species were correlated with *DBH*, but only for size classes > 10 cm. Likewise, Park and Hattori (2002) showed that greater basal area, *BA*, was associated with higher *SF* yields in a deciduous broad-leaved forest in central Japan. However, in our study, when *DBH* was a significant ($p \leq 0.05$) factor influencing Group B *SF*% for 2 to < 5 mm, it was negatively related. (The negative correlation of *FR* with *DBH* for all three rain classes reflects that *BA* is in the denominator of the formula for *FR*). For smaller rain events typical of the study region, the storage capacity, P'' , of our largest trees was rarely met (André et al., 2008; Valente et al., 1997); consequently, higher *SF* yields for small rain events were generally associated with smaller trees and a suite of size- and age-related variables correlated with lower *DBH*. When moderately sized trees produced *SF* at low rain depths (e.g., 0.9 % *SF* was generated by B-9 for a 0.9 mm event), we could often identify one or more conducive traits such as smooth bark, multiple leaders, or upright branching habit as discussed in more detail below. For our study trees, *DBH* was significantly correlated (Spearman's $r \leq 0.05$) with canopy width, tree height, projected canopy area, canopy volume, wood cover, and bark relief index. These variables appeared to work together in the larger study trees, limiting penetration of small rainfalls to the *SF*-conducting woody infrastructure and promoting obstruction and absorption of potential *SF* over the height and width of trees with deeply furrowed bark as well as greater wood area and volume (Ford and Deans, 1978; Aboal et al., 1999). However, the same combination of traits was associated with relatively higher *SF* production for large rain events that more completely saturated the canopy: broader, taller, denser canopies tend to capture more rainfall, particularly in windy conditions (Xiao et al., 2000a; Van Stan et al., 2011), but whether this potential *SF* is efficiently funneled to the base of the bole depends on factors other than size as discussed below (Van Stan and Levia, 2010; Pypker et al., 2011).

While size-related variables clearly influence *SF* production, so did canopy shape for small rain events in our study. The height-to-width ratio, *HWR*, was significantly ($p \leq 0.05$) inversely correlated with Group A funneling ratio, *FR* (negatively), and Group B *SF %* (positively) for 2 to < 5 mm rain depths. The opposing relationships may reflect that broader crowns (lower *HWR*) facilitate funneling from a broader area relative to *BA* (higher *FR*) while columnar trees (high *HWR*) efficiently concentrate flow generated over smaller areas (higher *SF %*), at least in part due to highly inclined branch angles (Levia et al., 2013). A possible mechanism for this is the increased effective crown projection area (Xiao et al., 2000a) presented by relatively tall, narrow trees to wind-driven rain which can penetrate to the branches and bole more readily than in broader canopies (Van Stan et al., 2011). This pattern was echoed in the ≥ 10 mm rain class where *SF %* was inversely related to canopy width, *CW*, such that narrower canopies were associated with higher *SF* yields on a per-canopy-area basis. As an example, the columnar form of A-15 may have contributed to a high event *SF %* value of 27.9 % from a 5.2 mm rainfall.

Group A *SF %* in the smallest rain class only was significantly ($p \leq 0.05$) inversely correlated with canopy volume, *Vol_C*, consistent with size-related patterns noted above. Given lower P'' values associated with smaller trees, our finding likely reflects that trees with larger *Vol_C* generate little or no *SF* at rain depths < 5 mm. Few studies have found relationships with *Vol_C* in trees (particularly isolated trees), but our finding is in contrast with observations by Martinez-Meza and Whitford (1996) that *SF* volume was directly related to canopy volume of *Larrea tridentata*, a desert shrub, leading them to suggest that larger canopies in that species more efficiently redistribute limited rainwater to the roots as a drought-resistance mechanism.

2.4.2 Cover Metrics

As noted above, wood cover, *WC*, was correlated with *DBH* and higher *WC* values predicted greater *SF %* for one rain class each for single- and multi-leader trees. This is consistent with recent findings by Levia et al. (2013) that higher *SF* yields in European

beech saplings were associated with higher total dry woody biomass and much higher woody-to-foliar biomass ratios. Although canopy cover, *CC*, was not correlated with *DBH*, it was significantly ($p \leq 0.05$) positively related to Group A *SF* % for the largest rain depth class and Group B *SF* % for 5 to < 10 mm events; however, *CC* was inversely related to Group A *FR* for the latter rain depth class, suggesting that canopy density interacts in complex ways with *DBH*, branch angles, and bark relief index, *BRI*. A consistent finding in the literature is that leafless canopies produce more *SF* than those in full leaf (e.g., Xiao and McPherson, 2011), and appear to be more sensitive to an array of meteorological influences such as wind speed, rainfall intensity, and vapour pressure deficit, *VPD* (Van Stan et al., 2014). In a detailed study of a single beech canopy, Staelens et al. (2008) found that the defoliated condition was associated with lower interception loss, higher *SF* yields, and lower *SF* initiation thresholds (1.5 mm for leafless vs. 2.1 mm for leafed).

2.4.3 Leader and Branch Characteristics

The number of leaders, L_n , was significantly ($p \leq 0.05$) positively correlated with *SF* % for 2 to < 5 mm and ≥ 10 mm suggesting that, despite greater surface areas associated with multiple leaders, they may play an important role in the convergence of *SF* at the base of the canopy, particularly for smooth-barked trees. An example of this combination of traits is the American beech (B-9) in our study that had six leaders and a *BRI* of only 1.04; this tree produced *SF* at low rain depths and in consistently high volumes relative to other trees of its size. For example, *SF* % values for B-9 for 4.6 mm and 8.8 mm events were 12.1 % and 18.7 %, respectively. Variables with which L_n was significantly ($p \leq 0.05$) correlated included upper-canopy intersection angles, *AIU*, full-tree intersection angles, *AIF*, and branch count, B_n (all positive) and frequency of drainage discontinuity, *FD* (negative), reinforcing the importance of woody biomass and high branch inclination angles (Levia et al., 2013) and suggesting that optimal funneling

of rain to *SF* is seen in smooth-barked, multi-leader trees with many inclined branches draining continuously to the bole.

Branch count was a significant ($p \leq 0.05$) factor for *FR* in single-leader trees (inversely for class II and positively for class IV rain depth classes), but was not significant for either *SF %* or *FR* in multi-leader trees or *SF %* in single-leader trees. For small events, high B_n may increase P'' due to increased woody surface area, but for larger events when canopies are approaching saturation, additional branches serve as infrastructure for flow to the bole. While branch count was not significantly correlated with any other traits for multi-leader trees, it was correlated ($p \leq 0.05$) with *BRI* and *FD* (positively) and *AIU*, *AIF*, and *CW* (negatively) for single-leader trees, illustrating that for this group of trees, plentiful branches may be associated with *SF*-enhancing and/or *SF*-suppressing characteristics for storms of various rain depths. Levia et al. (2013) found that higher *SF* was associated with higher primary and secondary branch counts in beech saplings while Návar (1993) demonstrated this trend for semi-arid shrubs with the number of branches angled at $> 80^\circ$ and mean branch angle both contributing to the best predictive model. As noted before, this variable interacts with many others, and is likely more important in conjunction with other factors than alone.

Positively correlated *AIF* explained more variation in *SF %* than any other trait for single-leader trees (all rain depth classes), while upper-canopy average angle, *AAU*, was positively related to *SF %* for class III events and *AIU* was positively related to *FR* for Class II and III rain depths ($p \leq 0.05$). For these trees, including some markedly columnar individuals, steeper branch angles appeared to promote flow, a finding that is well supported in the literature (Herwitz and Levia, 1997a; Herwitz, 1987; Xiao and McPherson, 2011). For multi-leader trees, *AIU* was significantly ($p \leq 0.05$) positively correlated with *SF %* for class III events and on *FR* for class III and IV events; *AIF*, however, was inversely related to *SF %* for class III events and to *FR* for the largest rain-depth class. It is possible that when high-angle upper branches are efficiently conducting *SF*, lower branches (intersecting the bole at lower angles) best contribute by collecting *SF*

at the dripline, making sense of the relationship between lower *AIF* and higher *SF*. Individual trees with high branch angles in this study often had the highest mean and/or event *SF %* and *FR* values; for example, A-14 generated 22.8 % *SF* from a 25.6 mm event while A-1 had a mean *FR* of 20.8 ± 14.5 for 2 to < 5 mm rain depths and an event *FR* of 56.4 for a 4.6 mm event. In synthesizing findings on this topic, Pypker et al. (2011) point out the trade-off between capture efficiency and *SF* generation as influenced by branch angle, projected branch area, and total branch area, a trade-off that varies vertically within individual trees as well as between individuals and species. Návar (1993) documented that dominant branches in the upper canopies of three semi-arid shrub species conducted a disproportionate quantity of *SF*, a result also found for trees. For example, Hutchinson and Roberts (1981) concluded that 98 % of *SF* was generated in the upper half of Douglas-fir canopies while Levia and Wubbena (2006) suggested that part of the explanation may be smoother upper-bole bark water storage capacities that can be half those of the lower bole.

2.4.4 Bark Relief

Bark relief had a variable effect depending on rain depth class and single- vs. multi-leader form, a departure from patterns noted in other studies (Levia and Herwitz, 2005; Van Stan and Levia, 2010; Livesley et al., 2014). The fact that higher *BRI* was associated with higher *SF %* and *FR* in single-leader trees for the largest rain depth class suggests that, once saturated, the increased surface area of more deeply fissured bark may enhance *SF*. However, this pattern was reversed for multi-leader trees for all except *SF %* for the smallest rain depth class, implying that smooth bark works with other characteristics associated with multiple leaders (e.g., greater wood volume and area) to promote *SF*. For rain events < 2 mm in our study, the two trees with the highest *FR* value in their respective groups were A-5 (21.5 from a 1.4 mm event) and B-3 (30.8 from a 1.6 mm event), likely reflecting the contribution of their smooth bark to funneling efficiency.

2.4.5 Leaf Size

Median leaf size was not significant ($p \leq 0.05$) for either tree group in any of the rain depth classes, which is not surprising given that this factor is only rarely reported in the literature. In a study of six species in a laurel forest, Aboal et al. (1999) theorized that relatively high *SF* efficiency of *Erica arborea* may have been due, in part, to its much smaller leaf size.

2.4.6 Assessment of Predicted Patterns on an Individual Tree Basis

Among single-leader trees, *SF %* values for two trees stood out: A-14 and A-15. In examining their traits relative to those in the regression equations, it is clear that they are unremarkable in some aspects (*DBH*, *BRI*), but represent extremes of other traits. Their height-to-width ratios are 4.1 (A-14) and 2.9 (A-15) compared to a group mean of 1.5 and consequently their *AAU*, *AIU*, and *AIF* values are among the highest of Group A trees and their canopy volumes are the lowest. Canopy cover measures are the highest in the group, while *WC* values are in the upper end of the range. These two trees do illustrate a seemingly optimal interaction of these traits, which have varying effects at different rain depth classes, when calculated per *PCA*. On the other hand, *FR* is calculated per *BA*, eliminating the “advantage” of tall, narrow trees. Figure 2.2c illustrates that *FR*, for A-14 and A-15, was significantly ($p \leq 0.05$) greater than for other individuals, making it clear that *SF %* and *FR* are distinct measures of *SF* efficiency, emphasizing the contribution of a canopy relative to the tree’s *PCA* or *BA*, respectively (Návar, 1993).

For multi-leader trees, B-9 had the greatest mean *SF %* values in all rain depth classes as well as the highest event percentages, 12.1% for a 4.6 mm event and 18.7 % for an 8.8 mm event. In the 2 to < 5 mm depth class, *SF %* was correlated with *DBH* (inversely) as well as *HWR* and *L_n* (positively); the only trait for which B-9 departs from the group average is the number of leaders (6 compared to Group B average of 3.6). While *BRI* was not significant ($p \leq 0.05$) at this rain depth, it is in the 5 to < 10 mm category and, in combination with above-average *AIU* and below-average *AIF*, the

smooth bark of B-9 ($BRI = 1.04$) may have contributed to group-maximum values for this American beech.

High FR values were observed for three single-leader trees at various rain depths: A-1, A-3, and A-5. For the 2 to < 5 mm rain depth class, the smallest tree (A-1, 10.2 cm DBH) had the highest mean FR (20.8 ± 14.5) and event FR (56.4 for a 4.6 mm event), reflecting the importance of DBH and HWR (both inverse) and AIU (relatively high for A-1 at 58.7°); given a value of B_n close to the group average, this tree's small, smooth branches were likely of secondary importance. For rain depths from 5 to < 10 mm, A-3 had a group-maximum FR of 117.8 from a 9.7 mm event; this tree's small DBH (18.8 cm) and slightly above-average AIU were conducive to SF production, but the other significant ($p \leq 0.05$) trait for this rain depth class, CC , was above average for this tree, whereas the regression indicated that lower CC was associated with higher FR . We suggest that the exceptionally smooth bark of B-3 (BRI 1.01) magnified the importance of other conducive traits. Finally, the highest event FR for multi-leader trees for rain depths < 2 mm was 21.5 for a 1.4 mm event for A-5, which also had the highest mean FR of 58.6 ± 12.0 for the ≥ 10 mm category. For both small (2 to < 5 mm) and the largest depth classes, FR was inversely related to DBH (relatively small at 14.6 cm for A-5); at small depths, the small HWR , high AIU , and very low B_n of A-5 explain its high SF production, whereas at depths ≥ 10 mm, its small DBH is the only significant ($p \leq 0.05$) variable associated with high FR . Its semi-smooth bark (BRI 1.07) and low B_n should not promote SF , but this may be a case where the interaction of smooth bark with other traits results in patterns that don't fully reflect the regression equations based on group data.

For multi-leader trees, high mean and event FR was noted for three trees: B-3, B-5, and B-9. At the smallest rain depths, an event high FR of 30.8 was recorded for a 1.6 mm event for B-3; this same tree had a mean FR of 28.6 ± 15.0 for the 2 to < 5 mm depth class. The only factor that was significant ($p \leq 0.05$) for Group B FR in that depth class was BRI , explaining such high production from B-3 ($BRI = 1.01$). In this same depth class, B-5 had a FR of 96.8 from a 4.6 mm event; BRI was moderate in this tree (1.10),

but the presence of four leaders and above-average branching angles may explain this high *FR* (as may the trend in single-leader trees of high *SF %* and *FR* for trees with deeply furrowed bark during large events). Once again, B-9 emerged as a high producer with a *FR* mean of 81.3 ± 64.9 for events ≥ 10 mm and an event maximum of 196.9 for a 25.6 mm event. The very smooth bark of this tree (*BRI* = 1.04), its high *AIU* (54.5 vs. group average of 46.0), and its low *AIF* (36.8 vs. group average of 44.8) support the relevance of variables identified as significant ($p \leq 0.05$) in the regression equation for this depth category.

2.5 CONCLUSION

This systematic investigation of the influence of various canopy traits on stemflow percent and funneling ratio has generally confirmed the importance of some deciduous tree characteristics found by other researchers to be correlated with increased stemflow, including small diameter at breast height (primarily for single-leader funneling ratios) and high branch angles. An exception to the latter trend in our study was the inverse relationships between 1) full-canopy average branch angles and stemflow percent for rain depths of 5 to < 10 mm and 2) full-canopy intersection angles and funneling ratios for rain depths ≥ 10 mm for multi-leader trees.

By identifying inconsistencies in some patterns, our study has emphasized the importance of understanding the differential importance of certain traits for various rain depth classes and in trees of different forms. For example, bark relief index was directly correlated with stemflow percent and funneling ratio for rain depths ≥ 10 mm, but only for single-leader trees; however, higher stemflow percent and funneling ratio in multi-leader trees were correlated with smoother bark. To our knowledge, this is the first study that has found the number of leaders converging at the base of a canopy to be significantly ($p \leq 0.05$) correlated with stemflow production; we look forward to future research on this morphological trait.

As found in virtually all stemflow studies to date, the variability in stemflow yields, stemflow percentages, and funneling ratios is high, even when a relatively uniform sample of trees is available. Chapter 3 will address meteorological characteristics that tend to interact with canopy structure differently in each season as well as potential stemflow yield patterns associated with different precipitation types. Based on generalized findings of this and other studies, we recommend the following in order to promote stemflow production and minimize stormwater runoff in urban environments:

- Ensure that sufficient infiltration capacity is available at the base of trees for stemflow volumes estimated with the region's storm regime and tree's mature size in mind. Spatially concentrated stemflow has the potential to be more readily managed than highly dispersed throughfall.
- In climates with mostly small rain events, select trees that will stay small as they tend to produce stemflow at lower rain depths and in greater quantities than large trees. If large rain events are frequent, larger canopies tend to produce more stemflow once they are saturated.
- In combination with other traits, canopy and wood cover were positively associated with stemflow production. Prepare for potentially greater stemflow yields from leafless canopies in the dormant season, particularly if mixed precipitation is common in your region.
- Select trees with multiple leaders or many major branches converging at the base of the canopy; this trait was correlated with high stemflow production for a range of rain depths, particularly in concert with high branch angles and smooth bark.
- Select trees with relatively high branch intersection angles as this trait promotes stemflow at all rain depths.
- In general, select trees with smooth bark as they tend to have lower storage capacities (and thus lower stemflow initiation thresholds) and higher stemflow yields. However, if planting or managing single-leader trees, be aware that deeply

furrowed bark was correlated with efficient stemflow production for rain events ≥ 10 mm, possibly reflecting enhanced conduction over a greater saturated surface area.

Further research is needed on stemflow as well as throughfall and interception-loss in isolated cultivated trees, both deciduous and coniferous, in urban areas representing a wide range of climatic conditions. Evidence is growing that canopy water balance in these solitary urban trees reflects different interactions of canopy traits and storm characteristics than those observed in closed-canopy forests.

2.6 REFERENCES

- Aboal, J., Morales, D., Hernández, M., Jiménez, M., 1999. The measurement and modelling of the variation of stemflow in a laurel forest in Tenerife, Canary Islands. *Journal of Hydrology* 221, 161–175.
- Akbari, H., Pomerantz, M., Taha, H., 2001. Cool surfaces and shade trees to reduce energy use and improve air quality in urban areas. *Solar Energy* 70, 295–310.
- André, F., Jonard, M., Ponette, Q., 2008. Influence of species and rain event characteristics on stemflow volume in a temperate mixed oak–beech stand. *Hydrological Processes* 22, 4455– 4466.
- Asadian, Y., Weiler, M., 2009. A new approach in measuring rainfall interception by urban trees in coastal British Columbia. *Water Quality Research Journal of Canada* 44, 16–25.
- Brooks, K., Ffolliott, P., Gregersen, H., DeBano, L., 2003. *Hydrology and the Management of Watersheds*, 2nd ed. Iowa State Press, Ames, IA.
- Carlyle-Moses, D.E., Gash, J.H.C., 2011. Rainfall interception loss by forest canopies, in: Levia, D.F., Carlyle-Moses, D., Tanaka, T. (Eds.), *Forest Hydrology and Biochemistry: Synthesis of Past Research and Future Directions*, Ecological Studies. Springer Netherlands, Dordrecht, pp. 407–424.
- Carlyle-Moses, D.E., Lishman, C.E., McKee, A.J., 2014. A preliminary evaluation of throughfall sampling techniques in a mature coniferous forest. *Journal of Forestry Research* 25, 407–413.
- Crabtree, R., Trudgill, S., 1985. Hillslope hydrochemistry and stream response on a wooded, permeable bedrock: The role of stemflow. *Journal of Hydrology* 80, 161–178.
- Dwyer, J., McPherson, E., Schroeder, H., Rowntree, R., 1992. Assessing the benefits and costs of the urban forest. *Journal of Arboriculture* 18, 227–234.
- Environment Canada. 2014. Canadian Climate Normals. Station Name: Kamloops A*. Webpage. URL http://climate.weather.gc.ca/climate_normals/index_e.html (accessed June 1, 2014).
- Ford, E., Deans, J., 1978. The effects of canopy structure on stemflow, throughfall and interception loss in a young Sitka spruce plantation. *Journal of Applied Ecology* 15, 905–917.
- Frost, E.E., Levia, D.F., 2013. Hydrologic variation of stemflow yield across co-occurring dominant canopy trees of varying mortality. *Ecohydrology*. doi: 10.1002/eco.1397.
- Germer, S., Werther, L., Elsenbeer, H., 2010. Have we underestimated stemflow? Lessons from an open tropical rainforest. *Journal of Hydrology* 395, 169–179.

- Goddard, M., Dougill, A., Benton, T., 2010. Scaling up from gardens: Biodiversity conservation in urban environments. *Trends in Ecology & Evolution* 25, 90–98.
- Goodall, D., 1965. Plot-less tests of interspecific association. *Journal of Ecology* 53, 197–210.
- Gorman, J., 2004. Residents' opinions on the value of street trees depending on tree location. *Journal of Arboriculture* 30, 36–44.
- Grubbs, F., 1950. Sample criteria for testing outlying observations. *The Annals of Mathematical Statistics* 21, 27–58.
- Guevara-Escobar, A., González-Sosa, E., Véliz-Chávez, C., Ventura-Ramos, E., Ramos-Salinas, M., 2007. Rainfall interception and distribution patterns of gross precipitation around an isolated *Ficus benjamina* tree in an urban area. *Journal of Hydrology* 333, 532–541.
- Hair, J., Anderson, R., Tatham, R., Black, W., 1998. *Multivariate Data Analysis*, 5th edition. Prentice Hall, Upper Saddle River, NJ.
- Herwitz, S., Levia, D., 1997. Mid-winter stemflow drainage from bigtooth aspen in central Massachusetts. *Hydrological Processes* 11, 169–175.
- Herwitz, S.R., 1986. Infiltration-excess caused by stemflow in a cyclone-prone tropical rainforest. *Earth Surface Processes and Landforms* 11, 401–412.
- Herwitz, S.R., 1987. Raindrop impact and water flow on the vegetative surfaces of trees and the effects on stemflow and throughfall generation. *Earth Surface Processes and Landforms* 12, 425–432.
- Hutchinson, I., Roberts, M.C., 1981. Vertical variation in stemflow generation. *Journal of Applied Ecology* 18, 521–527.
- Inkiläinen, E.N.M., McHale, M.R., Blank, G.B., James, A.L., Nikinmaa, E., 2013. The role of the residential urban forest in regulating throughfall: A case study in Raleigh, North Carolina, USA. *Landscape and Urban Planning* 119, 91–103.
- Johnson, M.S., Lehmann, J., 2006. Double-funneling of trees: Stemflow and root-induced preferential flow. *Ecoscience* 13, 324–333.
- Levia, D., Carlyle-Moses, D., Tanaka, T. (Eds.), 2011. *Forest Hydrology and Biogeochemistry: Synthesis of Past Research and Future Directions*, Ecological Studies. Springer Science+Business Media.
- Levia, D., Frost, E., 2003. A review and evaluation of stemflow literature in the hydrologic and biogeochemical cycles of forested and agricultural ecosystems. *Journal of Hydrology* 274, 1–29.
- Levia, D.F., Frost, E.E., 2006. Variability of throughfall volume and solute inputs in wooded ecosystems. *Progress in Physical Geography* 30, 605–632.

- Levia, D.F., Herwitz, S.R., 2005. Interspecific variation of bark water storage capacity of three deciduous tree species in relation to stemflow yield and solute flux to forest soils. *Catena* 64, 117–137.
- Levia, D.F., Michalzik, B., Nätke, K., Bischoff, S., Richter, S., Legates, D.R., 2013. Differential stemflow yield from European beech saplings: The role of individual canopy structure metrics. *Hydrological Processes* 2–9.
- Levia, D.F., Wubbena, N.P., 2006. Vertical variation of bark water storage capacity of *Pinus strobus* L. (Eastern White Pine) in Southern Illinois. *Northeastern Naturalist* 13, 131–137.
- Li, X.-Y., Liu, L.-Y., Gao, S.-Y., Ma, Y.-J., Yang, Z.-P., 2008. Stemflow in three shrubs and its effect on soil water enhancement in semiarid loess region of China. *Agricultural and Forest Meteorology* 148, 1501–1507.
- Liang, W.-L., Kosugi, K., Mizuyama, T., 2009. A three-dimensional model of the effect of stemflow on soil water dynamics around a tree on a hillslope. *Journal of Hydrology* 366, 62–75.
- Liu, C., Li, X., 2012. Carbon storage and sequestration by urban forests in Shenyang, China. *Urban Forestry & Urban Greening* 11, 121–128.
- Livesley, S.J., Baudinette, B., Glover, D., 2014. Rainfall interception and stem flow by eucalypt street trees – The impacts of canopy density and bark type. *Urban Forestry & Urban Greening* 13, 192–197.
- Lohr, V.I., Pearson-Mims, C.H., Tarnai, J., Dillman, D.A., 2004. How urban residents rate and rank the benefits and problems associated with trees in cities. *Journal of Arboriculture* 30, 28–35.
- Martinez-Meza, E., Whitford, W.G., 1996. Stemflow, throughfall and channelization of stemflow by roots in three Chihuahuan desert shrubs. *Journal of Arid Environments* 32, 271–287.
- Masukata, H., Garden, B., Science, F., 1990. Throughfall, stemflow and interception of rainwater in an evergreen broadleaved forest. *Ecological Research* 5, 303–316.
- McPherson, E., Nowak, D., Heisler, G., Grimmond, S., Souch, C., Grant, R., Rowntree, R., 1997. Quantifying urban forest structure, function, and value: The Chicago Urban Forest Climate Project. *Urban Ecosystems* 1, 49–61.
- McPherson, E., Simpson, J., Peper, P., Xiao, Q., 1999. Benefit-cost analysis of Modesto's municipal urban forest. *Journal of Arboriculture* 25, 235–248.
- McPherson, E.G., Simpson, J.R., Xiao, Q., Wu, C., 2011. Million trees Los Angeles canopy cover and benefit assessment. *Landscape and Urban Planning* 99, 40–50.
- Michopoulos, P., 2011. Biogeochemistry of urban forests, in: Levia, D.F., Carlyle-Moses, D., Tanaka, T. (Eds.), *Forest Hydrology and Biogeochemistry: Synthesis of Past Research and Future Directions*. Springer Netherlands, pp. 341–353.

- Miller, R.W., 1997. Planning and Urban Forestry, in: *Urban Forestry: Planning and Managing Urban Greenspaces*. Prentice Hall, pp. 167–185.
- Návar, J., 1993. The causes of stemflow variation in 3 semiarid growing species of northeastern Mexico. *Journal of Hydrology* 145, 175–190.
- Nowak, D., Crane, D., Stevens, J., 2006. Air pollution removal by urban trees and shrubs in the United States. *Urban Forestry & Urban Greening* 4, 115–123.
- Nowak, D.J., Hirabayashi, S., Bodine, A., Hoehn, R., 2013. Modeled PM_{2.5} removal by trees in ten U.S. cities and associated health effects. *Environmental Pollution* 178, 395–402.
- Park, H.-T., Hattori, S., 2002. Applicability of Stand Structural Characteristics to Stemflow Modeling. *Journal of Forest Research* 7, 91–98.
- Peng, H., Zhao, C., Feng, Z., Xu, Z., Wang, C., Zhao, Y., 2014. Canopy interception by a spruce forest in the upper reach of Heihe River basin, Northwestern China. *Hydrological Processes* 28, 1734–1741.
- Peper, P., McPherson, E., Simpson, J., Gardner, S., Vargas, K., Xiao, Q., 2007. *New York City Municipal Forest Resource Analysis*. New York City, New York.
- Peper, P., McPherson, E., Simpson, J., Vargas, K., Xiao, Q., 2008. *City of Indianapolis Municipal Forest Resource Analysis*. Indianapolis, Indiana.
- Pothier, A., Millward, A., 2013. Valuing trees on city-centre institutional land: An opportunity for urban forest management. *Journal of Environmental Planning and Management* 56, 1380–1402.
- Pypker, T., Levia, D., Staelens, J., Van Stan, J., 2011. Canopy structure in relation to hydrological and biogeochemical fluxes, in: Levia, Delphis F., Carlyle-Moses, DE, Tanaka, T. (Ed.), *Forest Hydrology and Biochemistry: Synthesis of Past Research and Future Directions*. Springer, Dordrecht, pp. 371–388.
- Roy, S., Byrne, J., Pickering, C., 2012. A systematic quantitative review of urban tree benefits, costs, and assessment methods across cities in different climatic zones. *Urban Forestry & Urban Greening* 11(4), 351–363.
- Rutter, A., Morton, A., Robin, P., 1975. A Predictive Model of Rainfall Interception in Forests. II. Generalization of the Model and Comparison with Observations in Some Coniferous and Hardwood Stands. *The Journal of Applied Ecology* 12, 367–380.
- Saito, T., Matsuda, H., Komatsu, M., Xiang, Y., Takahashi, A., Shinohara, Y., Otsuki, K., 2013. Forest canopy interception loss exceeds wet canopy evaporation in Japanese cypress (Hinoki) and Japanese cedar (Sugi) plantations. *Journal of Hydrology* 507, 287–299.
- Sander, H., Polasky, S., Haight, R.G., 2010. The value of urban tree cover: A hedonic property price model in Ramsey and Dakota Counties, Minnesota, USA. *Ecological Economics* 69, 1646–1656.

- Sanders, R.A. 1986. Urban vegetation impacts on the hydrology of Dayton, Ohio. *Urban Ecology* 9, 361–376.
- Soares, A.L., Rego, F.C., McPherson, E.G., Simpson, J.R., Peper, P.J., Xiao, Q., 2011. Benefits and costs of street trees in Lisbon, Portugal. *Urban Forestry & Urban Greening* 10, 69–78.
- Staelens, J., De Schrijver, A., Verheyen, K., Verhoest, N.E.C., 2008. Rainfall partitioning into throughfall, stemflow, and interception within a single beech (*Fagus sylvatica* L.) canopy: Influence of foliation, rain event characteristics, and meteorology. *Hydrological Processes* 22, 33–45.
- Stagoll, K., Lindenmayer, D.B., Knight, E., Fischer, J., Manning, A.D., 2012. Large trees are keystone structures in urban parks. *Conservation Letters* 5, 115–122.
- Tanaka, T., 2011. Effects of the canopy hydrologic flux on groundwater, in: Levia, Delphis F., Carlyle-Moses, D., Tanaka, T. (Eds.), *Forest Hydrology and Biochemistry: Synthesis of Past Research and Future Directions*. Springer, Dordrecht, pp. 499–518.
- Tanaka, T., Taniguchi, M., Tsujimura, M., 1996. Significance of stemflow in groundwater recharge. 2. A cylindrical infiltration model for evaluating the stemflow contribution to groundwater recharge. *Hydrological Processes* 10, 81–88.
- Taniguchi, M., Tsujimura, M., Tanaka, T., 1996. Significance of stemflow in groundwater recharge. 1: Evaluation of the stemflow contribution to recharge using a mass balance approach. *Hydrological Processes* 10, 71–80.
- Tukey, J.W. 1953. The problem of multiple comparisons. Department of Statistics, Princeton University, Princeton, NJ. Unpublished report.
- Tyrväinen, L., Pauleit, S., Seeland, K., Vries, S. De, 2005. Benefits and Uses of Urban Forests and Trees, in: Konijnendijk, C., Nilsson, K., Randrup, T., Schipperijn, J. (Eds.), *Urban Forests and Trees: A Reference Book*. Berlin, pp. 81–114.
- Tzoulas, K., Korpela, K., Venn, S., Yli-Pelkonen, V., Kaźmierczak, A., Niemela, J., James, P., 2007. Promoting ecosystem and human health in urban areas using Green Infrastructure: A literature review. *Landscape and Urban Planning* 81, 167–178.
- Valente, F., David, J.S., Gash, J.H.C., 1997. Modelling interception loss for two sparse eucalypt and pine forests in central Portugal using reformulated Rutter and Gash analytical models. *Journal of Hydrology* 190, 141–162.
- Van Stan, J., Jarvis, M., Levia, D., 2010. An automated instrument for the measurement of bark microrelief. *IEEE Transactions on Instrumentation and Measurement* 59, 491–493.

- Van Stan, J., Levia, D., 2010. Inter- and intraspecific variation of stemflow production from *Fagus grandifolia* Ehrh. (American beech) and *Liriodendron tulipifera* L. (yellow poplar) in relation to bark microrelief in the eastern United States. *Ecohydrology* 3, 11–19.
- Van Stan, J.T., Siegert, C.M., Levia, D.F., Scheick, C.E., 2011. Effects of wind-driven rainfall on stemflow generation between codominant tree species with differing crown characteristics. *Agricultural and Forest Meteorology* 151, 1277–1286.
- Van Stan, J.T., Van Stan, J.H., Levia, D.F., 2014. Meteorological influences on stemflow generation across diameter size classes of two morphologically distinct deciduous species. *International Journal of Biometeorology* (online) 1–11.
- Vico, G., Revelli, R., Porporato, A., 2014. Ecohydrology of street trees: Design and irrigation requirements for sustainable water use. *Ecohydrology* 7, 508–523.
- Wei, X., Liu, S., Zhou, G., Wang, C., 2005. Hydrological processes in major types of Chinese forest. *Hydrological Processes* 19, 63–75.
- Whitford, W.G., Anderson, J., Rice, P.M., 1997. Stemflow contribution to the “fertile island” effect in creosotebush, *Larrea tridentata*. *Journal of Arid Environments* 35, 451–457.
- Xiao, Q., McPherson, E., 2011. Rainfall interception of three trees in Oakland, California. *Urban Ecosystems* 14, 755–769.
- Xiao, Q., McPherson, E.G., Ustin, S.L., Grismer, M.E., 2000a. A new approach to modeling tree rainfall interception. *Journal of Geophysical Research* 105, 29173–29188.
- Xiao, Q., McPherson, E.G., Ustin, S.L., Grismer, M.E., Simpson, J.R., 2000b. Winter rainfall interception by two mature open-grown trees in Davis, California. *Hydrological Processes* 14, 763–784.
- Yarranton, G., 1967. An instrument for measuring the microrelief of bark. *Canadian Journal of Botany* 45, 1173–1178.
- Zar, J.H. 1984. *Biostatistical Analysis*. 2nd edition. Prentice-Hall Inc. Englewood Cliffs, NJ. 718 pp.
- Zhongjie, S., Yanhui, W., Lihong, X., Wei, X., Pengtao, Y., Jixi, G., Linbo, Z., 2010. Fraction of incident rainfall within the canopy of a pure stand of *Pinus armandii* with revised Gash model in the Liupan Mountains of China. *Journal of Hydrology* 385, 44–50.

CHAPTER 3

TREE TRAITS AND METEOROLOGICAL FACTORS INFLUENCING THE INITIATION AND RATE OF STEMFLOW FROM ISOLATED DECIDUOUS TREES

3.1 INTRODUCTION

Given the hydrological implications of vegetation-related planning and management decisions in forested, agricultural, and urban settings, it is critical to refine our understanding of the processes at this interface of the atmospheric and terrestrial hydrological cycles. Tree canopy water balances have been most actively studied and modelled since the 1970s (Rutter et al., 1971; Gash, 1979) from single-tree (David et al., 2006; Guevara-Escobar et al., 2007) to stand scales (Carlyle-Moses and Price, 1999, 2007), in semi-arid (Návar, 2011) and arid (Llorens and Domingo, 2007) to tropical ecosystems (Herwitz, 1985; Germer et al., 2010), and from the varied perspectives of canopy architecture (Park and Cameron, 2008), meteorology (Van Stan et al., 2011), biogeochemistry (Neary and Gizyn, 1994; Michopoulos, 2011), and groundwater recharge (Taniguchi et al., 1996).

Precipitation incident on vegetation canopies is partitioned into 1) interception loss, the portion directly evaporated from leaf and wood surfaces; 2) throughfall, *TF*, which reaches the ground directly through gaps or drips from the canopy; and 3) stemflow, *SF*, which is funneled to the base of the plant via the branch infrastructure and bole (Helvey and Patric, 1965; Valente et al., 1997). In broadleaf deciduous forests, understory precipitation in the form of *TF* and *SF* can represent from 70–80 % and 3–10 % of rain incident on the canopy, respectively (Llorens and Domingo, 2007; Van Stan et al., 2011). However, compared to the dispersed nature of *TF* inputs to the forest floor, the concentration of *SF* in a much smaller area means that this volumetrically minor quantity can have a disproportionate impact on the terrestrial hydrological cycle (Levia and Frost, 2003; Staelens et al., 2007; Germer et al., 2010; Levia et al., 2010). As in natural and managed forests, areas at the base of urban tree trunks can constitute hot spots (and hot

moments) of hydrological and biogeochemical enrichment (e.g., McClain et al., 2003; Staelens et al., 2007). Implications of this concentrated flux are intensified in urban landscapes characterized by impervious surfaces, compacted and constrained soils, and high pollutant levels (Xiao and McPherson, 2011). Extremes of drought and flood are common outcomes of meteorological variability in cities, making trees appealing as potential rainfall interceptors (Xiao et al., 2007; Inkiläinen et al., 2013; Livesley et al., 2014). Trees of certain forms in some climates (e.g., Germer et al., 2010) may funnel sufficient *SF* to create water quantity and quality issues in urban conditions. In conducive planting sites, however, high *SF* producers have the potential to self-irrigate and self-nourish (Levia and Frost, 2003), to direct pollutants from canopies to soils for biofiltration (Xiao et al., 2007), and even to recharge groundwater via preferential pathways along roots (Tanaka, 2011).

There is some evidence that *SF* processes in urban trees, particularly those isolated from their neighbours, differ from those observed in natural forest stands (Xiao et al., 2000; Guevara-Escobar et al., 2007), meaning that findings from forested environments cannot necessarily be applied in single-tree situations (Livesley et al., 2014). The empirically based model developed by Xiao et al. (2000) confirms the relevance of three broad influences on *SF*: 1) magnitude and duration of rain; 2) meteorological conditions during the storm; and 3) canopy characteristics of the tree. Research on these factors in non-urban forests around the world is now readily available (e.g., Staelens et al., 2008; Levia et al., 2011), but fewer studies have been done in urban settings and for isolated trees (Xiao et al., 2000; Guevara-Escobar et al., 2007; Livesley et al., 2014).

Rain depth is commonly the dominant meteorological predictor of *SF* volume (Germer et al., 2010; Návar, 2011), but there is evidence that other meteorological factors can play a role, including storm duration (Levia, 2004), rainfall intensity (Calder, 2001; Price and Carlyle-Moses, 2003), wind speed (André et al., 2008b) and direction (Van Stan et al., 2011), rainfall inclination angle (Van Stan et al., 2011), and vapour pressure deficit, *VPD* (Van Stan et al., 2014b). Little study has been done on the importance of within-storm break duration; however, André et al. (2008a) found, for a temperate oak-

beech forest in Belgium, that both storage capacities and *SF* initiation thresholds were affected by the ratio of cumulated potential evaporation for the dry period preceding the storm to volume of rainfall associated with the previous storm event.

In general, studies focusing on canopy traits point to the collective importance of a tree's *SF*-conducting infrastructure (Pypker et al., 2011; Levia et al., 2013). Diameter at breast height, *DBH*, is usually a strong predictor of *SF* production (Deguchi et al., 2006; André et al., 2008b; Šraj et al., 2008; Germer et al., 2010; Van Stan and Levia, 2010), but studies showing high yields for small trees (Germer et al., 2010; Levia et al., 2013) are stimulating further research.

Other factors influencing *SF* production include effective canopy area, which is greater for columnar trees where inclined rainfall is common (Xiao et al., 2000; Guevara-Escobar et al., 2007), particularly in sparse forests and for isolated trees (Herwitz and Slye, 1995). Canopy cover fraction, canopy volume, and leaf area index, *LAI*, have been explored (e.g., Marin et al., 2000; Park and Hattori, 2002; Xiao and McPherson, 2011), but their influence cannot be generalized across species, ecosystems, or rainfall regimes (Pypker et al., 2011).

Wood cover fraction and the volume of wood within the tree canopy have implications for *SF*, particularly during seasonal defoliation; increased *SF* in leaf-off condition has often been observed (André et al., 2008b; Dunkerley, 2013). Recently, Levia et al. (2013) measured woody as well as foliar biomass for 10 European beech saplings, concluding that greater *SF* yields were associated with both higher woody surface area per unit projected canopy area, *PCA*, and higher ratios of woody to foliar biomass; other influential metrics included branch count per unit *PCA* and mean branch inclination angle. Increasing branch inclination is conducive only to a point as nearly vertical branches present minimal surface area to rain and drip *TF* while being subject to greater drip loss themselves; Herwitz (1987) observed linear (dry branches) then logarithmic (saturated branches) increases in detention of droplets, with > 80 % of rainfall captured at inclinations above 60°.

Bark relief is one trait that clearly limits SF through at least two mechanisms: increased storage capacity per unit area (Herwitz, 1985; Levia and Herwitz, 2005) and greater surface areas associated with deeply furrowed bark (Van Stan and Levia, 2010).

Leaf size has been studied less than composite canopy measures, although hydrophobicity and inclination angles have been explored (Holder, 2012). In their model, Xiao et al. (2000) found high sensitivity of SF to increases in leaf zenith angles.

In general, research to date suggests that, for trees of comparable size, SF production tends to be greater if a tree has a moderately dense canopy, high woody-to-foliar biomass ratio, highly inclined branching angles, and smooth bark, acknowledging that different meteorological regimes can enhance or diminish the importance of these characteristics. Such generalizations are based on numerous different studies of diverse species from different climatic regions, making definite conclusions on the role of individual traits and meteorological factors problematic. This study took a systematic approach, focusing on diverse and detailed canopy traits at a relatively contained site (ensuring that all trees were subject to similar meteorological forces). Specific objectives of the study were to:

1. derive, for each tree, the threshold rain depth, P'' , and the flow rate once P'' has been satisfied, Q_{SF} ;
2. characterize relationships between canopy traits and SF threshold, rate, and yield; and
3. identify meteorological and seasonal variables that influence SF yield.

3.2 STUDY AREA AND METHODS

3.2.1 Study Area

McArthur Island Park (MIP) in the City of Kamloops, British Columbia, Canada (50° 41' 43" N, 120° 22' 38" W, elevation 344 m a.m.s.l.), is a 51-ha multi-use sport and leisure facility on the north shore of the Thompson River (Figures B.1 and B.2). The site

encompasses several tree stands, including fairly continuous tree and shrub cover in the riparian zone of the slough that borders the park on the east, north, and west. However, many trees within the perimeter access road at MIP are isolated, which, for the purpose of this study, refers to those trees with no obstructions, including other tree canopies, extending into a field of view 35° from vertical and centred where the lowest branch meets the bole. (Methods described below were used to verify that no inclined rainfall was obstructed by neighbouring trees during this study.) Most trees at MIP are deciduous, including cultivated species of maple (*Acer* spp.), ash (*Fraxinus* spp.), and oak (*Quercus* spp.).

Environment Canada's "Kamloops A*" climate station, located approximately 4.4 km west-north-west of MIP at an elevation of 345 m a.m.s.l., has an associated mean annual (1981–2010) temperature of 9.3°C and mean monthly temperatures ranging from –2.8°C (January) to 21.5°C (July). Of mean annual precipitation (277.6 mm), rain accounts for 81 % (224.3 mm) and snow for the remainder. A climograph for the "Kamloops A*" station is provided in Figure 3.1. The area has an average of 101.1 rain-days per year; approximately 83.3 (82 %) of the rain-days have associated rain depths between 0.2 and < 5 mm. On average, 4.3 rain-days per year have associated rain depths of between 10.0 and < 25.0 mm, while rain-days with depths ≥ 25.0 mm occur, on average, once every 5 years. MIP is extensively irrigated to meet tournament-standard turf conditions and sustain cultivated, non-native tree species. As a result, the study site's climate is more aligned with a moist continental Cwb Köppen climate type than its native mid-latitude, semi-arid steppe climate (BSk Köppen climate type; Ross, 2013).

3.2.2 Tree Selection and the Measurement and Derivation of Tree Traits

Using the City of Kamloops' ArcGIS inventory and on-site evaluation, study trees were selected according to criteria outlined in section 2.2.3. Trait terminology is defined below; section 2.2.3 provides a more detailed methodology of trait measurement and derivation.

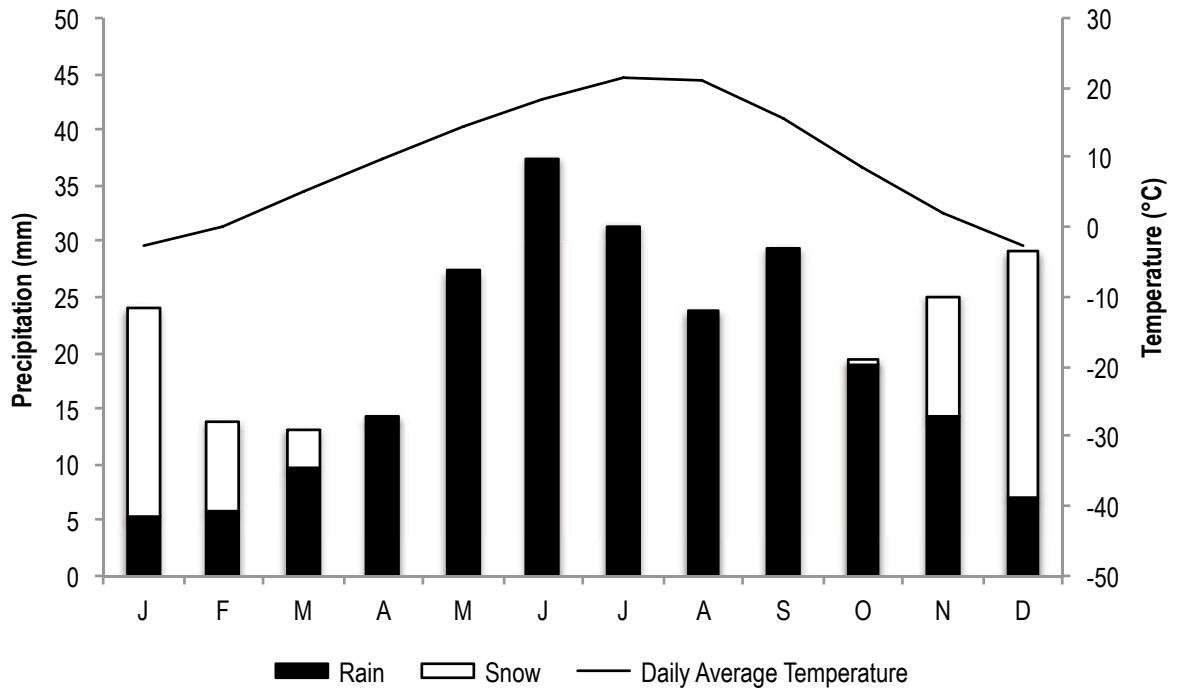


Figure 3.1. Climograph for the Meteorological Service of Canada’s “Kamloops A*” climate station (50° 42' 08" N, 120° 26' 31" W) (1981–2010 normals; Environment Canada, 2014).

For each study tree, we measured DBH (cm), tree height, H (m), and average canopy width, CW (m), then calculated projected canopy area, PCA (m²), projected wood area, PWA (m²), canopy height-to-width ratio, HWR (dimensionless), canopy volume, $Volc$ (m³), and wood volume, $Volw$ (m³).

Beneath-canopy skyward photographs were used to calculate leaf-on canopy cover, CC (%), and leaf-off wood cover, WC (%), values for the full canopy (adapted from Korhonen and Heikkinen, 2009).

The number of secondary leaders was noted (and used to calculate total number of leaders, L_n , at the base of the canopy); counts (but not angles) of branches intersecting secondary leaders were used to generate a total branch count, B_n , for the tree while angles of “feeder” branches intersecting only the primary leader were calculated. Four angles were used in final analyses: the angle of intersection of the branch and leader in the upper third of the canopy, AIU (mean, deg. from horizontal), and in the full canopy, AIF (mean, deg. from horizontal); and average (overall) angle from intersection to furthest extent of the branch in the upper, $A AU$ (mean, deg. from horizontal), and full canopy, $A AF$ (mean, deg. from horizontal). For each tree, an overall frequency of discontinuous branch segments, FD , was calculated by assigning a branch a “discontinuous” rating if the inner or mid-third of the branch drained away from the bole.

A quantitative bark relief index, BRI , was calculated using the ratio of the furrowed circumference of the tree bole to the surface (unfurrowed) circumference at breast height (1.3 m, or slightly higher or lower to avoid branches and deep scars). This measure essentially represents bark microrelief as discussed in section 2.2.3.

A sample of leaves or leaflets (13 to 49 per tree) was sorted by size and the median leaf was scanned. Its area was calculated using Photoshop® CC to yield median leaf size, MLS (cm²), for each tree.

3.2.3 Precipitation and Stemflow Measurement

Measurement of precipitation and stemflow, SF , was made on an event basis from June 12, 2012 to November 3, 2013. An Onset® tipping bucket rain gauge (Model # S-RGB-M002) connected to an Onset® Hobo® U-30 USB data logger (Model # U30-NRC) recorded rainfall depth and intensity. The opening of the tipping bucket (receiving diameter 15.4 cm, resolution 0.2 mm tip⁻¹) was 1 m off the ground. Accompanying the tipping bucket rain gauge (TBRG) in the unobstructed yard of a private residence directly north of MIP was a manually read polyethylene gauge (diameter 29 cm, depth 36 cm, opening height 1 m). The tipping bucket and adjacent manually read rain gauge were

between 80 and 770 m from the study trees. In addition to these gauges, eight manually read gauges were distributed throughout MIP (gauge density $\sim 0.04 \text{ km}^2 \text{ gauge}^{-1}$). The furthest distance between a manually read gauge and a study tree was approximately 215 m.

Stemflow collection collars were fabricated using black corrugated polyethylene hose (diameter of 3.2 cm for 32 trees and 3.8 cm for the five largest trees). After a lengthwise section of hose was removed, the collar was wrapped twice around the tree at an angle to promote drainage to the reservoir (collar lengths 1.2–5.2 m). One edge was stapled to the trunk and 100 % silicone was used to seal the seam and staples; collars were inspected and repaired regularly. Each collar drained through an intact section of hose to a 17-L polyethylene pail inside a 114-L lidded polyethylene tote to accommodate overflow; to guard against strong winds and contamination of collected *SF* by rain, each tote was weighted and its PVC plastic cover secured with elastic cord.

3.2.4 Measurement and Derivation of Meteorological Variables

In addition to logging rain depth via the tipping bucket rain gauge, the data logger reported the following variables every minute (equipment by Onset Computer Corporation):

- wind speed (m s^{-1}) and maximum 3-second gust speed (m s^{-1} ; S-WSA-M003);
- wind direction (degrees clockwise from 0° = north; S-WDA-M003);
- solar radiation (W m^{-2} ; SOLAR-RS3);
- barometric pressure (mbar; S-BPB-CM50), and
- temperature ($^\circ\text{C}$) and relative humidity (%) (S-THB-M003).

Event and 5-minute averages were calculated for each of these, and the latter two were used to derive event and 5-minute averages for vapour pressure deficit, *VPD* (kPa), as follows:

$$VPD = SVP - AVP \text{ where}$$

$$SVP = 0.611 \cdot \exp\left(\frac{17.27 T}{237.3 + T}\right) \text{ and}$$

$$AVP = \frac{RH}{100} \cdot SVP$$

where SVP is saturated vapour pressure (kPa), AVP is actual vapour pressure (kPa), T is average temperature ($^{\circ}\text{C}$) and RH is relative humidity (%). Since net radiant energy has been shown to be a minor contributor to evaporation of wetted canopies (see Carlyle-Moses and Gash, 2011), an introduced evaporation coefficient, E , based on the aerodynamic approach to estimating evaporation from wetted surfaces (Dalton, 1802; see Ward and Robinson, 2000), was calculated based on VPD and wind speed:

$$E = W \cdot VPD$$

where W is wind speed (m s^{-1}). Average wind directions and standard deviations were calculated through vector decomposition as described by Van Stan et al. (2011).

Tipping bucket records were used to identify the start and end of each rain event; for the purposes of this study, events were separated by rain-free breaks of at least 12 hours. By the same method, timing and duration of breaks (≥ 30 minutes without a tip) were documented, yielding the total duration of intra-storm breaks, D_B (h) and total rain duration, D_R (h). Two measures of intensity were calculated: 1) 5-minute maximum intensity, I_{max5} , (mm h^{-1}), the maximum intensity that occurred in any 5-minute period of the event and 2) 5-minute weighted intensity, I_{wt5} (mm h^{-1}). To derive 5-minute weighted averages, 5-minute (unweighted) averages were multiplied by the depth of rain that fell in those 5 minutes (yielding zero for rain-free 5-minute periods); these values were totalled then divided by total rainfall depth to give averages that more accurately reflect conditions during precipitation.

Event and 5-minute average rainfall inclination angles were also calculated using rainfall intensity, wind speed, and relationships with drop size and terminal fall velocity

(Herwitz and Slye, 1995). The Laws and Parsons (1943) best-fit equation is the basis for droplet size:

$$D = 2.23 (0.03937 PI)^{0.102}$$

where D is median raindrop diameter (mm) and PI is rainfall intensity (mm h^{-1}). The following empirical best-fit equation (Gunn and Kinzer, 1949) yields terminal fall velocity:

$$U_v = (3.378(\ln(D))) + 4.213$$

where U_v is terminal velocity (m s^{-1}) of any droplet of diameter D . Substituting this value and wind speed allows for calculation of inclination angle:

$$\tan P_{inc} = \frac{W_{wt5}}{U_v}$$

where P_{inc} is rainfall inclination angle (degrees from vertical), W_{wt5} is 5-minute weighted average wind speed (m s^{-1}), and U_v is terminal fall velocity (m s^{-1}).

3.2.5 Data Analysis

As described in section 2.2.4, we used exploratory cluster analysis to assign the 37 study trees to clusters reflecting two general canopy morphologies: single-leader ($n = 20$) and multi-leader ($n = 17$). Herwitz (1987) and others have documented that SF drains to and along the undersides of upright branches, suggesting that SF production processes might differ in trees with single trunks vs. multiple major leaders.

The TBRG rainfall depths were evaluated against those collected in the adjacent manually read rain gauge using double mass analysis (Searcy and Hardison, 1960). The double mass analysis found that, respectively, the slope and intercept of the regression of TBRG depth vs. manual gauge depth were not significantly different ($\alpha = 0.05$) than unity or zero prior to April 1, 2013; however, and although the cause is not clear, the

slope and intercept of the TBRG depth vs. manual gauge depth were found to be significantly ($p \leq 0.05$) different for the period after April 1, 2013. Thus, the following correction factor was applied to all recorded TBRG depths after that date:

$$TBRG_{corr} = (1.112 \cdot TBRG_{meas}) - 0.142$$

where $TBRG_{corr}$ is the corrected event rain depth value and $TBRG_{meas}$ is the value originally logged by the TBRG.

For all valid rainfall events for each study tree in full leaf, transitional, and leaf-off condition, rainfall depths (mm) and corresponding SF volumes (L) were sorted from smallest to largest rainfall depth. Data for events with rain depths equal to or greater than the first event that yielded $SF \geq 0.01$ L, even if some of these larger events produced no SF , were plotted (P in mm vs. SF in L). Linear regression yielded the threshold of SF initiation, P'' (absolute value of the intercept divided by the slope), and the flow rate once P'' had been satisfied (slope, Q_{SF}).

There is precedent in the SF literature for using multiple regression to analyze the influences of both trait and meteorological variables (e.g., Staelens et al., 2008; Van Stan et al., 2014b). We elected to use stepwise-up multiple regression to identify the major variables influencing the dependent variables (Armstrong and Hilton, 2010), and addressed concerns regarding multicollinearity between independent variables by ensuring that $r^2 < 0.64$ (Hair et al., 1998). All multiple linear regressions (stepwise-up) were run in Smith's Statistical Package (SSP) following transformations of dependent and independent variables (if necessary) as described in section 2.2.4. To facilitate comparison of Q_{SF} for trees of widely varying sizes, leaf-on multiple regression analyses at the group level were done for flow rate per unit PCA , $Q_{SF} PCA^{-1}$ ($L mm^{-1} m^{-2}$), as well as for P'' and Q_{SF} . Using a total of 18 trait variables, we identified those which significantly ($p \leq 0.05$ and $p \leq 0.10$) explained variation in P'' , Q_{SF} , and $Q_{SF} PCA^{-1}$ for each of the tree groups. Group A analyses used 17 variables as L_n was constant.

On an individual tree basis, we explored the role of actual canopy cover, ACC , during spring and fall using multiple regression (SSP) of SF volume on P and ACC , calculated as:

$$ACC = WC + LF(CC - WC)$$

where LF = observed leaf fraction at event date. The influence of storm meteorology on SF volume was also analyzed at the tree level with multiple regression yielding an equation of significant ($p \leq 0.10$) meteorological variables (out of 8 potential variables for leaf-on and leaf-off condition or 9 variables including ACC for transitional leaf condition). Occurrence or non-occurrence of a significant ($p \leq 0.10$) meteorological variable in each tree's equation formed the basis of a full-sample analysis (both groups combined) using a one-way ANOVA with Tukey HSD post-hoc (Tukey, 1953; see Zar, 1984) in IBM® SPSS® Statistics Version 22 (hereafter SPSS®) to detect associations between meteorological variables and canopy characteristics of trees for which they were influential.

3.3 RESULTS

3.3.1 Precipitation Profile

Between June 12, 2012 and November 2, 2013, 101 events with precipitation depths ≥ 0.2 mm were recorded; frequencies of depth by precipitation type are presented in Figure 3.2. A total of 394.4 mm fell: 327.9 mm as rain (86 events), 9.3 mm as mixed (4 events), and 57.2 mm as snow (11 events). We collected 89.8 % of this total depth and estimated the remainder (primarily snow) using Environment Canada data for the nearby “Kamloops A*” station. Frequency of rain by depth class approximated 1981–2010 normals for Kamloops (in parentheses): 80.7 % (82.4 %) for 0.2 to 5 mm, 10.2 % (13.4 %) for 5 to < 10 mm, and 9.1 % (4.3 %) for ≥ 10 mm. The higher frequency of larger events reflects that the study extended through two summers: July and August have the highest rain-day values for storms ≥ 10 mm.

3.3.2 Influence of Canopy Characteristics

In total, 37 isolated trees of 21 cultivated species were chosen (10.2–68.7 cm *DBH*, Table 2.1). Table 2.2 summarizes means and ranges for these trait metrics for each group. Derived values for P'' , Q_{SF} , and $Q_{SF} PCA^{-1}$ for individual Group A and B leaf-on trees are provided for reference in Tables A.1 and A.2, respectively, along with measured and calculated trait variables. Leaf-on, transitional, and leaf-off P'' and Q_{SF} values are listed in Tables A.3, A.4, and A.5. Results of multiple regressions of P'' , Q_{SF} , and $Q_{SF} PCA^{-1}$ for Group A and B trees on canopy trait variables are presented in Table 3.1.

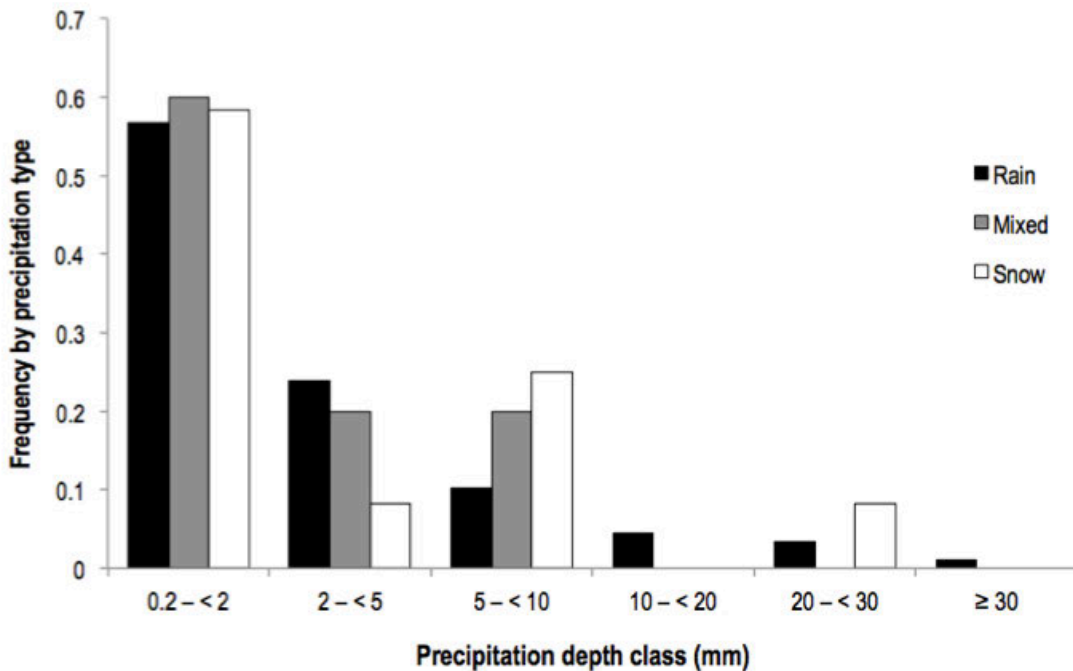


Figure 3.2. Frequency of precipitation events by type and depth class.

For rain events < 3 mm while trees were either in full leaf or completely leafless, SF volume was plotted against rain depth. Figure 3.3 depicts, for four variously sized trees (two each from Groups A and B), the patterns that were evident for most trees.

Table 3.1. Multiple regression equations for stemflow initiation thresholds, P'' (mm), flow rates post-initiation, Q_{SF} ($L\ mm^{-1}$) and flow rates per unit projected canopy area $Q_{SF}\ PCA^{-1}$, ($L\ mm^{-1}\ m^{-2}$) as functions of tree morphological traits, generated for single-leader (Group A, $n = 20$) and multi-leader trees (Group B, $n = 17$).

Equation	R^2	SEE	$p \leq$
P'' Group A			
$-18.10 \frac{1}{DBH} + 1.34 BRI^3 + 2.56$	0.528	0.69	0.05
$-11.85 \frac{1}{DBH} - 313.76 \frac{1}{CC} + 1.57 BRI^3 + 32.19 \frac{1}{AIU}$	0.660	0.62	0.10
P'' Group B			
$-10.63 \frac{1}{BRI} + 2.34 \ln H$	0.546	1.31	0.05
$-9.11 \frac{1}{BRI} + 2.72 \ln H - 0.010 L_n^3$	0.632	1.22	0.10
Q_{SF} Group A			
$(0.23 \sqrt{H} + 2.62 BRI - 0.015 B_n + 0.12 \ln Vol_c - 0.47 \frac{1}{MLS} - 2.64)^2$	0.860	0.16	0.05
Q_{SF} Group B			
$e^{(0.51 L_n + 3.51E-06 WC^3 - 0.67 BRI^3 + -36.35 \frac{1}{AIF} - 0.0002 CW^3)}$	0.952	0.22	0.05
$Q_{SF}\ CPA^{-1}$ Group A			
$e^{(0.0006 AIF^2 - 2.48 \frac{1}{BRI} - 1.14 \frac{1}{MLS} - 2.17)}$	0.853	0.33	0.05
$e^{(0.0004 AIF^2 + 7.76E-06 WC^3 - 6.09 \frac{1}{BRI} - 6.31E-06 B_n^3 - 5.23E-06 DBH^3 - 1.22 \frac{1}{MLS})}$	0.931	0.25	0.10
$Q_{SF}\ CPA^{-1}$ Group B			
$-0.062 \ln CW + 1.48E - 07 WC^3 - 0.10 BRI + 1.15E - 07 AIF^3 + 0.0004 L_n^3 + 0.25$	0.901	0.013	0.05

Stemflow from leafless trees generally started at lower threshold rain depths than when leaves were present, and when it was produced, volumes were often higher for leafless trees at a given rain depth. For rain depths > 2 mm, the pattern was less consistent with SF production from leafed canopies occasionally exceeding that for leafless trees.

3.3.3 Influence of Meteorological and Seasonal Factors

For leafed and leafless trees with data for ≥ 9 rain events, *SF* volume was regressed on eight core meteorological variables; a ninth variable, *ACC*, was used for trees in leaf transition with ≥ 10 events. Table 3.2 indicates if meteorological variables were significantly positively or inversely related to *SF* volume for all leaf conditions. Squares, circles, and triangles, in columns beneath each meteorological variable, represent leaf-on, leaf-transition, and leaf-off conditions, respectively; solid symbols indicate a positive correlation, while open symbols reflect an inverse relationship. Where an “x” symbol is shown, this variable was not significant ($p \leq 0.10$) in the regression. Finally, blank cells indicate that there was insufficient data to run the regression for that tree in that leaf condition. Corresponding regression equations for individual trees are provided in Tables A.6, A.7, and A.8.

For each leaf condition, at least one meteorological variable’s presence in a group of trees’ regression equations was associated with a significantly ($p \leq 0.10$) different trait mean compared to the group for which that variable was absent. Table 3.3 summarizes these relationships between meteorological and trait variables for our study trees.

Figure 3.4 presents graphs for a subset of trees (representative of most study trees) showing the general tendency for *SF* volumes to be greatest for mixed precipitation, intermediate for rain, and least for snow events. For example, for tree A-2, less than 0.4 mm of *SF* each was measured for 5.8-mm (SWE) and 6.4-mm (SWE) snow events while a 5.3-mm (SWE) mixed event produced 2.84 L and a 6.7-mm rain event produced 3.33 L of *SF*. For A-7, the highest volume of *SF* for events < 2.2 mm was 4.83 L for a 1.6-mm (SWE) mixed event. All other rain events in this depth range produced ≤ 2.59 L of *SF* (less than 54 % of the mixed-event volume). In even greater contrast, a 3.2-mm (SWE) snow event produced no *SF* for B-2 whereas 4.0 mm (SWE) of mixed precipitation generated 5.76 L of *SF*. However, the same tree produced only 0.22 L of *SF* from a larger 5.3-mm (SWE) mixed event.

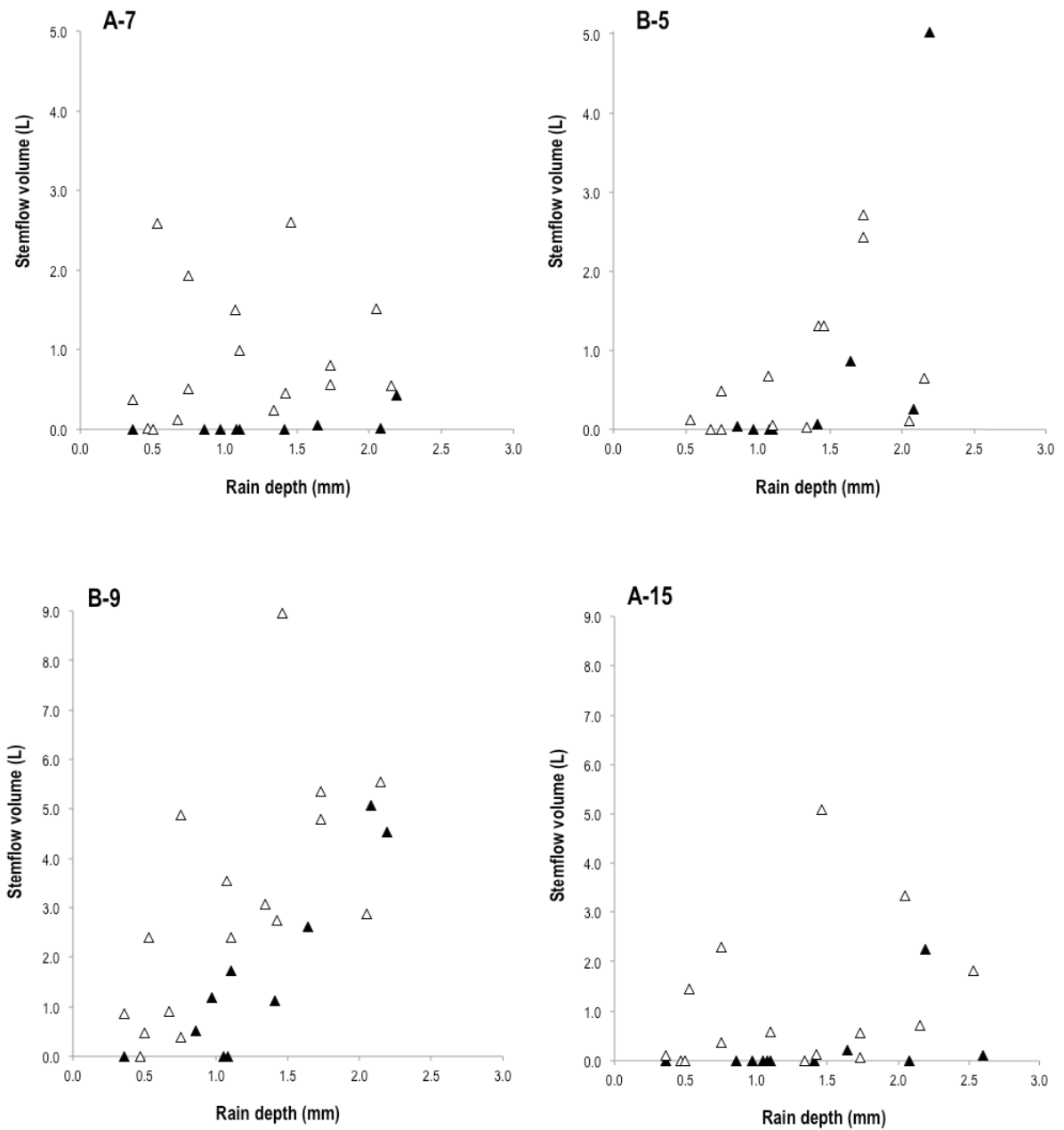


Figure 3.3. Comparison of stemflow volume (L) produced from rain events less than 3 mm by trees in full leaf (▲) vs. leafless (△) conditions.

Table 3.2. Summary of meteorological variables significantly ($p \leq 0.10$) related to stemflow volume during leaf-on (square), transitional (circle), and leaf-off (triangle) conditions per regression equations presented in Tables A.6, A.7, and A.8.

Tree ID	P	D_R	D_B	I_{wt5}	I_{max5}	P_{inc}	W_{wt5}	VPD^1	ACC
A-1	■ ▲	× ×	× △	× ▲	× ×	× ×	■ ×	× ×	
A-2	■●▲	×××	×○×	×××	×××	×××	■××	■××	×
A-3	■ ▲	× ×	× ×	× ×	× ×	× ▲	× ×	× ×	
A-4	■●×	×××	×○×	×××	×○×	■××	×●▲	■××	○
A-5	■●▲	×××	○××	×××	×××	■×▲	×××	■××	○
A-6	■●▲	×××	□×△	×××	××△	■××	××▲	■××	○
A-7	■ ▲	× ×	× ×	× ×	× ×	■ ×	× ▲	× ×	
A-8	■ ▲	× ×	× ×	× ×	× ×	× ×	× ▲	× ×	
A-9	■ ▲	× ×	× △	× ×	× △	■ ×	× ▲	■ ×	
A-10	■●▲	×××	×○×	×××	××▲	■××	×●▲	×××	○
A-11	■ ▲	× ×	× ×	× ×	× ×	■ ▲	× ×	■ ×	
A-12	■●	××	××	××	××	××	××	×○	○
A-13	■	×	×	×	×	■	×	■	
A-14	■ ▲	× ×	× ×	× ×	□ ▲	■ ×	■ ▲	■ ×	
A-15	■ ▲	× ×	× ×	× ×	× ×	× ×	■ △	× ▲	
A-16	■●×	×××	×××	×××	××▲	×××	××▲	××▲	×
A-17	■●	××	×○	××	×○	■×	××	××	○
A-18	■	×	×	×	×	×	×	■	
A-19	×●▲	■××	×○×	×××	■○×	×××	××▲	××▲	○
A-20	■	×	×	×	×	×	■	■	
B-1	×●×	■××	×××	××▲	×●×	■××	×××	×××	×
B-2	■ ▲	× ×	× ×	× ×	× ×	■×▲	× ×	■ ×	
B-3	■●▲	×××	□×△	■×▲	■××	×××	■××	■××	○
B-4	■●▲	×××	×××	×××	×××	××▲	×●×	×××	×
B-5	■ ▲	× ×	× △	× ×	× ×	× ×	■ ×	× ×	
B-6	■ ▲	× ×	× ×	× ×	× ×	× ×	××▲	×××	×
B-7	■	×	■	■	×	×	×	■	
B-8	■	×	×	×	×	■	×	■	
B-9	■ ▲	× ×	□ ×	× ×	× ×	× ×	■ △	■ ▲	
B-10	■ ▲	× ×	× ×	× ×	× ×	× ×	× ▲	□ ×	
B-11	■ ▲	× ×	× ×	× ×	× ×	×	■ ▲	■ ×	
B-12	■	×	×	×	×	×	×	×	
B-13	■	×	×	■	■	×	×	×	
B-15	▲	×	×	×	×	×	×	×	
B-17	■	×	×	×	×	×	■	■	

Legend for occurrence and sign of regression coefficients (significance level per individual equations, see Tables A.6, A.7, and A.8):

Leaf-on: ■ = positive, □ = negative, × = non-occurrence

Leaf transition: ● = positive, ○ = negative, × = non-occurrence

Leaf-off: ▲ = positive, △ = negative, × = non-occurrence

Blanks reflect trees and leaf conditions for which there was insufficient data for regression analysis (e.g., too few events were available for analysis of B-14, B-15, and B-16 in any leaf condition).

Table 3.3. Summary of means and standard deviations for canopy traits of trees grouped by whether or not each meteorological variable was significant (“occurred”, $p \leq 0.10$) in the individual tree’s *SF* volume regression equation (between-group differences analyzed via one-way ANOVA, $p \leq 0.10$).

Meteorological Variable (sign indicates positive/ negative relationship with stemflow volume)	Trait Variable	Non-occurrence group mean \pm SD (n)	Occurrence group mean \pm SD (n)	<i>p</i> - value
LEAF-ON CONDITION				
+ Rainfall intensity (5-min weighted average)	Bark relief index	1.10 \pm 0.08 (32)	1.26 \pm 0.22 (2)	0.018
	Frequency (discontinuity)	0.15 \pm 0.15 (32)	0.36 \pm 0.33 (2)	0.081
+ Rainfall inclination angle (5-min weighted average)	<i>DBH</i> (cm)	32.9 \pm 16.9 (21)	20.4 \pm 7.4 (13)	0.018
	Average canopy spread (m)	8.4 \pm 4.0 (21)	6.1 \pm 1.9 (13)	0.054
	Canopy volume (m ³)	690.4 \pm 895.6 (21)	214.8 \pm 158.5 (13)	0.068
	Wood volume (m ³)	75.9 \pm 103.4 (21)	15.2 \pm 18.2 (13)	0.045
	Intersection angle, full tree (deg. above horizontal)	41.9 \pm 13.0 (21)	49.0 \pm 9.9 (13)	0.100
	Branch count	46.9 \pm 20.8 (21)	32.2 \pm 15.2 (13)	0.035
+ Wind speed (5-min weighted average)	Canopy volume (m ³)	382.6 \pm 408.6 (26)	917.7 \pm 1322.1 (8)	0.074
	Wood volume (m ³)	35.7 \pm 46.0 (26)	107.8 \pm 152.4 (8)	0.037
	Median leaf size (cm ²)	21.6 \pm 13.4 (26)	35.7 \pm 26.4 (8)	0.050
+ Inverse vapour pressure deficit (variable transformed)	Average angle, full tree (deg. above horizontal)	47.6 \pm 18.2 (18)	37.1 \pm 14.2 (15)	0.080
TRANSITIONAL LEAF CONDITION				
– Total break duration (h)	No. branches, full tree	42.7 \pm 21.4 (6)	25.3 \pm 9.7 (6)	0.100
	No. leaders at canopy base	1.83 \pm 1.0 (6)	1.0 \pm 0.0 (6)	0.065
LEAF-OFF CONDITION				
+ Rainfall inclination angle (5-min weighted average)	Wood cover (%)	27.0 \pm 10.3 (20)	14.6 \pm 2.7 (5)	0.015
+ Inverse vapour pressure deficit (variable transformed)	<i>DBH</i> (cm)	21.7 \pm 12.0 (21)	36.7 \pm 12.3 (4)	0.032
	Tree height (m)	9.1 \pm 2.5 (21)	12.2 \pm 1.5 (4)	0.027
	Wood cover (%)	22.8 \pm 10.3 (21)	33.4 \pm 7.0 (4)	0.062

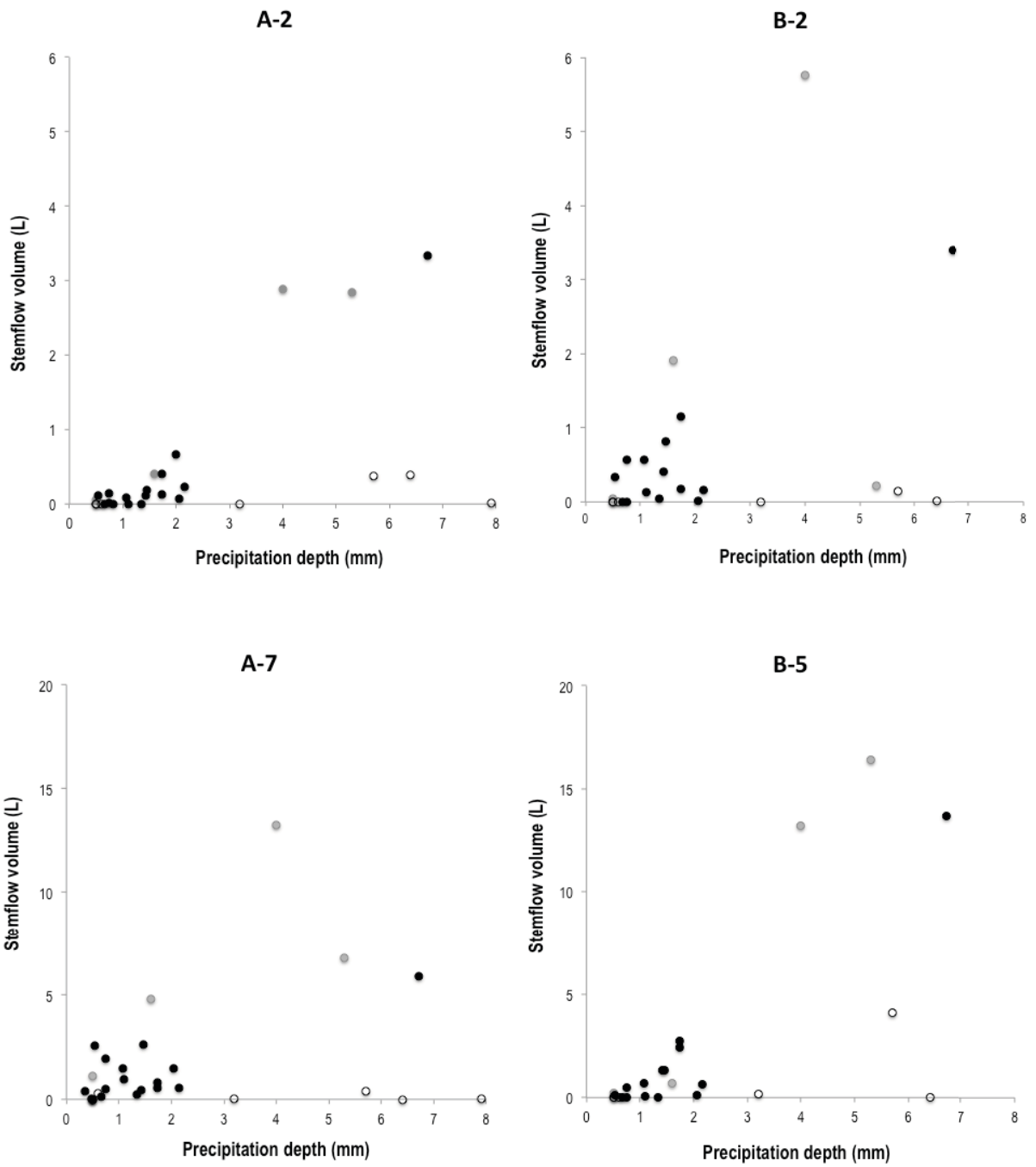


Figure 3.4. Graphs of measured SF generated from rain events (●) and from snow–water equivalent (SWE) depths for snow (○) and mixed (●) precipitation events.

3.4 DISCUSSION

3.4.1 Canopy Traits Influencing Stemflow from Rain in Leaf-on Condition

Derived measures of stemflow— SF as a percentage of incident rain on a projected canopy area, PCA , basis, $SF\%$, and the SF funneling ratio, FR (Herwitz, 1986)—are commonly used to report and compare SF production (e.g., Levia and Frost, 2003; Carlyle-Moses et al., 2010; Germer et al., 2010). Prior to discussing our findings in these terms, we examine the influence at the tree group level of canopy traits on threshold rain depth for SF initiation, P'' and post-initiation SF rate, Q_{SF} (the combination of which determines SF volume), as well as on Q_{SF} standardized per m^2 PCA ($Q_{SF} PCA^{-1}$).

3.4.2 Stemflow Initiation Threshold

Examination of the multiple regression equations in Table 3.1 reveals some common factors within and between groups for different dependent variables. Firstly, P'' was directly related to diameter at breast height, DBH , but only for single-leader trees; on the other hand, bark relief index, BRI , was positively related to P'' for both single- and multi-leader trees. The influence of BRI is apparent when comparing P'' for Group A and B trees of similar size whereby smoother bark (in concert with other traits) is associated with lower P'' :

- A-6 ($DBH = 15.1$ cm, $BRI = 1.01$, $P'' = 2.0$ mm) vs. B-1 ($DBH = 15.2$ cm, $BRI = 1.22$, $P'' = 3.6$ mm)
- A-9 ($DBH = 19.0$ cm, $BRI = 1.09$, $P'' = 3.7$ mm) vs. B-3 ($DBH = 18.8$ cm, $BRI = 1.01$, $P'' = 1.3$ mm)
- A-18 ($DBH = 43.0$ cm, $BRI = 1.15$, $P'' = 3.9$ mm) vs. B-11 ($DBH = 43.0$ cm, $BRI = 1.25$, $P'' = 3.8$ mm)

For Group A, additional trait variables were significant at the $p \leq 0.10$ level: canopy cover, CC (positive) and angle of branch intersection in the upper canopy, AIU

(negative, such that higher P'' was associated with lower branch angles as measured from horizontal). Neither of these variables was significant ($p \leq 0.10$) for multi-leader P'' while tree height was a factor only for Group B trees. Finally, the number of leaders was inversely related to P'' for the multi-leader trees.

In this study, the smallest events to generate $SF \geq 0.1$ % of incident rainfall were 1.0 mm for A-1 and 0.9 mm for B-3 and B-9. These compare to mean SF initiation thresholds of 3.4 ± 0.3 mm for beech and 10.9 ± 1.2 mm for oak in a temperate mixed forest (André et al., 2008b), > 1 mm and > 4 mm for urban *Eucalyptus saligna* and *E. nichollii* trees, respectively (Livesley et al., 2014), and 1.4–4.8 mm for six species in a laurel forest in the Canary Islands (Aboal et al., 1999a). Study trees with the lowest derived thresholds included A-1 (small DBH with smooth bark and numerous, steeply inclined branches), A-3 (small, smooth bark, high CC), B-3 (small, smooth, with numerous branches), and B-9 (medium-sized but extremely smooth-barked with many leaders). These examples serve to confirm the importance of conducive traits identified by others including smooth bark (Levia and Herwitz, 2005; Van Stan and Levia, 2010) and high branch inclination angles (Herwitz, 1987; Xiao et al., 2000; Levia et al., 2013). As we did for single-leader trees, André et al. (2008) found that lower P'' (reflecting lower apparent storage capacity) was associated with smaller DBH trees; for our multi-leader trees, tree height, H , was highly correlated with DBH (Spearman $r \leq 0.01$), and may have been acting as a proxy for the latter size-related variable. The fact that the number of leaders converging at the base of the canopy, L_n , was inversely related to P'' for Group B suggests that the benefits of having multiple major SF flowpaths to the base of the canopy outweighed the disadvantages associated with increased wood area to be saturated, particularly for smooth-barked trees.

3.4.3 Stemflow Rate

While Q_{SF} was significantly ($p \leq 0.05$) correlated with BRI in both Group A and B trees, it was positively correlated for single-leader trees, but inversely related for multi-

leader trees. This implies that, for single-leader trees, more deeply furrowed (now saturated) bark may contribute to higher SF rates, particularly if furrows are linear rather than diamond-shaped or forked (Levia and Herwitz, 2005). In fact, the five highest Q_{SF} values among Group A trees (1.97–3.61 L mm⁻¹) were for trees with moderate bark relief (BRI ranging from 1.15–1.20) and bark with linear furrows. The highest $Q_{SF}PCA^{-1}$ value was for A-14, an English columnar oak with linearly furrowed bark of moderate relief. Others have documented the promotion of SF production (and resistance to evaporative forces) by such linear microrelief, despite its association with higher normative bark water storage and delay of SF initiation (Levia and Herwitz, 2005). Our findings confirm that, certainly for single-leader trees, bark with moderate relief and linear furrows was associated with high Q_{SF} . Most smooth- and flaky-barked trees had lower rates, although two of the highest $Q_{SF}PCA^{-1}$ values were for trees with extremely low BRI , suggesting that other traits (such as high branch angles) in association with bark relief may contribute to high rates on a per-canopy-area basis.

It is possible that greater wood surface areas associated with multi-leader trees may result in a gradual increase in Q_{SF} during the time between satisfaction of P'' (SF begins) and full saturation, but as discussed below, L_n appeared to be more important than any other factor for Group B trees. Tree height explained more variability in Q_{SF} (57 %) than any other factor for Group A trees, though it was not significant ($p \leq 0.10$) for Group B trees and is not identified frequently in the literature (e.g., Germer et al., 2010). It is possible that H was acting as a proxy for DBH (as discussed above) or other closely correlated size-related variables in this study. Branch count, B_n , was inversely related to Q_{SF} in single-leader trees only. Reduced SF with more branches was also found by Herwitz (1985), who attributed this effect to increased storage capacities, but Návar (1993), Aboal et al., (1999b), and Levia et al. (2013) all found higher B_n to promote SF . Specifically, Levia et al. (2013) concluded that woody biomass, branch count (both per unit PCA), and mean inclination angles were the most important factors governing $SF PCA^{-1}$ in their study of European beech saplings. For Group A trees, higher canopy

volume, Vol_c , was associated with higher Q_{SF} , which is consistent with the findings of Martinez-Meza and Whitford (1996) for certain desert shrubs, Crockford and Richardson (1990) for pine and eucalypts (crown size per DBH), and Aboal et al. (1999b) for a laurel forest. Aboal et al. (1999b) also noted that small leaves contributed to more efficient SF production, counter to the positive relationship between median leaf size, MLS , and Q_{SF} for our Group A study trees. For Group B trees, L_n explained 52 % of variation in Q_{SF} while WC was also positively related; given that L_n has not been examined to our knowledge (although both factors are consistent with findings of Levia et al. [2013] that woody biomass is associated with high SF), we recommend further study to refine understanding of its potential role. The regression equation for Group B Q_{SF} suggests that L_n may be of particular importance when a tree also has smooth bark and high full-canopy intersection angles, AIF , and when canopy width, CW , is relatively small (minimizing the distance that SF needs to travel to reach the bole). Few specific results are published on CW , but many authors corroborate the importance of associated traits such as high branch inclination angles for SF in trees and shrubs (Martinez-Meza and Whitford, 1996; Crockford and Richardson, 2000; Barbier et al., 2009; Levia et al., 2013; Van Stan et al., 2014b). Herwitz (1987) observed that > 80 % of impacting rain became branchflow for branch angles > 60° in the laboratory, but there is a “tipping point” at which the benefits of high branch angles in conducting SF will be offset by a tree’s smaller projected canopy area (Pypker et al., 2011; Levia et al., 2013).

Derived Q_{SF} for single-leader trees ranged from 0.33 L mm⁻¹ (A-3: small, smooth, relatively few branches) to 3.61 L mm⁻¹ (A-20: tallest study tree, large volume, moderate BRI , disproportionately low branch count). For multi-leader trees, Q_{SF} ranged from 0.48 L mm⁻¹ (B-4: moderate BRI , only one secondary leader, low wood cover, WC , and AIF , relatively high CW for its size) to 7.45 L mm⁻¹ (B-9: very smooth bark, many leaders, moderate WC , relatively low branch angles, average CW). The low P'' and high Q_{SF} for B-9 contribute to exceptional SF % and FR values as discussed below despite moderate branch angles and a broad canopy. This tree’s early and voluminous SF

production in this study is consistent with findings of others studying beech species (e.g., Levia et al., 2013, 2010; Staelens et al., 2008; Van Stan et al., 2014b). Based on observations of SF on the study tree's trunk (Videos B.1–B.4), it is possible that the bark may be not only smooth but hydrophobic, a condition that may have been enhanced by the presence of water-repellent lichen (Shirtcliffe et al., 2006) which we observed along preferential flowpaths on the trunk of B-9 (and other study trees). Water repellency in *Acacia* bark has been linked to presence of a waxy substance called suberin (Borgin and Corbett, 1974), which has also been extracted from beech bark (Perra et al., 1993).

For comparison, a sample of SF rates observed by others includes $0.08 \pm 0.04 \text{ L mm}^{-1}$ for oak and $0.09 \pm 0.02 \text{ L mm}^{-1}$ for beech in a mixed stand (André et al., 2008b), and a range of 0.070 ± 0.011 to $0.172 \pm 0.013 \text{ L mm}^{-1}$ for five tropical tree species (Park and Cameron, 2008). The derived rate for B-9 in our study is over 43 times greater than the highest rate calculated by Park and Cameron (2008), which even the lowest rates for our study trees exceed. Researchers in urban environments have long been aware that SF rates and yields tend to be greater for isolated trees (e.g., Xiao et al., 2000; David et al., 2006; Guevara-Escobar et al., 2007) though the magnitude of this effect depends on climate, rainfall depth, and storm meteorology, as well as tree species and size. In general, gains due to unobstructed precipitation from all directions more than offset losses from an open-grown canopy to evaporative forces (Gash et al., 1995) and direct wind that can dislodge potential SF from leaves and woody surfaces.

For $Q_{SF} PCA^{-1}$, BRI was again positively related for Group A trees and inversely related for Group B trees; standardizing the Q_{SF} rate per unit PCA did not remove these effects. Angle of intersection (full tree) explained over 73 % of variation in $Q_{SF} PCA^{-1}$ for Group A and was also a positive factor for Group B; this once again agrees with the results of many studies cited above (e.g., Levia et al., 2013), and confirms that this factor remains highly influential once rate is standardized per unit PCA . Remaining factors for Group A were MLS and WC (both positive) and B_n and DBH (both inverse) of which WC was inversely related to $Q_{SF} PCA^{-1}$ for Group B (WC appears to promote SF when there's

a primary bole, but suppresses it when multiple leaders convey flow to the base of the canopy). The inverse relationship between DBH and $Q_{SF} PCA^{-1}$ indicates that single-leader trees with lower basal areas tended to have higher rates per PCA , as well as lower P'' , meaning that for small events especially, they are likely to out-produce larger- DBH trees. Canopy width explained 38 % of variability in $Q_{SF} PCA^{-1}$ for Group B trees; given that it was inversely related, this likely reflects that traits associated with narrower trees (e.g., high branch angles and CC) promote SF in multi-leader trees. The final positive factor for Group B trees, one also significant ($p \leq 0.10$) for P'' and Q_{SF} , was L_n : more leaders meant higher yields due to both lower thresholds and higher rates. Highest derived $Q_{SF} PCA^{-1}$ for Group A trees was $0.202 \text{ L mm}^{-1} \text{ m}^{-2}$ for A-14 (the tightly columnar oak with relatively high BRI and WC as well as exceptionally high branch angles) and for Group B was $0.113 \text{ L mm}^{-1} \text{ m}^{-2}$ for B-9 (the American beech with very low BRI and numerous leaders but moderate values for other conducive traits).

3.4.4 Stemflow Percent

Mean $SF\%$ values for Group A trees for the 2 to < 5 mm, 5 to < 10 mm, and ≥ 10 mm rain depth classes were $0.9 \pm 0.9\%$, $2.8 \pm 3.3\%$, and $3.1 \pm 2.8\%$ while for Group B trees, mean $SF\%$ values for these rain depth classes were $0.8 \pm 1.2\%$, $2.0 \pm 2.5\%$, and $2.7 \pm 2.6\%$, respectively. The highest mean $SF\%$ values for individual Group A trees for the 2 to < 5 mm, 5 to < 10 mm, and ≥ 10 mm rain depth classes were $3.6 \pm 4.8\%$ (A-15), $12.0 \pm 10.1\%$ (A-15), and $12.3 \pm 8.4\%$ (A-14). For Group B, the highest means in the same depth classes were $4.3 \pm 3.6\%$, $9.6 \pm 6.7\%$, and $9.9 \pm 1.4\%$, all for B-9. Event maximum $SF\%$ for the single-leader and multi-leader groups, respectively, were 27.9% for A-15 for a 5.2-mm event and 18.7% for B-9 for an 8.8-mm event.

For context, Livesley et al. (2014) observed average $SF\%$ values of 0.2–0.3 % and 1.5–1.7 % for *E. nichollii* and *E. saligna*, respectively, over three years in Melbourne, Australia. Guevara-Escobar et al. (2007) measured $SF\%$ of 0–5.7 % (mean 2.20 %) beneath a *Ficus benjamina* tree in Queretaro City, Mexico. Levia et al. (2013) reported an

average *SF* % of 2.4 ± 1.5 % for the European beech saplings in east-central Germany, while Staelens et al. (2008) found *SF* % ranging from 3.3 % for precipitation depths of 2 to < 5 mm to 8.9 % for depths of 15–35 mm with an average of 6.4 % for a dominant beech tree in Belgium. Van Stan et al. (2014a) found mean *SF* % of 0.9 % for yellow poplar in contrast to 5.3 % for American beech in the northeastern United States, a difference they attributed primarily to steeper branch angles and smoother bark (i.e., lower canopy storage capacity) of beech canopies. High branch angles ($> 67^\circ$) were measured for both A-14 (English columnar oak) and A-15 (Armstrong Freeman maple) (these two trees had by far the greatest height-to-width ratios in our study); A-15 was smooth-barked, but A-14 had convoluted bark with linear furrows, an illustration of the apparent advantage of furrowed bark once *P*'' is satisfied. Once again, the American beech (B-9) out-produced all Group B trees in terms of *SF* % means and event maximums, reflecting the combination of conducive traits noted above including smooth bark and many leaders fed by moderately angled branches.

3.4.5 Funneling Ratios

The highest mean *FR* values for individual trees for the 2 to < 5 mm, 5 to < 10 mm, and ≥ 10 mm rain depth classes were, respectively, 31.5 ± 20.9 (A-5), 50.7 ± 33.6 (A-1), and 58.6 ± 12.0 (A-5) for Group A trees and 24.1 ± 19.9 , 53.5 ± 37.1 , and 81.3 ± 64.9 , all for B-9. These compare to means of 13.0 ± 1.3 and 53.0 ± 4.0 for two American beech trees with *DBH* 74.9 cm and 10.3 cm, respectively (Levia et al., 2010) and a maximum mean *FR* of 47.2 for five intermediate-sized beech trees over 10 months (Van Stan and Levia, 2010). Gómez et al. (2002) documented funneling ratios of 51, 60, and 85 over 12 rain events for three olive trees. Event maximum *FR* values for Group A and B trees, respectively, were 117.8 for A-3 for a 9.7-mm event and 196.9 for B-9 for a 25.6-mm event, exceeding values reported in the literature for trees which include 100.6 for a 10.3 cm *DBH* beech during a 2.5-mm rain event (Levia et al., 2010) and 71 for small palm trees (Germer et al., 2010). A detailed discussion of factors influencing *SF* % and *FR* is provided in Chapter 2. Once again, we expect that the absence of neighbouring

canopies for our study trees enhanced the effects of conducive canopy architecture and exposure to wind-driven rainfall as discussed below.

3.4.6 Influence of Leaf Condition on Stemflow from Rain

The tendency of leafless trees in both groups to produce *SF* at smaller rain depths and in greater quantities for a given rain depth < 3 mm compared to full leaf condition (Figure 3.3) is consistent with the significance ($p \leq 0.10$) of actual canopy cover, *ACC*, in regression equations for over half of the study trees analyzed in transitional leaf states (Table A.7): *SF* volume varied inversely with *ACC* for these trees in our climate. While many researchers have observed this pattern (Helvey and Patric, 1965; Xiao et al., 2000; André et al., 2008; Staelens et al., 2008), others have found the reverse (Liang et al., 2009b) or no significant difference between seasons (Deguchi et al., 2006). The observed pattern of increased *SF* yields from defoliated trees was less distinct as rain depth increased, implying that storm characteristics and other canopy traits may supersede *ACC* in importance. For example, Van Stan et al. (2014b) found that 1) presence of leaves increased direct associations between *SF* and rainfall intensity for yellow poplar and American beech; 2) a positive relationship between *SF* and wind speed for leafed canopies switched to an inverse one for leafless canopies; 3) beech exhibited strengthened differences between leaf states for *SF*–rainfall depth and *SF*–wind speed associations; and 4) relationships were further modified by *DBH* class.

3.4.7 Meteorological Influences on Stemflow from Rain for Various Leaf Conditions

Table 3.2 shows the dominant influence of rain depth, *P*, on *SF* volume for individual trees: in only two cases did rain duration (usually closely correlated with depth) supercede *P*. This finding is supported by most studies including André et al. (2008b) for oak and beech and Levia et al. (2010) and Van Stan et al. (2014b) for beech and yellow poplar. Xiao et al. (2000) made the distinction that *SF* for saturated canopies was tightly controlled by *P* while *SF* from unsaturated canopies reflected storage capacity

and the various morphological and meteorological factors associated with wetting-up. Carlyle-Moses and Price (2006) found that *FR* increased with greater rain depths up to a threshold for a growing-season mixed deciduous forest; once this level of saturation was reached, the authors speculated that flowpaths were overloaded and more intercepted rain was diverted to throughfall, *TF*.

Break duration was inversely related to *SF* (except for B-7), and was significant ($p \leq 0.10$) for various trees and leaf conditions. While some studies have explored intra-storm variability of *SF* (e.g., Levia et al., 2010), very few have quantified the influence of storm breaks. For an oak–beech stand, André et al. (2008b) did discern that while *SF* rate was not significantly affected by meteorological conditions preceding a storm event, storage capacity and rainfall threshold appeared to increase with the ratio of potential dry-period evaporation to preceding rain volume. In light of our findings, this relationship may also apply to intra-storm breaks.

Weighted 5-minute rainfall intensity was positively related to *SF* for only the smallest single-leader tree in leaf-off condition, but was significant ($p \leq 0.10$) for a few multi-leader trees in all except transitional leaf states. Maximum 5-minute intensity was inconsistent, being positively and inversely related to *SF* for trees in both groups and in all leaf conditions. According to Levia and Frost (2003) and exemplified by Carlyle-Moses and Price (2006) for red oak, sugar maple, and American beech, *SF* is often found to vary inversely with rainfall intensity; on the other hand, Van Stan et al. (2014b) observed positive correlations between *SF* and rainfall intensity for American beech and yellow poplar, but emphasize that tree size, bark relief, and other meteorological factors interact with intensity in complex ways. The variability in our results with respect to 5-minute weighted and maximum intensity likely reflects the morphological diversity of our study trees (37 individuals of 21 species and widely ranging sizes) and meteorological variability associated with our semi-arid climate.

When it was significant ($p \leq 0.10$), rainfall inclination angle, P_{inc} , was always positively correlated with *SF*, occurring frequently for Group A trees and occasionally for

Group B trees in leaf-on and leaf-off but not transitional states. Herwitz and Slye (1995) found differential *SF* generation from rain inclined $> 19^\circ$ from vertical across varying storm depths, durations, and intensities. Using this angle to categorize rainfall as inclined or not, Van Stan et al. (2011) found significant correspondences between wind-driven inclined rain and *SF* production in American beech and yellow poplar for almost all storm events. They observed preferential *SF* generation in both species when winds were from particular directions, and noted that the vertically deeper canopy (i.e., greater effective canopy area) of beech trees enhanced efficiency of inclined rainfall capture and funneling as *SF*. Among our trees, P_{inc} was a significant ($p \leq 0.10$) factor for *SF* volume for highly columnar A-14 in leaf-on condition, but there was no consistent association with greater height-to-width ratios. In our study, event average P_{inc} was $\geq 20^\circ$ for only 3 of 60 rain events (5 %), 10° to $< 20^\circ$ for 20 % of events, 5° to $< 10^\circ$ for 30 % of events, and $< 5^\circ$ for 45 % of events: the significance ($p \leq 0.10$) of P_{inc} for many trees in leafed and leafless conditions suggests that *SF* in isolated deciduous trees may be sensitive to rain falling at less inclined angles (from vertical) than observed in forest studies.

With two exceptions, 5-minute weighted average wind speed, W_{wt5} , was always positively related to *SF*; it occurred more commonly for leaf-on and leaf-off than transitional conditions. This is in agreement with findings of Xiao et al. (2000) for isolated oak and pear trees and André et al. (2008b) that higher wind speeds during rain enhanced *SF* production for oak and beech, apparently by reducing *SF* initiation thresholds. This direct association was strongly demonstrated by Van Stan et al. (2014b) for three size classes of American beech and yellow poplar during the growing season; for leafless canopies (particularly smaller ones), however, *SF* was inversely related to wind speed, possibly reflecting increased evaporation from bark in the absence of shelter from leaves.

After P , inverse vapour pressure deficit, VPD (i.e., transformed to enhance linearity for regressions), was the second-most common factor influencing *SF* volume, certainly for leaf-on trees; since the inverse variable influenced *SF* positively, higher values of

VPD were associated with lower *SF* volumes. Staelens et al. (2008) documented this relationship for a beech forest while Van Stan et al. (2014b) confirmed the inverse effect of *VPD* for leafed American beech and yellow poplar, noting that the effect was enhanced for taller trees.

3.4.8 *Stemflow from Snow and Mixed Events Compared to Rain*

Figure 3.4 shows actual *SF* volumes measured from four selected trees for four mixed and 11 snow events graphed along with *SF* generated by rain events in the same depth range using snow-water-equivalent (SWE) on the x-axis. The sample size is small and there is high variability in the actual *SF* values from mixed and snow events, but, with few exceptions, more *SF* was generated from mixed events (over three times more for some events) and less from snow events (not uncommonly zero or close to it). While data is limited, it seems that mixed precipitation in our climate may have properties relating to air and bark temperature that optimize adhesion (as opposed to snow that is less likely to adhere and subject to being dislodged by wind). Herwitz and Levia (1997) found substantial mid-winter *SF* drainage from bigtooth aspen in the northeastern United States (5–10 % of incident precipitation per *PCA*, despite below-zero temperatures), particularly when snow events coated bare trees in icy glaze; they theorized that the bark's low albedo promotes melting and drainage of intercepted snow and ice, a process subject to much lower *VPD* than in warmer seasons. Consistent with our findings, they also noted that *SF* from snow did not reliably increase with precipitation depth (as for rain), a lack of predictability that was even more pronounced for seven trees of three different deciduous species in Massachusetts (Levia, 2004). For a northern red oak examined in detail by Levia (2004), funneling ratios associated with snow events were significantly lower than for other precipitation types (as in our study), yet mean ratios (± 1 SE) overlapped for rain, rain-to-snow, and snow-to-rain, suggesting that precipitation type was less influential than other meteorological factors, particularly duration and intensity of precipitation in concert with high wind speeds. Our observation that mixed events often resulted in more *SF* than comparable rain and snow events is

consistent with findings of Levia (2003) who related low levels of *SF* chemical enrichment for rain, sleet, and snow events to short residence times (for all three) as well as low interception for sleet and snow, a factor that we suggest is particularly limiting for small trees.

Based on observations that larger trees in our study retained more snow than small ones, canopy architecture can be important. For example, we noted that smaller trees had minimal reservoirs at branch intersections, limited branch surface area, smaller projected bole area in the face of wind-driven snow, and smoother bark (which decreases storage capacity and also limits snow retention associated with rougher bark). Enhanced *SF* was observed for upright bigtooth aspen branches (Herwitz and Levia, 1997). Though they are beyond the scope of the current study, a number of hypotheses and conceptual models were proposed by Levia and Underwood (2004) related to snowmelt-induced *SF*, a process potentially influenced by 1) albedo of snow-covered and snow-free wood surfaces, 2) snow-to-rain nature of the precipitation (vs. pure snow), and 3) longwave radiative flux within the canopy.

3.5 CONCLUSION

This study of isolated deciduous park trees confirms the volumetric importance of stemflow and the influence of various canopy traits and meteorological characteristics on stemflow initiation thresholds and stemflow rates. Smooth bark and steeply inclined branch angles are among traits previously associated with high stemflow yields; we also found that stemflow initiation threshold rain depth decreased and stemflow rate increased with higher numbers of leaders converging at the base of a canopy. These traits were apparent in the sole American beech in our study that exhibited the lowest stemflow initiation threshold, highest stemflow rate, and highest mean and event stemflow % and funneling ratio values among multi-leader trees. Single-leader trees tended to have higher stemflow yields if they had 1) high branch angles, 2) low diameter at breast height and canopy cover (associated with lower thresholds), 3) greater tree height, bark relief index

(particularly when furrows are linear), canopy volume, and median leaf size, and 4) fewer branches (associated with higher stemflow rates). Given that bark relief increased both the stemflow initiation threshold and rate for single-leader trees, resultant stemflow yield depended on rainfall depth, duration, and other storm and trait variables.

Despite the diversity of study tree species and size, patterns emerged regarding event meteorology including 1) the dominance of rainfall depth, 2) the influence of inclined rainfall at smaller angles from vertical than previously observed, and 3) the already-established relationships between *SF* yield and wind speed (positive) and vapour pressure deficit (inverse). The effects of intra-storm break duration and rainfall intensity were less clear and warrant further study. Like others, we found a seasonal pattern of enhanced stemflow from leafless canopies, especially at low rain depths; for eight of 13 study trees in transitional leaf states, stemflow yield was significantly ($p \leq 0.10$) inversely related to actual canopy cover. We observed, as other researchers have, very high variability for non-rain events, but in general, for small events, stemflow yield was greatest for mixed precipitation followed by rain then snow.

Among the many reasons our findings may depart from earlier results are differences in climate, tree species, and event profiles, but the primary one in most cases is likely our focus on isolated trees in an urban park situation. We expect that our trees' canopies were subject to influences undetectable (or at least complicated) in a forest setting. What is clear is that stemflow, in the volumes we measured, must be managed in an urban setting, either as a resource in the form of supplemental irrigation where infiltration is possible, or as a hazard if excess stemflow becomes runoff on polluted impervious surfaces. While interception loss by urban trees is substantial, stemflow can no longer be dismissed as insignificant; in fact, planting trees that divert intercepted rain to stemflow could reduce throughfall, which typically falls on paving. Future work should address stemflow quantity and quality (nutrients and pollutants) for isolated deciduous and coniferous trees of diverse ages and sizes in a range of climates and urban conditions. This body of knowledge will provide valuable guidance as we respond to the need for urban trees and their ecosystem services in ever-densifying cities.

3.6 REFERENCES

- Aboal, J., Jiménez, M., Morales, D., Hernández, J., 1999a. Rainfall interception in laurel forest in the Canary Islands. *Agricultural and Forest Meteorology* 97, 73–86.
- Aboal, J., Morales, D., Hernández, M., Jiménez, M., 1999b. The measurement and modelling of the variation of stemflow in a laurel forest in Tenerife, Canary Islands. *Journal of Hydrology* 221, 161–175.
- André, F., Jonard, M., Ponette, Q., 2008a. Influence of species and rain event characteristics on stemflow volume in a temperate mixed oak–beech stand. *Hydrological Processes* 22, 4455– 4466.
- André, F., Jonard, M., Ponette, Q., 2008b. Effects of biological and meteorological factors on stemflow chemistry within a temperate mixed oak-beech stand. *Science of the Total Environment* 393, 72–83.
- Barbier, S., Balandier, P., Gosselin, F., 2009. Influence of several tree traits on rainfall partitioning in temperate and boreal forests: A review. *Annals of Forest Science* 66, 602 (11 pp.).
- Borgin, K., Corbett, K., 1974. The hydrophobic and water-repellent properties of wattle bark extractives. *Wood Science and Technology* 8, 138–147.
- Calder, I.R., 2001. Canopy processes: Implications for transpiration, interception and splash induced erosion, ultimately for forest management and water resources. *Plant Ecology* 153, 203–214.
- Carlyle-Moses, D., Price, A., 1999. An evaluation of the Gash interception model in a northern hardwood stand. *Journal of Hydrology* 214, 103–110.
- Carlyle-Moses, D., Price, A., 2006. Growing-season stemflow production within a deciduous forest of southern Ontario. *Hydrological Processes* 20, 3651–3663.
- Carlyle-Moses, D., Price, A., 2007. Modelling canopy interception loss from a Madrean pine-oak stand, Northeastern Mexico. *Hydrological Processes* 21, 2572–2580.
- Carlyle-Moses, D.E., Gash, J.H.C., 2011. Rainfall interception loss by forest canopies, in: Levia, D.F., Carlyle-Moses, D., Tanaka, T. (Eds.), *Forest Hydrology and Biochemistry: Synthesis of Past Research and Future Directions, Ecological Studies*. Springer Netherlands, Dordrecht, pp. 407–424.
- Carlyle-Moses, D.E., Park, A.D., Cameron, J.L., 2010. Modelling rainfall interception loss in forest restoration trials in Panama. *Ecohydrology* 3, 272–283.
- Crockford, R.H., Richardson, D.P., 1990. Partitioning of rainfall in a eucalypt forest and pine plantation in southeastern Australia: II Stemflow and factors affecting stemflow in a dry sclerophyll eucalypt forest and a *Pinus radiata* plantation. *Hydrological Processes* 4, 145–155.

- Crockford, R.H., Richardson, D.P., 2000. Partitioning of rainfall into throughfall, stemflow and interception: Effect of forest type, ground cover and climate. *Hydrological Processes* 14, 2903–2920.
- Dalton, J., 1802. Experimental essays on the constitution of mixed gases. *Manchester Literary and Philosophical Society Memoirs* 5, 535–602.
- David, T.S., Gash, J.H.C., Valente, F., Pereira, J.S., Ferreira, M.I., David, J.S., 2006. Rainfall interception by an isolated evergreen oak tree in a Mediterranean savannah. *Hydrological Processes* 20, 2713–2726.
- Deguchi, A., Hattori, S., Park, H.-T., 2006. The influence of seasonal changes in canopy structure on interception loss: Application of the revised Gash model. *Journal of Hydrology* 318, 80–102.
- Dunkerley, D., 2013. Stemflow on the woody parts of plants: Dependence on rainfall intensity and event profile from laboratory simulations. *Hydrological Processes* (online), 1–14.
- Environment Canada. 2014. Canadian Climate Normals. Station Name: Kamloops A*. Webpage. URL http://climate.weather.gc.ca/climate_normals/index_e.html (accessed June 1, 2014).
- Gash, J., Lloyd, C., Lachaud, G., 1995. Estimating sparse forest rainfall interception with an analytical model. *Journal of Hydrology* 170, 79–86.
- Gash, J.H.C., 1979. An analytical model of rainfall interception by forests. *Quarterly Journal of the Royal Meteorological Society* 105, 43–55.
- Germer, S., Werther, L., Elsenbeer, H., 2010. Have we underestimated stemflow? Lessons from an open tropical rainforest. *Journal of Hydrology* 395, 169–179.
- Gómez, J., Vanderlinden, K., Giráldez, J., Fereres, E., 2002. Rainfall concentration under olive trees. *Agricultural Water Management* 55, 53–70.
- Guevara-Escobar, A., González-Sosa, E., Véliz-Chávez, C., Ventura-Ramos, E., Ramos-Salinas, M., 2007. Rainfall interception and distribution patterns of gross precipitation around an isolated *Ficus benjamina* tree in an urban area. *Journal of Hydrology* 333, 532–541.
- Hair, J., Anderson, R., Tatham, R., Black, W., 1998. *Multivariate Data Analysis*, 5th edition. Prentice Hall, Upper Saddle River, NJ.
- Helvey, J.D., Patric, J.H., 1965. Canopy and litter interception of rainfall by hardwoods of eastern United States. *Water Resources Research* 1, 193–206.
- Herwitz, S., Levia, D., 1997. Mid-winter stemflow drainage from Bigtooth Aspen (*Populus grandidentata* Michx.) in central Massachusetts. *Hydrological Processes* 11, 169–175.
- Herwitz, S., Slye, R., 1995. Three-dimensional modeling of canopy tree interception of wind-driven rainfall. *Journal of Hydrology* 168, 205–226.

- Herwitz, S.R., 1985. Interception storage capacities of tropical rainforest canopy trees. *Journal of Hydrology* 77, 237–252.
- Herwitz, S.R., 1986. Infiltration-excess caused by stemflow in a cyclone-prone tropical rainforest. *Earth Surface Processes and Landforms* 11, 401–412.
- Herwitz, S.R., 1987. Raindrop impact and water flow on the vegetative surfaces of trees and the effects on stemflow and throughfall generation. *Earth Surface Processes and Landforms* 12, 425–432.
- Holder, C.D., 2012. The relationship between leaf hydrophobicity, water droplet retention, and leaf angle of common species in a semi-arid region of the western United States. *Agricultural and Forest Meteorology* 152, 11–16.
- Inkiläinen, E.N.M., McHale, M.R., Blank, G.B., James, A.L., Nikinmaa, E., 2013. The role of the residential urban forest in regulating throughfall: A case study in Raleigh, North Carolina, USA. *Landscape and Urban Planning* 119, 91–103.
- Korhonen, L., Heikkinen, J., 2009. Automated analysis of *in situ* canopy images for the estimation of forest canopy cover. *Forest Science* 55, 323–334.
- Laws, J.O., Parsons, D.A., 1943. The relation of raindrop-size to intensity. *Transactions, American Geophysical Union* 24, 452–460.
- Levia, D., Frost, E., 2003. A review and evaluation of stemflow literature in the hydrologic and biogeochemical cycles of forested and agricultural ecosystems. *Journal of Hydrology* 274, 1–29.
- Levia, D.F., 2003. Winter stemflow leaching of nutrient-ions from deciduous canopy trees in relation to meteorological conditions. *Agricultural and Forest Meteorology* 117, 39–51.
- Levia, D.F., 2004. Differential winter stemflow generation under contrasting storm conditions in a southern New England broad-leaved deciduous forest. *Hydrological Processes* 18, 1105–1112.
- Levia, D.F., Herwitz, S.R., 2005. Interspecific variation of bark water storage capacity of three deciduous tree species in relation to stemflow yield and solute flux to forest soils. *Catena* 64, 117–137.
- Levia, D., Keim, R., Carlyle-Moses, D., Frost, E., 2011. Throughfall and stemflow in wooded ecosystems, in: Levia, D., Carlyle-Moses, D., Tanaka, T. (Eds.), *Forest Hydrology and Biochemistry: Synthesis of Past Research and Future Directions*. Springer, Dordrecht, pp. 426–443.
- Levia, D.F., Michalzik, B., Näthe, K., Bischoff, S., Richter, S., Legates, D.R., 2013. Differential stemflow yield from European beech saplings: The role of individual canopy structure metrics. *Hydrological Processes* 2–9.

- Levia, D.F., Underwood, S.J., 2004. Snowmelt induced stemflow in northern hardwood forests: A theoretical explanation on the causation of a neglected hydrological process. *Advances in Water Resources* 27, 121–128.
- Levia, D.F., Van Stan, J.T., Mage, S.M., Kelley-Hauske, P.W., 2010. Temporal variability of stemflow volume in a beech-yellow poplar forest in relation to tree species and size. *Journal of Hydrology* 380, 112–120.
- Liang, W.-L., Kosugi, K., Mizuyama, T., 2009. Characteristics of stemflow for tall *Stewartia monadelphica* growing on a hillslope. *Journal of Hydrology* 378, 168–178.
- Livesley, S.J., Baudinette, B., Glover, D., 2014. Rainfall interception and stem flow by eucalypt street trees – The impacts of canopy density and bark type. *Urban Forestry & Urban Greening* 13, 192–197.
- Llorens, P., Domingo, F., 2007. Rainfall partitioning by vegetation under Mediterranean conditions. A review of studies in Europe. *Journal of Hydrology* 335, 37–54.
- Marin, C.T., Bouten, W., Sevink, J., 2000. Gross rainfall and its partitioning into throughfall, stemflow and evaporation of intercepted water in four forest ecosystems in western Amazonia. *Journal of Hydrology* 237, 40–57.
- Martinez-Meza, E., Whitford, W.G., 1996. Stemflow, throughfall and channelization of stemflow by roots in three Chihuahuan desert shrubs. *Journal of Arid Environments* 32, 271–287.
- McClain, M.E., Boyer, E.W., Dent, C.L., Gergel, S.E., Grimm, N.B., Groffman, P.M., Hart, S.C., Harvey, J.W., Johnston, C.A., Mayorga, E., McDowell, W.H., Pinay, G., 2003. Biogeochemical hot spots and hot moments at the interface of terrestrial and aquatic ecosystems. *Ecosystems* 6, 301–312.
- Michopoulos, P., 2011. Biogeochemistry of urban forests, in: Levia, D.F., Carlyle-Moses, D., Tanaka, T. (Eds.), *Forest Hydrology and Biogeochemistry: Synthesis of Past Research and Future Directions*. Springer Netherlands, pp. 341–353.
- Návar, J., 1993. The causes of stemflow variation in 3 semiarid growing species of northeastern Mexico. *Journal of Hydrology* 145, 175–190.
- Návar, J., 2011. Stemflow variation in Mexico's northeastern forest communities: Its contribution to soil moisture content and aquifer recharge. *Journal of Hydrology* 408, 35–42.
- Neary, A., Gizyn, W., 1994. Throughfall and stemflow chemistry under deciduous and coniferous forest canopies in south-central Ontario. *Canadian Journal of Forest Research* 24, 1089–1100.
- Park, A., Cameron, J.L., 2008. The influence of canopy traits on throughfall and stemflow in five tropical trees growing in a Panamanian plantation. *Forest Ecology and Management* 255, 1915–1925.

- Park, H.-T., Hattori, S., 2002. Applicability of Stand Structural Characteristics to Stemflow Modeling. *Journal of Forest Research* 7, 91–98.
- Perra, B., Haluk, J.-P., Metche, M., 1993. Extraction of suberin and lignin from beech barks (*Fagus sylvatica* L.). *Holzforschung* 47, 486–490.
- Price, A., Carlyle-Moses, D., 2003. Measurement and modelling of growing-season canopy water fluxes in a mature mixed deciduous forest stand, southern Ontario, Canada. *Agricultural and Forest Meteorology* 119, 69–85.
- Pypker, T., Levia, D., Staelens, J., Van Stan, J., 2011. Canopy structure in relation to hydrological and biogeochemical fluxes, in: Levia, Delphis F., Carlyle-Moses, DE, Tanaka, T. (Eds.), *Forest Hydrology and Biochemistry: Synthesis of Past Research and Future Directions*. Springer, Dordrecht, pp. 371–388.
- Ross, S., 2013. *Weather and Climate*. Oxford University Press, Don Mills, Ontario.
- Rutter, A.J., Kershaw, K.A., Robins, P.C., Morton, A.J., 1971. A predictive model of rainfall interception in forests, 1. Derivation of the model from observations in a plantation of Corsican pine. *Agricultural Meteorology* 9, 367–384.
- Searcy, J., Hardison, C., 1960. Double mass curves. *Manual of hydrology: Part 1. General surface water techniques*, Water-Supply Paper.
- Shirtcliffe, N.J., Pyatt, F.B., Newton, M.I., McHale, G., 2006. A lichen protected by a super-hydrophobic and breathable structure. *Journal of Plant Physiology* 163, 1193–1197.
- Šraj, M., Brilly, M., Mikoš, M., 2008. Rainfall interception by two deciduous Mediterranean forests of contrasting stature in Slovenia. *Agricultural and Forest Meteorology* 148, 121–134.
- Staelens, J., De Schrijver, A., Verheyen, K., 2007. Seasonal variation in throughfall and stemflow chemistry beneath a European beech (*Fagus sylvatica*) tree in relation to canopy phenology. *Canadian Journal of Forest Research* 37, 1359–1372.
- Staelens, J., De Schrijver, A., Verheyen, K., Verhoest, N.E.C., 2008. Rainfall partitioning into throughfall, stemflow, and interception within a single beech (*Fagus sylvatica* L.) canopy: Influence of foliation, rain event characteristics, and meteorology. *Hydrological Processes* 22, 33–45.
- Tanaka, T., 2011. Effects of the canopy hydrologic flux on groundwater, in: Levia, Delphis F., Carlyle-Moses, D., Tanaka, T. (Eds.), *Forest Hydrology and Biochemistry: Synthesis of Past Research and Future Directions*. Springer, Dordrecht, pp. 499–518.
- Taniguchi, M., Tsujimura, M., Tanaka, T., 1996. Significance of stemflow in groundwater recharge. 1: Evaluation of the stemflow contribution to recharge using a mass balance approach. *Hydrological Processes* 10, 71–80.

- Tukey, J.W. 1953. The problem of multiple comparisons. Department of Statistics, Princeton University, Princeton, NJ. Unpublished report.
- Valente, F., David, J.S., Gash, J.H.C., 1997. Modelling interception loss for two sparse eucalypt and pine forests in central Portugal using reformulated Rutter and Gash analytical models. *Journal of Hydrology* 190, 141–162.
- Van Stan, J., Levia, D., 2010. Inter- and intraspecific variation of stemflow production from *Fagus grandifolia* Ehrh. (American beech) and *Liriodendron tulipifera* L. (yellow poplar) in relation to bark microrelief in the eastern United States. *Ecohydrology* 3, 11–19.
- Van Stan, J.T., Levia, D.F., Jenkins, R.B., 2014a. Forest canopy interception loss across temporal scales: Implications for urban greening initiatives. *The Professional Geographer* 00 (online), 1–11.
- Van Stan, J.T., Siegert, C.M., Levia, D.F., Scheick, C.E., 2011. Effects of wind-driven rainfall on stemflow generation between codominant tree species with differing crown characteristics. *Agricultural and Forest Meteorology* 151, 1277–1286.
- Van Stan, J.T., Van Stan, J.H., Levia, D.F., 2014b. Meteorological influences on stemflow generation across diameter size classes of two morphologically distinct deciduous species. *International Journal of Biometeorology* (online) 1–11.
- Ward, R., Robinson, M., 2000. *Principles of Hydrology*, 4th edition. McGraw-Hill Publishing Company, London, UK.
- Xiao, Q., McPherson, E., 2011. Rainfall interception of three trees in Oakland, California. *Urban Ecosystems* 14, 755–769.
- Xiao, Q., McPherson, E., Simpson, J., Ustin, S., 2007. Hydrologic processes at the urban residential scale. *Hydrological Processes* 21, 2174–2188.
- Xiao, Q., McPherson, E.G., Ustin, S.L., Grismer, M.E., Simpson, J.R., 2000. Winter rainfall interception by two mature open-grown trees in Davis, California. *Hydrological Processes* 14, 763–784.
- Zar, J.H. 1984. *Biostatistical Analysis*. 2nd edition. Prentice-Hall Inc. Englewood Cliffs, NJ. 718 pp.

CHAPTER 4 CONCLUSIONS AND RECOMMENDATIONS

4.1 SYNTHESIS: TRAIT AND METEOROLOGICAL FACTORS IN STEMFLOW GENERATION

The breadth and depth of this study have allowed us to test the relevance of key variables identified in past studies on stemflow, SF , while identifying factors not previously investigated. For the precipitation regime in Kamloops, British Columbia, and for this sample of 20 single-leader (Group A) and 17 multi-leader (Group B) isolated deciduous trees, we found the following tree traits to influence SF processes and yields.

- **Branch Angles:** With only one exception (Group B funneling ratio, FR , for events ≥ 10 mm), full-canopy intersection angle, AIF , was positively correlated with SF , including for 1) Group A $SF\%$, 2) Group B stemflow rate, Q_{SF} , and 3) Group A and B rate per m^2 projected canopy area, $Q_{SF} PCA^{-1}$. Also, upper-canopy intersection angle, AIU , was positively correlated with Group A and B funneling ratio, FR , and inversely correlated with SF initiation threshold rain depth, P'' (thus contributing to a lower threshold), while upper-canopy average angle, AAU , was a positive factor for Group A $SF\%$. We conclude that, except for cases where lower branching angles are associated with a broader canopy and smooth bark, high branch angles were associated with greater SF production.
- **Bark Relief:** Intuitively, smoother bark should promote SF , and for multi-leader trees in our study, it tended to. It was also inversely related to P'' , which supports many other observations that rougher bark requires greater rain depths to become saturated. However, we found that bark relief index, BRI , was positively correlated with $SF\%$, FR , Q_{SF} , and $Q_{SF} PCA^{-1}$ for single-leader trees, particularly for greater rain depths. Our study quantified bark relief, or topography, in the form of the BRI rather than the storage capacity of each tree's bark, and we suggest that greater surface areas associated with high BRI may promote SF production, particularly for

higher rain depths that have largely saturated the bark and for trees with linearly furrowed bark and high branch angles. We conclude that it is unwise to make assumptions that trees with deeply furrowed bark will produce less SF , and recommend that other climatic and trait factors be considered.

- **Cover Metrics:** Both canopy cover, CC , and wood cover, WC , were positively correlated with $SF\%$ for Group A and B trees, though for the 5 to < 10 mm rain depth class, CC was inversely related to Group A FR . There was a positive correlation between CC and P'' for Group A trees, reflecting that most denser trees require more rain depth to saturate. Finally, WC was positively associated with Q_{SF} for Group B trees and with $Q_{SF} PCA^{-1}$ for both groups. We conclude that, while CC interacted unpredictably with other factors, WC was consistently positively correlated with SF , reflecting the importance of woody infrastructure to the funneling of SF through a canopy.
- **Size Metrics:** For Group A trees, diameter at breast height, DBH , was directly related to P'' , in agreement with past research. For Group B trees, DBH was inversely related to $SF\%$ in the smallest rain class; the same relationship was seen for Group A trees with FR across all rain depth classes, and with $Q_{SF} PCA^{-1}$, confirming that smaller trees tend to produce more SF , at least early in a storm event. Canopy volume, Vol_C , was inversely correlated with $SF\%$ in Group A trees and positively related to Q_{SF} , suggesting that there are trade-offs whereby too great a volume results in higher P'' and too small a volume minimizes capture area. Shape of a canopy can interact with its volume: in our study, we found that height-to-width ratio, HWR , was positively correlated with $SF\%$ for Group B trees and inversely related to FR for Group A trees, both for the smallest rain depth class. Tree height, H , was directly related to Q_{SF} for Group A trees and to P'' for Group B trees, which may reflect that taller multi-leader trees tend to be broader as well. In fact, canopy width, CW , was inversely related to $SF\%$, Q_{SF} , and $Q_{SF} PCA^{-1}$ for

Group B trees, supporting the theory that too much breadth in multi-leader trees tends to be counter-productive in terms of *SF* generation.

- **Leader and Branch Counts:** The number of leaders, L_n , was consistently positively associated with *SF* ($SF\%$, Q_{SF} , and $Q_{SF} PCA^{-1}$) and inversely related to P'' . We therefore conclude that the benefits of many multiple leaders converging at the base of a tree's canopy more than compensate for the additional surface area and storage capacity associated with this woody infrastructure. For Group A trees, branch count, B_n , was positively related to *FR* for events ≥ 10 mm and inversely related to Q_{SF} and $Q_{SF} PCA^{-1}$, possibly reflecting that high B_n conferred an advantage only once a tree was fully saturated. We suggest that this is an example of a trait that varies in its relationship with *SF* depending on other morphological and meteorological factors.

The following meteorological variables were influential, and particularly so for groups of trees with lower or higher values for certain trait metrics.

- **Rain Depth and Duration:** For all except two trees (for which rain duration, D_R , was most important), this variable explained the most variability in *SF* volume.
- **Break Duration:** In general, this factor was inversely related to *SF* volume, likely reflecting the relatively dry climate of the study region. When it occurred during the leafed season, D_B was associated with trees having lower *CC* and thus being more exposed to the influence of other meteorological variables. During leaf transition, the influence of D_B was associated with lower L_n and B_n , suggesting that smaller trees with less wood infrastructure dry out faster during intra-storm breaks.
- **Rainfall Intensity:** When 5-minute weighted average rainfall intensity, I_{wt5} , influenced *SF* volume, it tended to be in trees with more convoluted bark and more discontinuously draining branches (leaf-on) or lower *CC* (leaf-off) and it was always positively related to *SF*. There was no clear pattern associating 5-minute maximum

rainfall intensity, I_{max5} , positively or negatively with SF , and no tree traits were associated with the influence of this variable.

- **Rainfall Inclination Angle:** When it was a factor for leaf-on or leaf-off SF , rainfall inclination angle, P_{inc} , was always positively related to SF volume. Its influence was associated with small, narrow, trees with relatively high branch angles and few branches (leaf-on) or with trees having high WC (leaf-off), a reasonable profile of a tree exposed to inclined rain by virtue of its effective crown projection area.
- **Wind Speed:** As found in past studies, wind speed positively influenced SF generation in study tree canopies in all leaf conditions. For leafed canopies, 5-minute weighted average wind speed, W_{wt5} , was influential for trees with high canopy and wood volumes and larger leaves. Leafless trees influenced by wind speed tended to have wider canopies and higher WC , implying that large, broad, dense trees respond to windy conditions with increased SF .
- **Vapour Pressure Deficit:** Commonly, VPD was inversely related to SF volumes in leafed canopies, and occasionally in leafless canopies. It was influential in leafed trees with higher full-canopy average branch angles, AAF , and in leafless canopies with lower DBH , WC , and tree height.

Finally, we found the following patterns related to seasonal conditions of the canopy and different types of precipitation:

- **Leaf-on vs. Leaf-off Condition:** As numerous other researchers have found, SF tended to start at lower rain depths when trees were leafless and SF volume, for small events at least, was generally greater for leafless canopies than those in full leaf. Our findings highlight the need to account for potentially increased SF generated by urban deciduous trees in the dormant season.
- **Precipitation Type:** Though variability was high, the general pattern for individual trees of both Groups A and B was that, for a given depth, the most SF volume was

generated by mixed precipitation, then rain, then snow. Urban forest managers in climates subject to mixed precipitation and high rainfall depths during winter months are advised to assess existing and proposed urban trees and planting sites with these findings in mind.

4.2 APPLICABILITY OF FINDINGS IN THE CONTEXT OF STORMWATER MANAGEMENT

While our discussion has focused largely on traits correlated with high stemflow production, deciduous trees with opposite traits such as low branching angles in combination with a large diameter at breast height and deeply furrowed bark do have the potential to minimize stemflow while partitioning more incident rain to interception-loss and throughfall. If the goal is to minimize stormwater generation, higher interception-loss is welcome in urban settings; however, greater throughfall is beneficial only if it falls on pervious surfaces beneath a tree's canopy. If trees are being planted in a largely paved area, trees shown to be high stemflow producers while generating minimal throughfall could be used to funnel stemflow to a suitably sized reservoir of growing medium at the base of a tree; here, nutrients and supplementary irrigation may be available to tree roots while biofiltration may reduce the impact of pollutants deposited on trees' leaves and wood surfaces. The wide range of stemflow colour observed in this study (Figure 4.1) suggests that there were between-tree and between-event differences in stemflow chemistry, likely reflecting interaction of canopy traits and meteorological variables analyzed in the main part of this study. This reinforces the importance of investment in an adequate volume and quality of growing medium increases the potential for an urban tree to achieve its mature size and provide valuable ecosystem services, including rainwater and pollutant management, for many years.

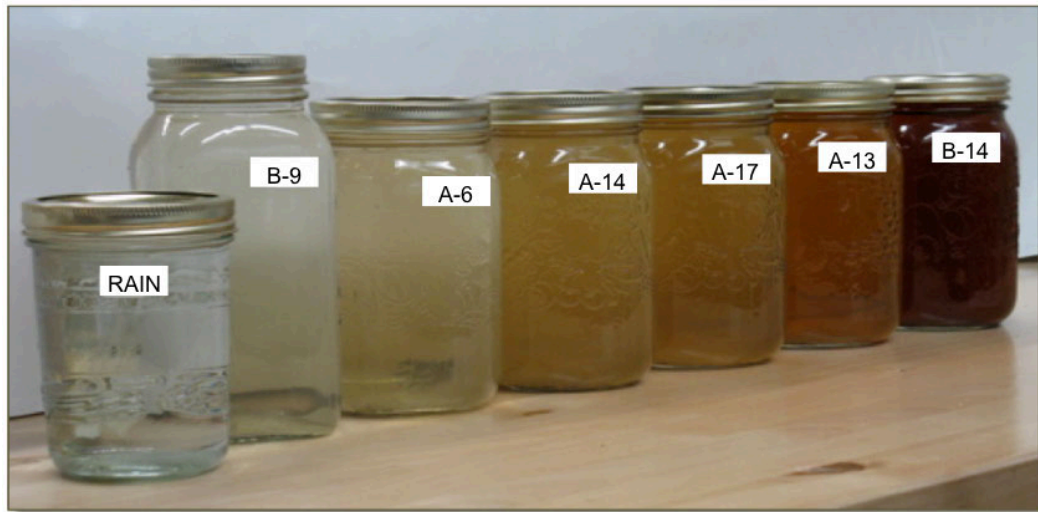


Figure 4.1. Range of stemflow colours observed for May 21–23, 2013 rain event (32.7 mm).

Using the City of Kamloops as a case study, and assuming 1) typical frequencies of rain depth classes (midpoint depth used), 2) mean stemflow % values based on this study for Group A and B trees (representing a wide range of sizes) for each rain depth class, and 3) mean *PCA* for each group, estimated annual stemflow from 11,200 City-managed deciduous trees ranges from 2,575 m³ to 3,585 m³ for single- and multi-leader trees, respectively. The volumetric and biogeochemical concentration of these quantities at the base of trees justifies careful evaluation of existing and potential tree planting sites and proactive management of potential infiltration and/or runoff.

It is essential to consider a tree's contribution to urban hydrology at all stages of its lifecycle. The mature form of the species may play a very different role in terms of canopy water balance compared to a newly established specimen. Canopy traits evolve with time, as do their interactions with meteorological variables. Climate matters: different tree species will be associated with more or less stemflow production depending on a region's storm regime.

4.3 LESSONS LEARNED

The innovative methodologies described above are applicable in most contexts, but it was the public park setting that presented the greatest logistical challenges for our research. We offer these recommendations to prepare researchers who may be working in heavily used parks or streetscapes for the first time.

- ***Collaborate early and often:*** It is critical to establish expectations and channels of communication with all groups that will benefit from or be impacted by research at an urban site. In the case of McArthur Island Park, this meant co-ordination with the City of Kamloops (use permits, pruning, turf maintenance, irrigation, signage, and our project website), the McArthur Island Lawn Bowling Club (equipment storage), an adjacent private property owner (secure site for our weather station), local police (vandalism prevention), and local media (project updates).
- ***Prepare to be in the public eye:*** Answering countless questions from curious onlookers took time but paid dividends as regular users started to watch out for the research equipment and let us know of vandalism. Provide links to information about the project as well as contacts via on-site signage (Figure B.7).
- ***Budget for vandalism:*** If there's public use of a project site, there will be abuse as well, particularly just after installation. We repaired and replaced stemflow collars, manual rain gauges, collection reservoirs, and water-filled jugs used to weight the reservoirs. Local police responded to our requests for increased patrols around the site during the study, and we suspect that this contributed to a relatively low rate of vandalism.
- ***Discourage urban wildlife:*** Species such as crows, deer, and bears had various impacts on our installations. One bear completely destroyed a tote and punctured the water-filled jugs; deer detached sections of collars with their antlers; and countless crows pecked holes in the black plastic used to cover each tote. We suspect that the behaviour of the bear and crows reflects repeated rewards of food

in black garbage bags (though clear bags weren't immune). We recommend alternate configurations or materials if possible.

- ***Weight or anchor everything:*** Prepare for above-average winds by anchoring collection equipment into the ground (e.g., bases for manual rain gauges) or placing weights within reservoirs.
- ***Provide adequate reservoir capacity:*** During larger rain events, we had to check high-producing trees and take interim measurements to prevent overflow. Even reservoirs of more than 100 L were no match for trees like our American beech that produced 224 L of stemflow during a 32.7 mm rain event!

4.4 FUTURE RESEARCH

The knowledge base regarding stemflow quantity and quality in natural and managed closed-canopy forests has expanded, particularly in the past decade, but research is needed to better understand and predict canopy interception processes in urban environments and for isolated trees. While our research focused on cultivated deciduous species, more work is needed on stemflow and throughfall in conifer species commonly used in urban landscapes. Our findings highlight the need to better distinguish stemflow processes according to rainfall depth and other meteorological variables, requiring systematic study of similar species in contrasting climates and pollutant regimes. Findings from such studies have the potential to support proactive management of urban stemflow as a resource in terms of supplementary irrigation and nourishment rather than as a potential stormwater source.

APPENDIX A

SUPPLEMENTARY TABLES

- Table A.1. Derived values for stemflow initiation threshold, P'' (mm), rate, Q_{SF} (L mm⁻¹), and rate per unit projected canopy area, $Q_{SF} PCA^{-1}$ (L mm⁻¹ m⁻²), along with measured values for an array of canopy traits for individual single-leader (group A) study trees (see Glossary for definition of acronyms and units).
- Table A.2. Derived values for stemflow initiation threshold, P'' (mm), rate, Q_{SF} (L mm⁻¹), and rate per unit projected canopy area, $Q_{SF} PCA^{-1}$ (L mm⁻¹ m⁻²), along with measured values for an array of canopy traits for individual multi-leader (group B) study trees (see Glossary for definition of acronyms and units).
- Table A.3. Regression coefficients for stemflow, SF , volume (L) as a function of rainfall depth (P , mm) for study trees in *leaf-on* condition.
- Table A.4. Regression coefficients for stemflow, SF , volume (L) as a function of rainfall depth (P , mm) and actual canopy cover (ACC , %) for study trees in *transitional* leaf condition.
- Table A.5. Regression coefficients for stemflow, SF , volume (L) as a function of rainfall depth (P , mm) for study trees in *leaf-off* condition.
- Table A.6. Multiple regression equations for stemflow, SF , volume (L) as a function of meteorological variables, generated for single-leader (group A, $n = 20$) and multi-leader trees (group B, $n = 17$) for n rain events during *leaf-on* condition.
- Table A.7. Multiple regression equations for stemflow, SF , volume (L) as a function of meteorological variables, generated for single-leader (group A, $n = 20$) and multi-leader trees (group B, $n = 17$) for rain events during *transitional leaf* condition.
- Table A.8. Multiple regression equations for stemflow, SF , volume (L) as a function of meteorological variables, generated for single-leader (group A, $n = 20$) and multi-leader trees (group B, $n = 17$) for rain events during *leaf-off* condition.

Table A.1. Derived values for stemflow initiation threshold, P'' (mm), rate, Q_{SF} (L mm⁻¹), and rate per unit projected canopy area, $Q_{SF}PCA^{-1}$ (L mm⁻¹ m⁻²), along with measured values for an array of canopy traits for individual single-leader (group A) study trees.

Tree ID	P''	Q_{SF}	$Q_{SF}CPA^{-1}$	DBH	H	CW	HWR	Vol _c	Vol _w	CC	WC	L _n	B _n	AIF	AAF	AIU	AAU	FD	BRI	MLS
A-1	1.42	0.36	0.032	10.2	5.7	3.66	1.28	28.3	1.6	76.0	15.1	1	26	45.8	62.0	58.7	72.4	0.00	1.06	12.14
A-2	2.96	0.48	0.036	10.5	4.9	4.00	1.09	52.2	1.0	90.6	10.5	1	23	45.6	37.0	51.1	45.8	0.13	1.08	92.22
A-3	1.62	0.33	0.019	11.4	6.3	5.12	1.11	85.9	1.7	94.2	11.7	1	20	40.2	38.8	50.4	54.6	0.10	1.00	30.89
A-4	3.11	0.46	0.023	12.7	7.2	4.50	1.24	103.3	3.6	83.3	18.6	1	23	37.3	33.5	34.9	42.5	0.26	1.00	17.65
A-5	2.72	1.66	0.049	14.6	7.9	6.89	1.17	206.5	5.7	84.6	12.1	1	12	57.9	59.6	69.0	65.5	0.00	1.07	9.54
A-6	1.95	0.53	0.012	15.1	9.9	6.36	1.31	320.6	6.0	74.9	12.4	1	20	42.9	34.3	39.5	40.7	0.25	1.01	1.37
A-7	2.98	1.28	0.063	15.9	9.6	5.13	1.56	120.2	5.5	91.7	19.6	1	18	60.5	61.8	68.0	70.4	0.00	1.00	33.89
A-8	3.74	0.51	0.029	17.2	8.1	4.57	1.40	90.4	6.1	97.9	24.1	1	27	47.7	38.7	55.0	61.4	0.22	1.00	33.42
A-9	3.75	1.76	0.065	19.0	10.5	5.99	1.52	244.3	13.0	95.3	24.0	1	31	46.6	47.5	54.3	61.5	0.13	1.09	9.15
A-10	3.82	1.28	0.057	19.0	11.3	5.24	1.72	167.4	6.0	95.4	20.3	1	26	52.8	60.6	55.3	13.5	0.00	1.02	22.54
A-11	4.51	1.97	0.077	19.7	10.6	5.58	1.53	172.3	8.6	94.6	17.3	1	21	43.5	58.4	30.4	65.2	0.00	1.15	15.91
A-12	4.13	0.42	0.010	20.3	10.1	7.26	1.25	311.7	12.8	88.2	21.2	1	52	14.3	23.7	20.4	39.3	0.48	1.09	30.87
A-13	4.09	2.27	0.061	21.5	9.8	7.49	1.10	271.4	16.7	92.3	23.6	1	39	47.9	32.3	53.0	44.7	0.26	1.20	56.72
A-14	3.70	1.28	0.202	23.5	14.6	2.79	4.13	51.6	8.6	99.6	39.8	1	36	68.1	77.0	75.1	83.0	0.00	1.15	21.59
A-15	2.13	1.26	0.114	24.1	13.1	3.50	2.87	81.7	8.6	98.4	32.1	1	19	66.8	75.2	66.2	76.5	0.00	1.08	23.05
A-16	3.85	0.95	0.034	31.0	10.8	5.83	1.74	280.5	18.1	95.9	33.0	1	28	38.6	18.2	45.2	27.6	0.29	1.04	27.49
A-17	2.78	1.27	0.025	34.3	9.6	8.48	0.94	290.6	41.6	90.3	41.0	1	26	35.4	25.1	32.0	30.6	0.42	1.02	12.72
A-18	3.89	1.99	0.013	43.0	14.1	13.59	0.79	1015.0	114.4	81.3	25.6	1	50	17.7	25.7	27.2	38.1	0.40	1.15	30.67
A-19	4.63	2.15	0.014	52.7	13.8	13.71	0.99	1801.2	105.6	83.6	26.0	1	42	24.9	32.0	39.1	40.3	0.29	1.23	25.57
A-20	4.12	3.61	0.022	60.7	24.7	14.21	1.04	1728.1	183.4	76.7	34.1	1	24	36.6	24.8	35.8	16.6	0.17	1.15	27.89
Avg.	3.29	1.29	0.048	23.8	10.64	6.69	1.49	371.2	28.4	89.2	23.1	1	28.2	43.6	43.3	48.0	49.5	0.17	1.08	26.76
Min.	1.42	0.33	0.010	10.2	4.95	2.79	0.79	28.3	1.0	74.9	10.5	1	12.0	14.3	18.2	20.4	13.5	0.00	1.00	1.37
Max.	4.63	3.61	0.202	60.7	24.75	14.21	4.13	1801.2	183.4	99.6	41.0	1	52.0	68.1	77.0	75.1	83.0	0.48	1.23	92.22

Table A.2. Derived values for stemflow initiation threshold, P'' (mm), rate, Q_{SF} (L mm⁻¹), and rate per unit projected canopy area, $Q_{SF} PCA^{-1}$ (L mm⁻¹ m⁻²), along with measured values for an array of canopy traits for individual multi-leader (group B) study trees.

Tree ID	P''	Q_{SF}	$Q_{SF} CPA^{-1}$	DBH	H	CW	HWR	Vol_c	Vol_w	CC	WC	L_n	B_n	AIF	AAF	AIU	AAU	FD	BRI	MLS
B-1	3.64	1.37	0.047	15.2	8.1	5.92	0.91	129.2	14.3	86.0	31.2	3	53	57.0	59.7	56.7	63.6	0.00	1.22	7.43
B-2	3.51	1.26	0.079	18.3	6.3	4.37	1.32	56.9	3.0	91.2	17.2	3	58	37.8	27.1	40.8	25.2	0.32	1.00	25.68
B-3	1.33	1.49	0.042	18.8	8.5	6.57	1.44	352.9	15.1	83.5	23.0	3	76	34.9	42.4	38.8	50.9	0.12	1.01	9.39
B-4	3.13	0.48	0.009	21.0	8.7	7.81	1.04	334.4	10.4	84.4	14.7	2	27	39.9	25.8	44.1	31.5	0.29	1.17	1.77
B-5	1.74	2.75	0.051	24.6	8.7	8.08	1.06	381.0	19.6	95.9	18.5	4	56	47.0	53.5	50.4	51.9	0.00	1.10	50.56
B-6	4.12	2.20	0.094	26.0	8.9	5.35	1.46	173.8	19.2	98.8	43.5	3	54	60.2	64.8	53.6	61.7	0.00	1.17	30.43
B-7	5.37	0.97	0.022	28.9	12.6	7.54	1.47	416.0	56.6	94.7	39.8	2	50	32.5	18.9	22.6	24.5	0.59	1.10	9.49
B-8	4.02	4.03	0.048	36.9	10.3	10.14	0.89	657.6	65.5	97.3	37.1	5	56	49.3	52.3	52.2	61.1	0.11	1.18	28.49
B-9	1.58	7.45	0.113	38.8	11.0	9.31	1.09	588.5	103.4	96.5	42.8	6	65	36.8	50.2	54.5	54.0	0.05	1.04	13.45
B-10	3.20	2.65	0.057	41.3	8.3	7.48	1.15	360.6	22.2	97.2	25.0	5	67	52.8	66.2	50.4	66.2	0.00	1.13	45.30
B-11	3.78	2.68	0.027	43.0	12.0	10.74	0.94	845.0	215.1	98.7	41.0	5	85	51.2	49.6	50.6	53.9	0.04	1.25	34.46
B-12	5.27	2.94	0.068	46.0	11.2	7.57	1.25	414.1	77.8	98.8	61.0	3	68	59.2	51.5	58.8	49.6	0.00	1.18	10.80
B-13	7.22	0.61	0.004	51.8	13.0	14.20	0.71	1284.2	183.1	93.8	41.1	4	74	44.6	37.4	44.9	45.0	0.13	1.42	8.90
B-14	4.97	0.32	0.003	54.3	10.5	11.21	0.99	947.5	162.8	96.2	68.4	2	49	25.0	6.5	34.1	11.9	0.55	1.43	5.55
B-15	6.83	1.34	0.017	58.0	14.2	9.51	1.31	860.9	115.6	92.2	39.0	4	66	48.7	35.0	58.6	49.2	0.29	1.33	71.58
B-16	7.23	0.72	0.003	66.8	16.8	15.10	1.02	1987.3	551.4	85.2	51.8	3	52	43.5	47.9	36.2	47.4	0.10	1.16	5.93
B-17	3.85	0.85	0.004	68.7	18.6	16.72	1.05	3872.0	418.3	80.7	47.2	4	52	41.5	13.1	34.4	-3.3	0.40	1.19	35.69
Avg.	4.17	2.01	0.041	38.7	11.05	9.27	1.12	803.6	120.8	92.4	37.8	3.6	59.3	44.8	41.3	46.0	43.8	0.18	1.18	23.23
Min.	1.33	0.32	0.003	15.2	6.29	4.37	0.71	56.9	3.0	80.7	14.7	2.0	27.0	25.0	6.5	22.6	-3.3	0.00	1.00	1.77
Max.	7.23	7.45	0.113	68.7	18.64	16.72	1.47	3872.0	551.4	98.8	68.4	6.0	85.0	60.2	66.2	58.8	66.2	0.59	1.43	71.58

Table A.3. Regression coefficients for stemflow, SF , volume (L) as a function of rainfall depth, P (mm) for study trees in *leaf-on* condition.

Tree ID	Q_{SF} (L mm ⁻¹)	SE	p - <i>value</i>	Intercept	SE	p - <i>value</i>	R^2	SEE	n	P'' (mm)
A-1	0.36	0.03	0.00	-0.51	0.33	0.07	0.847	1.26	27	1.4
A-2	0.48	0.04	0.00	-1.43	0.35	0.00	0.924	1.02	18	3.0
A-3	0.33	0.06	0.00	-0.54	0.63	0.20	0.605	2.18	26	1.6
A-4	0.46	0.03	0.00	-1.42	0.35	0.00	0.927	1.10	21	3.1
A-5	1.66	0.13	0.00	-4.51	-1.38	0.00	0.907	3.94	18	2.7
A-6	0.53	0.05	0.00	-1.04	0.46	0.02	0.874	1.33	22	2.0
A-7	1.28	0.11	0.00	-3.81	1.24	0.00	0.858	4.31	25	3.0
A-8	0.51	0.05	0.00	-1.89	0.55	0.00	0.876	1.66	20	3.7
A-9	1.76	0.22	0.00	-6.60	2.29	0.00	0.788	6.07	20	3.7
A-10	1.28	0.13	0.00	-4.90	1.56	0.00	0.840	4.94	21	3.8
A-11	1.97	0.15	0.00	-8.86	1.74	0.00	0.906	5.36	21	4.5
A-12	0.42	0.06	0.00	-1.73	0.58	0.00	0.721	1.66	21	4.1
A-13	2.27	0.19	0.00	-9.29	2.52	0.00	0.901	6.72	18	4.1
A-14	1.28	0.11	0.00	-4.73	1.36	0.00	0.886	4.04	20	3.7
A-15	1.26	0.11	0.00	-2.69	1.35	0.03	0.853	4.47	23	2.1
A-16	0.95	0.06	0.00	-3.64	0.71	0.00	0.931	2.18	21	3.9
A-17	1.27	0.08	0.00	-3.54	0.88	0.00	0.938	2.79	20	2.8
A-18	1.99	0.13	0.00	-7.74	1.53	0.00	0.921	4.78	23	3.9
A-19	2.15	0.32	0.00	-9.94	4.07	0.01	0.729	11.69	19	4.6
A-20	3.61	0.30	0.00	-14.84	3.01	0.00	0.908	7.90	17	4.1
B-1	1.37	0.20	0.00	-4.98	1.97	0.01	0.719	5.83	21	3.6
B-2	1.26	0.13	0.00	-4.41	1.42	0.00	0.818	4.85	24	3.5
B-3	1.49	0.07	0.00	-1.99	0.76	0.01	0.950	2.92	26	1.3
B-4	0.48	0.04	0.00	-1.52	0.43	0.00	0.913	1.08	17	3.1
B-5	2.75	0.27	0.00	-4.79	2.71	0.04	0.802	10.62	27	1.7
B-6	2.20	0.22	0.00	-9.08	2.77	0.00	0.851	8.11	19	4.1
B-7	0.97	0.10	0.00	-5.22	1.35	0.00	0.878	3.50	15	5.4
B-8	4.03	0.31	0.00	-16.23	3.01	0.00	0.907	8.64	19	4.0
B-9	7.45	0.35	0.00	-11.74	3.57	0.00	0.945	14.51	28	1.6
B-10	2.65	0.20	0.00	-8.49	2.24	0.00	0.901	7.51	22	3.2
B-11	2.68	0.13	0.00	-10.12	1.57	0.00	0.958	4.89	20	3.8
B-12	2.94	0.26	0.00	-15.51	3.51	0.00	0.900	8.98	16	5.3
B-13	0.61	0.04	0.00	-4.39	0.60	0.00	0.962	1.12	12	7.2
B-14	0.32	0.21	0.10	-1.57	3.04	0.31	0.312	4.28	7	5.0
B-15	1.34	0.24	0.00	-9.16	3.42	0.02	0.821	4.96	9	6.8
B-16	0.72	0.08	0.00	-5.20	1.14	0.00	0.944	1.58	7	7.2
B-17	0.85	0.16	0.00	-3.29	1.73	0.04	0.636	4.54	18	3.9

Table A.4. Regression coefficients for stemflow, SF , volume (L) as a function of rainfall depth, P (mm) and actual canopy cover, ACC (%) for study trees in *transitional* leaf condition.

Tree ID	Q_{SF} (L mm ⁻¹)	SE	p	ACC	SE	p	Intercept	SE	p	R^2	SEE	n	P'' (mm)
A-1													
A-2	0.62	0.02	0.00	-0.02	0.01	0.04	0.15	0.63	0.41	0.991	0.72	12	
A-3	1.50	0.07	0.00				-3.32	0.67	0.00	0.988	1.57	8	2.2
A-4	0.52	0.02	0.00	-0.02	0.01	0.01	0.02	0.35	0.48	0.980	0.51	17	
A-5	1.69	0.06	0.00	-0.05	0.03	0.05	-0.27	1.54	0.43	0.979	2.31	19	
A-6	0.63	0.02	0.00	-0.03	0.01	0.00	0.55	0.27	0.04	0.996	0.40	11	
A-7	1.92	0.09	0.00				-2.54	0.84	0.01	0.981	2.27	10	1.3
A-8	0.57	0.03	0.00				-0.89	0.29	0.01	0.984	0.68	8	1.6
A-9												2	
A-10	1.15	0.06	0.00				-1.79	0.51	0.00	0.969	1.50	13	1.6
A-11	1.63	0.07	0.00				-3.45	0.83	0.01	0.992	1.59	6	2.1
A-12	0.54	0.03	0.00				-1.19	0.37	0.01	0.975	1.02	11	2.2
A-13	2.05	0.05	0.00				-5.57	0.48	0.00	0.995	1.17	10	2.7
A-14	1.83	0.04	0.00				-4.23	0.41	0.00	0.998	0.88	7	2.3
A-15	1.68	0.13	0.00	0.17	0.07	0.04	-14.54	5.46	0.02	0.973	2.87	8	
A-16	1.32	0.06	0.00				-2.26	0.54	0.00	0.977	1.57	12	1.7
A-17	1.85	0.10	0.00	-0.12	0.06	0.02	5.26	4.12	0.11	0.962	2.58	17	
A-18	2.27	0.03	0.00	-0.05	0.02	0.01	-2.08	1.18	0.06	0.999	0.76	10	
A-19	2.67	0.10	0.00				-5.54	0.83	0.00	0.988	2.31	11	2.1
A-20	5.04	0.19	0.00	-0.37	0.20	0.05	10.21	12.43	0.22	0.991	6.07	10	
B-1	1.67	0.20	0.00				-4.31	2.33	0.04	0.856	7.18	14	2.6
B-2	0.60	0.02	0.00				-0.58	0.20	0.01	0.993	0.47	8	1.0
B-3	1.51	0.16	0.00	-0.03	0.02	0.07	0.23	0.91	0.40	0.913	1.21	13	
B-4	0.42	0.13	0.00				0.30	1.56	0.43	0.497	4.54	13	0.7
B-5	3.10	0.10	0.00				-4.92	0.92	0.00	0.993	2.29	9	1.6
B-6	2.31	0.12	0.00				-6.19	1.08	0.00	0.980	2.67	10	2.7
B-7	0.21	0.00	0.01	-0.01	0.00	0.03	0.18	0.05	0.09	1.000	0.02	4	
B-8	6.05	0.29	0.00				-18.48	2.94	0.00	0.987	6.45	8	3.1
B-9	5.64	0.18	0.00				-2.25	1.82	0.13	0.992	2.03	8	0.4
B-10	2.33	0.09	0.00				-4.91	0.90	0.00	0.992	2.16	8	2.1
B-11	3.88	0.07	0.00				-11.36	0.91	0.00	0.999	1.55	5	2.9
B-12	4.03	0.07	0.00	-0.20	0.05	0.00	5.04	4.69	0.16	0.998	1.40	9	
B-13												2	
B-14												3	
B-15	2.22	0.26	0.00				-7.86	4.96	0.11	0.961	7.44	5	3.5
B-16												3	
B-17	1.62	0.51	0.04				-6.80	11.02	0.30	0.832	13.71	4	4.2

Note: Shaded cells indicate that there was not sufficient data for analysis.

Table A.5. Regression coefficients for *stemflow, SF, volume (L) as a function of rainfall depth, P (mm) for study trees in leaf-off condition.*

Tree ID	Q_{SF} (L mm ⁻¹)	<i>SE</i>	<i>p</i>	Intercept	<i>SE</i>	<i>p</i>	R^2	<i>SEE</i>	<i>n</i>	P'' (mm)
A-1	0.40	0.01	0.00	-0.21	0.08	0.01	0.977	0.35	22	0.5
A-2	0.54	0.05	0.00	-0.54	0.10	0.00	0.909	0.26	16	1.0
A-3	0.32	0.03	0.00	-0.23	0.07	0.00	0.871	0.19	16	0.7
A-4	0.19	0.07	0.40	0.13	0.11	0.13	0.009	0.13	9	0.7
A-5	1.28	0.16	0.00	-0.50	0.37	0.08	0.863	0.87	12	0.4
A-6	0.81	0.02	0.00	-0.54	0.14	0.00	0.986	0.56	21	0.7
A-7	0.79	0.16	0.00	0.05	0.33	0.44	0.618	0.94	17	0.1
A-8	0.37	0.06	0.00	-0.25	0.13	0.03	0.773	0.31	15	0.7
A-9	1.54	0.05	0.00	-2.14	0.29	0.00	0.977	1.26	25	1.4
A-10	0.09	0.35	0.40	0.50	0.49	0.16	0.01	0.64	13	5.7
A-11	0.59	0.08	0.00	-0.63	0.17	0.00	0.815	0.44	15	1.1
A-12	0.32	0.09	0.01	-0.01	0.26	0.49	0.776	0.42	6	0.0
A-13									1	
A-14	0.33	0.17	0.05	0.21	0.42	0.32	0.317	0.91	10	0.6
A-15	0.71	0.57	0.12	0.20	0.82	0.40	0.11	1.46	15	0.3
A-16	-0.02	0.20	0.47	0.25	0.29	0.21	0.00	0.36	9	14.7
A-17	0.13	0.17	0.23	0.00	0.24	0.50	0.08	0.29	9	0.0
A-18	1.11	0.09	0.00	-1.16	0.22	0.00	0.958	0.47	9	1.0
A-19	1.21	0.17	0.00	-0.97	0.39	0.02	0.840	0.91	12	0.8
A-20	1.78	0.22	0.00	-1.56	0.56	0.01	0.902	1.18	9	0.9
B-1	-0.01	0.03	0.35	0.05	0.05	0.15	0.02	0.06	12	3.7
B-2	0.51	0.08	0.00	-0.30	0.18	0.06	0.777	0.44	14	0.6
B-3	2.11	0.05	0.00	-2.18	0.35	0.00	0.994	1.14	14	1.0
B-4	0.37	0.04	0.00	-0.42	0.09	0.00	0.861	0.23	15	1.1
B-5	2.22	0.21	0.00	-2.05	0.47	0.00	0.902	1.16	14	0.9
B-6	0.65	0.14	0.00	-0.37	0.32	0.13	0.63	0.80	14	0.6
B-7	0.93	0.06	0.00	-3.36	0.70	0.00	0.977	1.41	7	3.6
B-8									5	
B-9	5.14	0.41	0.00	-2.66	0.84	0.00	0.913	2.40	17	0.5
B-10	0.16	0.73	0.41	0.93	1.03	0.19	0.00	1.35	12	5.7
B-11	1.38	0.19	0.00	-1.70	0.46	0.00	0.860	0.95	11	1.2
B-12	1.15	0.17	0.00	-1.87	0.54	0.01	0.92	0.76	6	1.6
B-13	1.00	0.09	0.00	-4.51	1.31	0.04	0.98	1.82	4	4.5
B-14									0	
B-15	0.13	0.02	0.00	-0.14	0.04	0.00	0.88	0.08	12	1.1
B-16									1	
B-17	0.10	0.02	0.00	-0.08	0.06	0.10	0.724	0.12	9	0.9

Note: Shaded cells indicate that there was not sufficient data for analysis.

Table A.6. Multiple regression equations for stemflow, SF , volume (L) as a function of meteorological variables, generated for single-leader (group A, $n = 20$) and multi-leader trees (group B, $n = 17$) for rain events during *leaf-on* condition.

Tree ID	Stemflow Volume Regression Equation	R^2	SEE	n	$p \leq$
A-1	$0.36 P + 0.56 W_{wt5} - 1.07$	0.885	1.12	27	0.05
A-2	$0.43 P + 0.77 W_{wt5} + 0.19 \frac{1}{VPD} - 2.85$	0.967	0.71	18	0.05
A-3	$0.33 P$	0.605	2.18	26	0.05
A-4	$0.39 P + 0.12 P_{inc} + 0.23 \frac{1}{VPD} - 3.10$	0.967	0.79	21	0.05
A-5	$1.44 P + 0.30 P_{inc} + 0.75 \frac{1}{VPD} - 9.25$	0.955	2.92	18	0.05
A-6	$0.51 P - 0.076 D_B + 0.062 P_{inc} + 0.18 \frac{1}{VPD} - 1.76$	0.931	1.07	22	0.10
A-7	$1.30 P + 0.21 P_{inc} - 5.81$	0.880	4.05	25	0.05
A-8	$0.51 P - 1.89$	0.876	1.66	20	0.05
A-9	$1.44 P + 0.23 P_{inc} + 1.25 \frac{1}{VPD} - 13.27$	0.907	4.26	20	0.05
A-10	$1.32 P + 0.34 P_{inc} - 7.97$	0.867	4.63	21	0.05
A-11	$1.64 P + 0.43 P_{inc} + 1.01 \frac{1}{VPD} - 15.14$	0.939	4.58	21	0.05
A-12	$0.42 P - 1.73$	0.721	1.66	21	0.05
A-13	$1.98 P + 0.61 P_{inc} + 1.06 \frac{1}{VPD} - 17.27$	0.947	5.26	18	0.05
A-14	$1.34 P - 0.17 I_{max5} + 0.45 P_{inc} - 6.09$	0.916	3.68	20	0.10
A-15	$1.31 P + 2.60 W_{wt5} - 5.96$	0.925	3.28	23	0.05
A-16	$0.95 P - 3.64$	0.931	2.18	21	0.05
A-17	$1.30 P + 0.15 P_{inc} - 5.23$	0.953	2.50	20	0.05
A-18	$1.86 P + 0.44 \frac{1}{VPD} - 9.37$	0.931	4.60	23	0.10
A-19	$4.85 D_R + 0.51 I_{max5} - 19.37$	0.794	10.49	19	0.05
A-20	$3.33 P + 6.62 W_{wt5} + 0.82 \frac{1}{VPD} - 23.21$	0.941	6.80	17	0.05
B-1	$3.18 D_R + 0.40 P_{inc} - 9.36$	0.836	4.58	21	0.05
B-2	$0.96 P + 0.44 P_{inc} + 1.01 \frac{1}{VPD} - 11.65$	0.911	3.54	24	0.05
B-3	$1.42 P - 0.12 D_B + 1.46 W_{wt5} + 0.53 \frac{1}{VPD} - 4.73$	0.978	2.09	26	0.05
B-4	$0.48 P - 1.52$	0.913	1.08	17	0.05
B-5	$2.78 P + 3.37 W_{wt5} - 8.33$	0.828	10.11	27	0.05
B-6	$2.20 P - 9.08$	0.851	8.11	19	0.05
B-7	$0.69 P + 0.25 D_B + 0.23 I_{wt5} + 0.58 \frac{1}{VPD} - 10.74$	0.942	2.75	15	0.10
B-8	$3.46 P + 0.59 P_{inc} + 1.66 \frac{1}{VPD} - 26.45$	0.947	6.95	19	0.05
B-9	$8.22 P - 1.11 D_B - 9.35$	0.958	12.92	28	0.05
B-10	$2.96 P - 0.97 \frac{1}{VPD} - 5.15$	0.923	6.81	22	0.05
B-11	$2.52 P + 3.24 W_{wt5} + 0.53 \frac{1}{VPD} - 14.87$	0.968	4.53	20	0.10
B-12	$2.94 P - 15.51$	0.900	8.98	16	0.05
B-13	$0.62 P + 0.13 I_{wt5} + 0.061 I_{max5} - 6.62$	0.994	0.50	12	0.05
B-17	$0.72 P + 3.02 W_{wt5} + 0.71 \frac{1}{VPD} - 9.70$	0.902	2.51	18	0.05

Note: B-14, B-15, and B-16 were not analyzed due to an insufficient number of events.

Table A.7. Multiple regression equations for stemflow, SF , volume (L) as a function of meteorological variables, generated for single-leader (group A, $n = 20$) and multi-leader trees (group B, $n = 17$) for rain events during *transitional leaf* condition.

Tree ID	Stemflow Volume Regression Equation	R^2	SEE	n	$p \leq$
A-2	$0.70 P - 0.12 D_E - 0.91$	0.997	0.39	12	0.05
A-4	$0.55 P - 0.023 D_E - 0.10 I_{max5} + 0.44 W_{wt5} - 0.011 ACC$	0.992	0.37	17	0.10
A-5	$1.92 P - 0.40 D_E - 0.056 ACC$	0.997	0.81	19	0.05
A-6	$0.63 P - 0.028 ACC + 0.55$	0.996	0.41	11	0.05
A-10	$1.14 P - 0.36 D_E + 1.49 W_{wt5} - 0.036 ACC$	0.995	0.71	13	0.05
A-12	$0.60 P - 0.04 \frac{1}{VPD} - 0.014 ACC$.998	0.35	11	0.10
A-16	$1.32 P - 2.26$	0.977	1.57	12	0.05
A-17	$1.95 P - 0.15 D_E - 0.43 I_{max5} - 0.071 ACC$	0.983	1.87	17	0.10
A-19	$2.77 P - 0.89 D_E - 0.34 I_{max5} - 0.12 ACC + 6.31$	0.997	1.41	11	0.10
B-1	$1.08 P + 1.30 I_{max5} - 8.57$	0.951	4.37	14	0.05
B-3	$1.51 P - 0.034 ACC$	0.913	1.21	13	0.10
B-4	$0.41 P + 6.05 W_{wt5} - 3.04$	0.796	3.04	13	0.05

Note: A-1, 3, 7, 8, 9, 11, 13, 14, 15, 18, and 20 as well as B-2, 5, 6, 7, 8, 9, 10, 11, 12, 13, 14, 15, 16, and 17 were not analyzed due to an insufficient number of events.

Table A.8. Multiple regression equations for stemflow, SF , volume (L) as a function of meteorological variables, generated for single-leader (group A, $n = 20$) and multi-leader trees (group B, $n = 17$) for rain events during *leaf-off* condition.

Tree ID	Stemflow Volume Regression Equation	R^2	SEE	n	$p \leq$
A-1	$-0.042 D_B + 0.40 P + 0.047 I_{w\tau 5} - 0.28$	0.984	0.31	22	0.10
A-2	$0.54 P - 0.54$	0.909	0.26	16	0.05
A-3	$0.33 P + 0.011 P_{inc} - 0.33$	0.896	0.17	16	0.10
A-4	$0.064 W_{w\tau 5} + 0.082$	0.326	0.11	9	0.10
A-5	$1.33 P + 0.060 P_{inc} - 1.24$	0.910	0.75	12	0.05
A-6	$0.83 P - 0.029 D_B - 0.075 I_{max 5} + 0.49 W_{w\tau 5} - 0.61$	0.993	0.44	21	0.10
A-7	$0.87 P + 0.86 W_{w\tau 5} - 0.92$	0.897	0.50	17	0.05
A-8	$0.41 P + 0.27 W_{w\tau 5} - 0.57$	0.914	0.20	15	0.05
A-9	$1.59 P - 0.11 D_B - 0.27 I_{max 5} + 0.69 W_{w\tau 5} - 1.27$	0.987	1.03	25	0.05
A-10	$0.46 W_{w\tau 5} + 0.33 P + 0.062 I_{max 5} - 0.57$	0.927	0.19	13	0.05
A-11	$0.62 P + 0.028 P_{inc} - 0.90$	0.858	0.40	15	0.05
A-14	$0.081 I_{max 5} + 0.38 P + 0.61 W_{w\tau 5} - 1.20$	0.879	0.44	10	0.10
A-15	$-1.72 W_{w\tau 5} + 1.57 P + 0.12 \frac{1}{VPD} - 3.55$	0.802	0.75	15	0.10
A-16	$0.23 W_{w\tau 5} + 0.042 I_{max 5} + 0.038 \frac{1}{VPD} - 0.53$	0.886	0.14	11	0.10
A-19	$1.30 P + 0.93 W_{w\tau 5} + 0.17 \frac{1}{VPD} - 3.60$	0.955	0.54	12	0.05
B-1	$0.018 I_{w\tau 5} - 0.041$	0.886	0.02	12	0.05
B-2	$0.54 P + 0.033 P_{inc} - 0.65$	0.855	0.37	14	0.05
B-3	$2.13 P - 0.31 D_B + 0.12 I_{w\tau 5} - 1.87$	0.999	0.47	14	0.05
B-4	$0.38 P + 0.015 P_{inc} - 0.58$	0.897	0.20	15	0.05
B-5	$2.35 P - 0.076 D_B - 1.94$	0.917	1.12	14	0.10
B-6	$0.74 P + 0.69 W_{w\tau 5} - 1.22$	0.890	0.45	14	0.05
B-9	$5.42 P - 2.33 W_{w\tau 5} + 0.25 \frac{1}{VPD} - 7.53$	0.959	1.77	17	0.10
B-10	$1.23 W_{w\tau 5} + 0.91 P - 1.40$	0.784	0.66	12	0.05
B-11	$1.47 P + 0.78 W_{w\tau 5} - 2.66$	0.951	0.60	11	0.05
B-15	$0.13 P - 0.14$	0.884	0.08	12	0.05

Note: A-12, 13, 17, and 18 as well as B-7, 8, 12, 13, 14, 16 and 17 were not analyzed due to an insufficient number of events.

APPENDIX B

SUPPLEMENTARY MAPS, PHOTOGRAPHS, AND VIDEOS

Figure B.1. Map showing location of study trees, the meteorological station, and manual rain gauges within McArthur Island Park on the north shore of the Thompson River. The inset shows Kamloops in the context of British Columbia and the Pacific Northwest.

Figure B.2. Aerial view of McArthur Island Park taken from the northwest.

Figure B.3. Meteorological station complete with tipping bucket rain gauge (middle) and separate manual rain gauge (left).

Figure B.4. Stemflow collection system.

Figure B.5. Screen capture of a portion of leafless canopy. Deduction of selected sky pixels from total pixels in Adobe Photoshop[®] CC yielded canopy cover (%) and wood cover (%).

Figure B.6. Bark with measured bark relief index, *BRI*, values (from left to right) of 1.00, 1.20, and 1.43.

Figure B.7. Project sign produced by the City of Kamloops and attached to large maps at key access points around the park.

VIDEO DOCUMENTATION OF STEMFLOW

Video B.1. Pin oak

Video B.2. Silver maple

Video B.3. American beech

Video B.4. American beech (close-up)

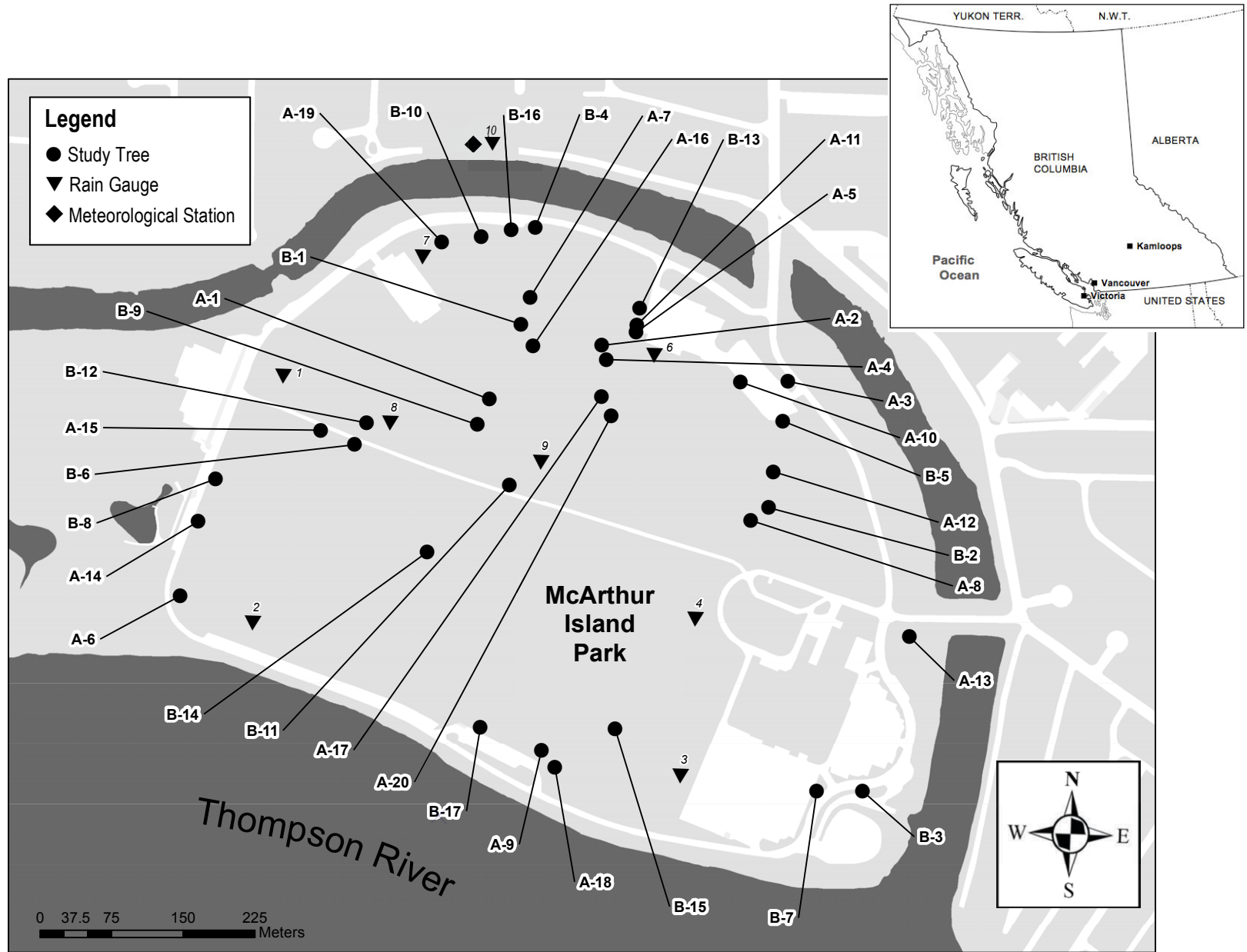


Figure B.1. Location of study trees, meteorological station, and manual rain gauges within McArthur Island Park. The inset shows Kamloops in the context of British Columbia and the Pacific Northwest.



Figure B.2. Aerial view of McArthur Island Park taken from the northwest.



Figure B.3. Meteorological station complete with tipping bucket rain gauge (middle) and separate manual rain gauge (left).



Figure B.4. Stemflow collection system.

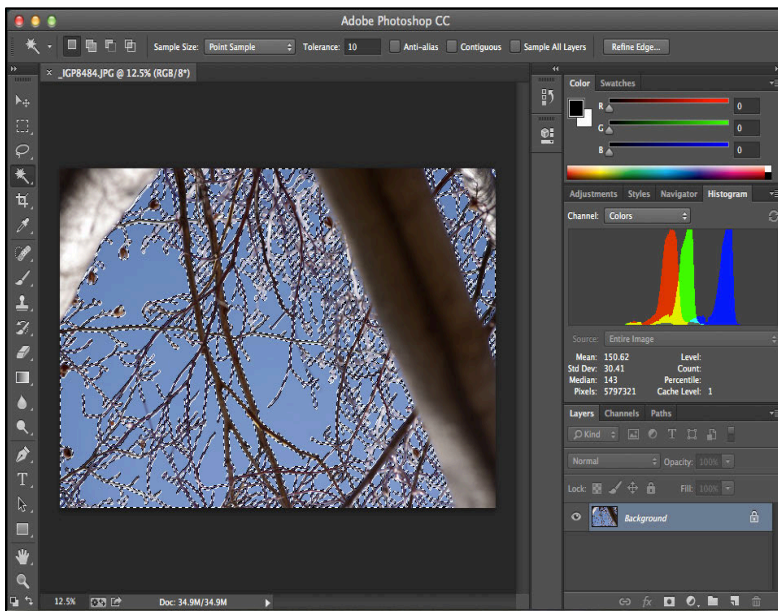


Figure B.5. Screen capture of a portion of leafless canopy. Deduction of selected sky pixels from total pixels in Adobe Photoshop[®] CC yielded canopy cover (%) and wood cover (%).



Figure B.6. Bark with measured bark relief index, *BRI*, values (from left to right) of 1.00, 1.20, and 1.43.

RESEARCH IN PROGRESS



We'll be set up when it rains from now until October, 2013.

A team of scientists from Thompson Rivers University is studying how much rain gets funnelled down the trunks of trees at McArthur Island Park. This research will help us understand which trees may recharge groundwater or minimize urban runoff, thus protecting stream habitat and water quality.

Please call the RCMP at (250) 828-3000 if you see vandalism of equipment.
For more information or to volunteer, visit www.kamloops.ca/stormwatertrees or email Julie.Schooling@gmail.com













Figure B.7. Project sign produced by the City of Kamloops and attached to large maps at key access points around the park.

Video Documentation of Stemflow

Footage taken during this study can be viewed at the following links:

Video B.1. Pin oak: <https://www.youtube.com/watch?v=8BBRvQ8xYfi>

Video B.2. Silver maple: <https://www.youtube.com/watch?v=wu7TxrjCDCI>

Video B.3. American beech: <https://www.youtube.com/watch?v=DqXwgD8u8Pg>

Video B.4. American beech (close-up): <https://www.youtube.com/watch?v=irFt1tRTvzI>